UNIVERSITY OF JYVÄSKYLÄ

Department of Chemistry

Synthesis and investigation of coordinative properties of biimidazole-derived ligands

Master's thesis

University of Jyväskylä

Department of Chemistry

Laboratory of Organic Chemistry

9th April 2015

Margarita Bulatova

ABSTRACT

For this thesis a study of the coordination properties of biimidazole-based compounds was performed. The thesis is divided into two parts: literature part, where the chemistry and application of biimidazole and its derivatives are discussed, and experimental part, where the synthesis and coordination properties of biimidazole-based ligands are studied and discussed.

The literature part contains a discussion of coordinative properties of biimidazole-derived ligands and a discussion of different types of weak interactions. Definition, nature and examples of hydrogen and different types of π-bonding were considered in detail. Due to chemical properties of biimidazole-derived compounds they have been applied in medicine, supramolecular chemistry, and coordination chemistry. A short overview of these applications presented in the literature part.

The experimental part contains synthetic procedures of several biimidazole-based ligands with promising supramolecular properties. The ability of the synthesized ligands to bind d-block transition metals such as Fe(II), Zn(II), Ru(II), Ag(I), Re(III), Pt(II), Au(I) was studied. A variety of coordination frameworks were synthesized using biimidazole-based compounds. In addition, a novel coordination compound of biimidazole-based ligand and potassium iodide was synthesized and investigated.

PREFACE

The literature and experimental part of the present thesis were done May 2014th - April 2015th at the University of Jyväskylä. The literature search was done using SciFinder, Reaxys, and the library of the University of Jyväskylä.

I would like to acknowledge my advisors Academy Professor Kari Rissanen, Professor Matti Haukka, and PhD researcher Rajendhraprasad Tatikonda for helpful advices, inspiration, support, and interest in the current research. Also, I would like to thank Elina Hautakangas for elemental analysis of my samples and both research groups for nice working atmosphere and advices. I would also like to thank my friends Sarah Harris and Samuel Conkovich, who have helped me with this thesis a lot. Especially I would like to thank my beloved husband Evgeny Bulatov who supported and cheered me a lot during all the time I was working on the thesis.

CONTENTS

ABBREVIATIONS

bpy – bipyridine

CDK inhibitor – cyclin-dependent kinase inhibitor

Cisplatin – (*SP*-4-2)-diamminedichloroplatinum(II)

d – day

DCM – dichloromethane

DNA – deoxyribonucleic acid

h – hour

H_2Biim – 1H,1H'-2,2'-biimidazole

ICR – ([ImH][trans-$RuCl_4(Im)_2$]), where Im = imidazole

IUPAC – International Union of Pure and Applied Chemistry

L1 – 1,1'-bis(pyridin-4-ylmethyl)-1H,1'H-2,2'-biimidazole

L2 – diethyl 2,2'-(1H,1'H-[2,2'-biimidazole]-1,1'-diyl)diacetate

L3 – 2,2'-(1H,1'H-[2,2'-biimidazole]-1,1'-diyl)diacetic acid

LED – light-emitting device

NAMI-A – imidazolium *trans*-[tetrachloride(dimethylsulfoxide)imidazole ruthenate(III)]

POM – polyoxometalate

r.t. – room temperature

S_E – electrophilic substitution reactions

LITERATURE PART

1. INTRODUCTION

It is a well-known fact coordination compounds are involved in many important areas of science, medicine, and industry, such as catalysis and photochemistry. Since the 18th century many novel organometallic and coordination compounds have been synthesized and investigated; they are used in modern devices.[1-2] Nevertheless, a wide range of existing ligands and coordination centers, and therefore the possibility of new discoveries, attracts attention of scientists in the field of coordination and organometallic chemistry.

Great possibilities for synthesis of coordination compounds are presented by multidentate ligands. This kind of ligands has several potential binding sides to attach to the coordination center. This provides the opportunity to synthesize different complexes and to investigate the options of ligand binding depending on coordination center or reaction conditions. An interesting fact is that even within the one coordination center, a ligand could coordinate differently which leads to diversity of compounds that possess different optical, electrochemical, and structural properties.[3] Good examples of multidentate ligands are imidazole-based ligands and their derivatives, which will be considered further.

2. COORDINATION COMPOUNDS DEFINITION

Despite the fact the IUPAC definition states that organometallic compounds are "compounds that having bonds between one or more metal atoms and one or more carbon atoms of an organyl group" and coordination compounds are "an assembly consisting of a central atom (usually metallic) to which is attached a surrounding array of other groups of atoms (ligands)"[4], the difference between the two concepts is not obvious. Thus, organometallic compounds would be called coordination compounds from here on in this thesis.

3. LIGAND DEFINITION AND CLASSIFICATION

A ligand could be defined as a coordination entity, that donates one or more electron pairs to the central atom[5], and can have an inorganic or organic nature. Neutral molecules, ions or radicals can act as a ligand in coordination compounds.

There are many ways how to classify ligands, for example:

1) By denticity:
   - monodentate – ligands that have one binding site like Cl^-, OH^-, NH_3 (Figure 1, a);
   - polydentate – ligands that have several binding sites like bipyridine (Figure 1, b);
   - ambidentate – ligands that have more than one potential binding sides consisting of different elements, usually act as monodentate, like DMSO, NCS^- (Figure 1, c);

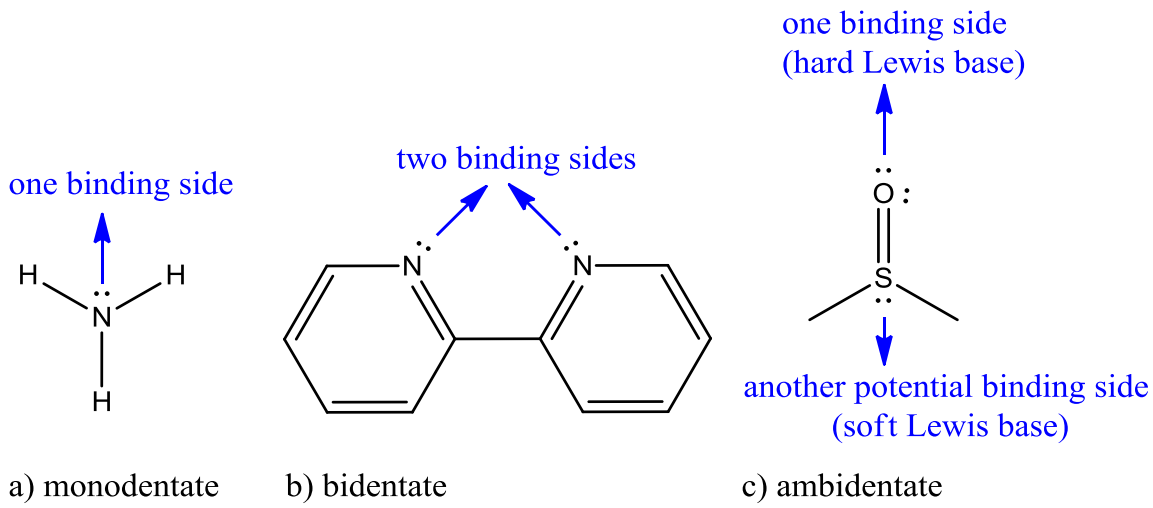

Figure 1. Examples of denticity of ligands: a) monodentate; b) polydentate; c) ambidentate.

2) By chelation:
   - chelate – polydentate ligand that is attached to one coordination center (Figure **2**, a and b);
   - bridging – ligand that is attached to more than one coordination center (Figure **2**, c and d);

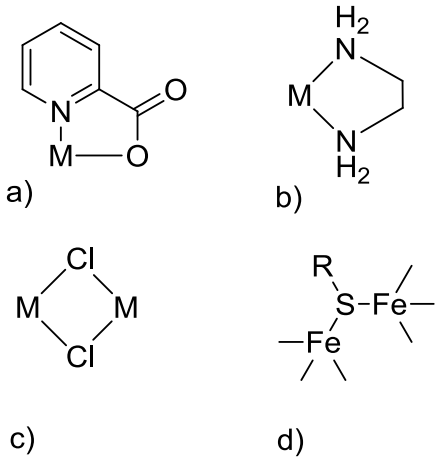

Figure 2. Type of chelation of ligands: a, b – chelate, c, d – bridging, where M – coordination center.

3) By type of bonding:
   - σ-bonding ligands – ligands that are bonded to a coordination center via σ-bond (Figure 3, a);[5]
   - π-bonding ligands - organic fragments containing a conjugated π-electronic system which can interact with one or more metal atoms (Figure 3, b).[6]

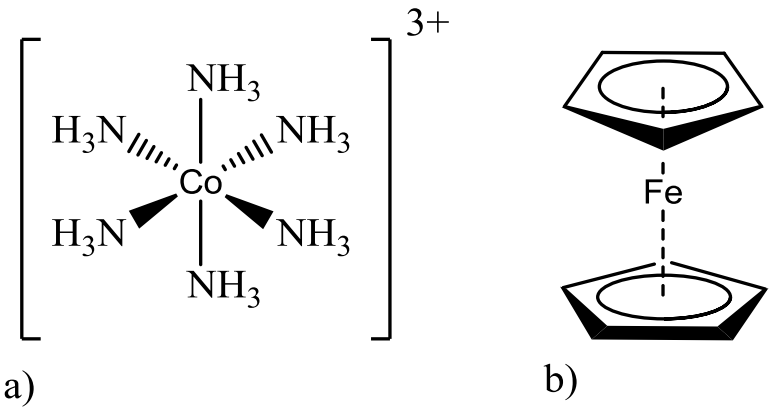

Figure 3. Examples of different types of bonding: a) σ-bonding NH_3 ligands; b) π-bonding cyclopentadienyl ligands.

There are other ways to classify ligands, but they will not be considered in this thesis.

Since ligands are used for complexation reactions it is necessary to understand what type of interactions are responsible for the formation of complexes, or even further supramolecular ensembles. Therefore further basics of supramolecular chemistry and different kinds of interactions will be discussed briefly.

4. SUPRAMOLECULAR CHEMISTRY

Supramolecular chemistry is an actively developing research area. It attracts researchers from all over the world, who are producing promising results with many applications of the research, such as different sensors, molecular storages and machines, and self-assembly materials.[7]

Supramolecular chemistry is the chemistry of molecules or molecular assemblies that are connected to each other by intermolecular interactions.[8] This chemistry is also well known as "guest-host" chemistry, when 'guest' molecule interacts with a 'host' molecule to produce a supramolecule (complex).

One of the main concepts in supramolecular chemistry is the lock and key concept. In 1894 it was created by Emil Fischer, a genius German chemist.[8] The main idea of this concept could be easily understood even just through it name. A key – is a guest molecule has a specific shape and size that opens one particular lock, which is the host molecule (Figure 4). Therefore, to make a host (lock) for a special guest one should know the properties (shape) of the guest.

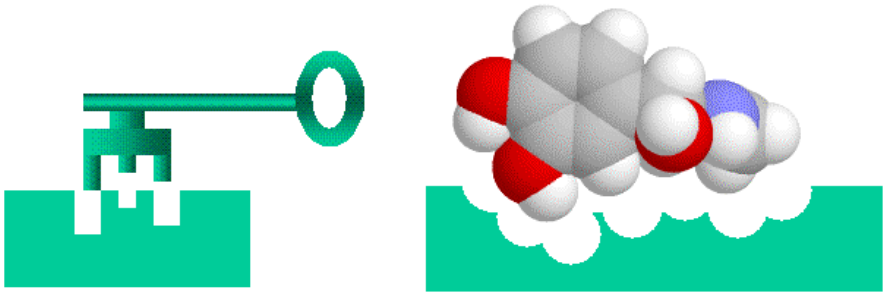

Figure 4. The lock and key concept.[9]

Usually, molecular interactions are associated with the creation of a new covalent bond which is formed when electron pair is shared between two atoms. Contrarily, intermolecular (or supramolecular) interactions do not lead to formation of a covalent bond, and electrostatic interactions are the basic in this case. Intermolecular interactions themselves are not as strong as covalent bonds, although when there are many intermolecular interactions, they are quite tough. The best example to illustrate supramolecular interactions is DNA, perhaps, the most important molecule in human life. Hydrogen bonds that tie two chains to make DNA double helix are quite weak

separately, but altogether they make a very strong bond between two chains, which makes the existence of many biological forms possible (Figure 5).

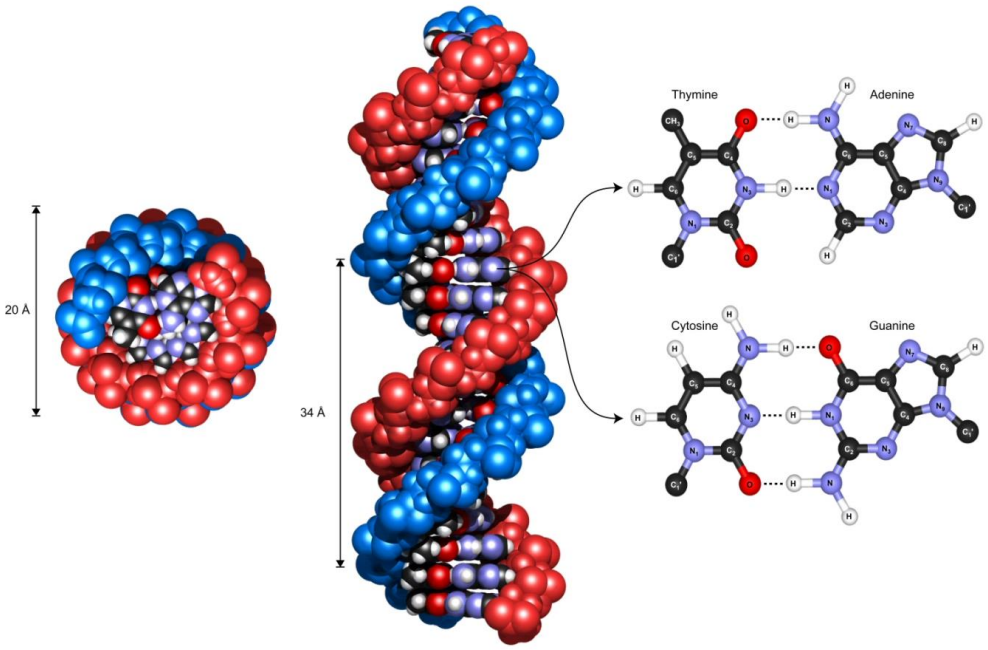

Figure 5. DNA string with hydrogen bonds indicated as the dashed lines.[10]

There are many factors in supramolecular chemistry that are important to know when planning an experiment: the size of the guest molecule, the special interactions between the host and guest based on the guest chemical properties such as degree of order, interactions between subunits, symmetry of packing, and, of course, intermolecular interactions should be considered.

There are some important properties that are similar for designing a host for anions and cations:

- Complementarity

In order to bond, the host binding sites must correspond to electron nature of the guest binding sites (electron deficient host needs electron rich guest). The binding sites should also be located in such a way they are easily available for the guest.

- Macrocyclic effect

Macrocyclic host molecules are more stable than acyclic analogues due to the special organization of binding sites in a space: guest molecule “wraps” around the host molecule to get the best chelation.

- Chelate effect

Due to the advantage of the entropy contribution monodentate ligands are less favorable than polydentate ligands for the same metal ion.

- Host preorganization

The host molecule builds up its structure to correspond to a guest molecules shape before the complexation.

There are, however, some important properties that are different for designing a host for anions then for cations:

- Size of guest

Cations are quite small whereas usually anions are simultaneously quite big in size, therefore for cations the host would be relatively smaller than for anions.

- Shape of guest

Most of the cations have a spherical shape whereas anions have wide range of shapes and geometries.

- Free energy of solvation

Anions have higher energy of solvation than cations and they have to compete with the surrounding medium in order to bind with the host. In general, non-polar solvents are the best for anions.

- Binding

Cations can bind via different kinds of binds, whilst anions provide only hydrogen and van der Waals binding. Nondirectional forces are very important in anion binding.

- pH dependence

Most of cations could exist in a wide range of pH whilst anions could exist in fairly narrow pH region.

- Charge

It is well known that cations are positively charged particles whilst anions are negatively charged. The host for such a particle should be designed according to the

nature of the charge. All this nuances show that special conditions are needed for complexation/hosting of anions, however cation hosting requires quite soft conditions and has been investigated more.

It is important to consider intermolecular interactions when investigating the supramolecular system. Biimidazole-based supramolecular systems usually possess hydrogen and different types of π-bonding, and these are considered in detail in next chapters.

5. HYDROGEN BONDING

Hydrogen bonding has been described as the 'masterkey interaction in supramolecular chemistry' due to its relatively strong and highly directional nature of bonding.[8] According to the Golden book of IUPAC, hydrogen bonds are a form of association between an electronegative atom and a hydrogen atom attached to a second, relatively electronegative atom.[4] A hydrogen bond could be considered as an electrostatic interaction due to the small size of a hydrogen atom, which permits the close proximity of the interacting dipoles or charges. In particular, a hydrogen bond may be presented as a kind of dipole–dipole interaction where a hydrogen atom attached to an electronegative atom (or electron withdrawing group) is attracted to a neighboring dipole on an adjacent molecule or functional group (Figure 6).

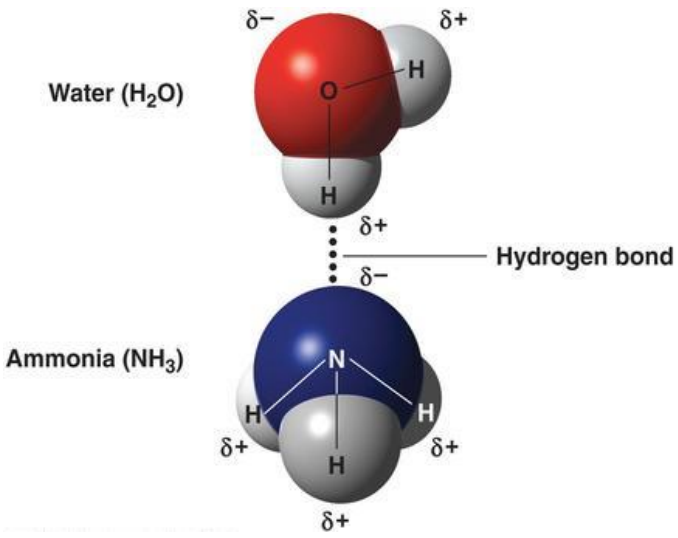

Figure 6. Dipole–dipole representation of hydrogen bond between water and ammonia molecules.[11]

Usually, both electronegative atoms are from the first row of the Periodic Table, i.e. N, O or F. Hydrogen bonds are generally labeled as a dash line D–H···A in between a donor (D) group, which is represented by an electronegative atom, and an acceptor (A) group, which is represented by an electronegative atom, bearing a lone electron pair.

The typical range of strength of hydrogen bonds is *ca*. 4–60 kJ/mol.[8] The strength of the hydrogen bond is significantly dependent on the environment: it is stronger for chlorine atoms, and for the larger halide acceptors it is weaker as a result of the reduced electronegativity.

The formation of carboxylic acid dimers is a very important hydrogen bonding example in supramolecular chemistry (Figure 7). The dimer formation causes the shift of the ν(OH) infrared stretching frequency from about 3400 cm^{-1} to about 2500 cm^{-1}. Moreover, the signal of the absorption is significantly broadened and intensified.

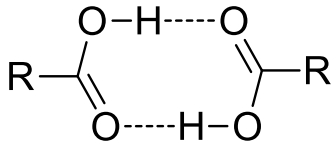

Figure 7. Carboxylic acid dimer.

Hydrogen bonds have different properties such as strength, length, and geometry. There are three categories of hydrogen bonds: strong, moderate, and weak. Strong interactions are similar to a covalent bond in character, have a linear geometry (with bond angles 175–180º), the energy of bond is 15 ± 40 kcal/mol,[12] and they take place when hydrogen atom is close to the center-point of the donor and acceptor atoms. Examples of strong interactions are the formation of gas phase dimers with strong acids/bases, hydrogen fluoride complexes, and proton sponges. Moderate interactions are mainly electrostatic in character, are slightly bent in geometry (with bond angles 130–180º), and the energy of this bond is 4±15 kcal/mol.[12] Examples of moderate interactions are amide interactions in proteins and the self-association of carboxylic acids. Weak interactions are electrostatic in character, highly non-linear geometry (with bond angles 90–150º), and take place when unconventional donors and acceptors are involved in forming the hydrogen bond, for example, C–H groups, the π-systems of aromatic rings or alkynes, transition metals, and transition metal hydrides. The energy of the weak hydrogen bond is <4 kcal/mol.[12]

There is a direct correlation between neutral species, hydrogen bond strength, and the crystallographically determined distance between hydrogen bond donor and acceptor. The strength of similar hydrogen bonds depends on the geometry of the hydrogen bond and on the type of electronegative atom attaching to the hydrogen. Partially those effects can be described by scales of hydrogen bond acidity and basicity. The acidity of the C—H proton increases significantly in the presence of electronegative atoms near the carbon of C–H donor hydrogen bonds, and a strong dipole is formed.

There are two different types of hydrogen bond interactions: primary and secondary. In primary hydrogen bond interactions there are direct interactions between the donor group and the acceptor group. This type of interaction is presented by different geometries in hydrogen bonding complexes: linear, bent, donating bifurcated, accepting bifurcated, trifurcated, and three centers bifurcated (Figure 8).

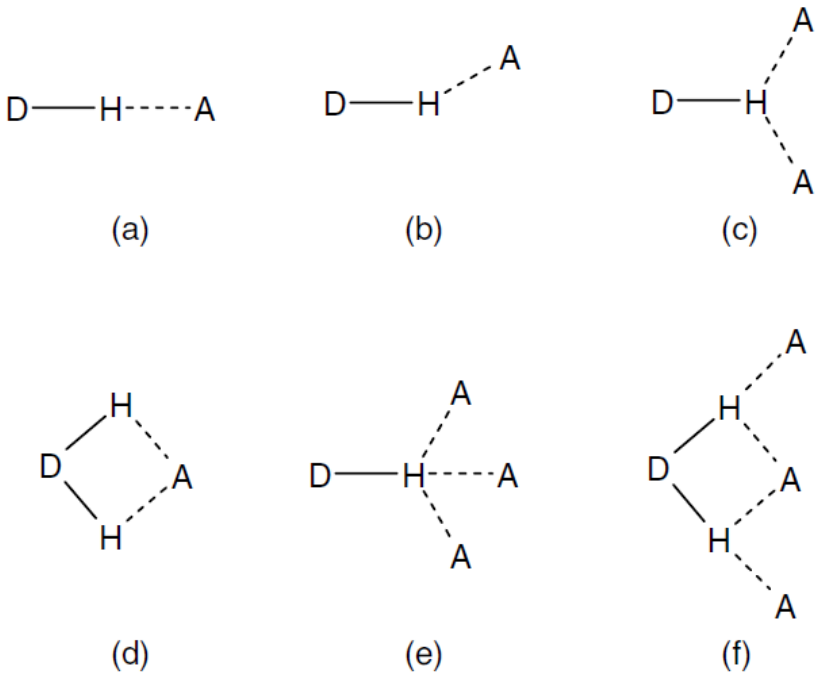

Figure 8. Primary interactions of various types of hydrogen bonding geometries: (a) linear; (b) bent; (c) donating bifurcated; (d) accepting bifurcated; (e) trifurcated; (f) three center bifurcated.[8]

In secondary interactions the interaction takes place between neighboring groups where partial charges on neighboring atoms can either increase the binding strength by virtue of the attraction between opposite charges or decrease the proximity due to repulsion between like charges (Figure 9).

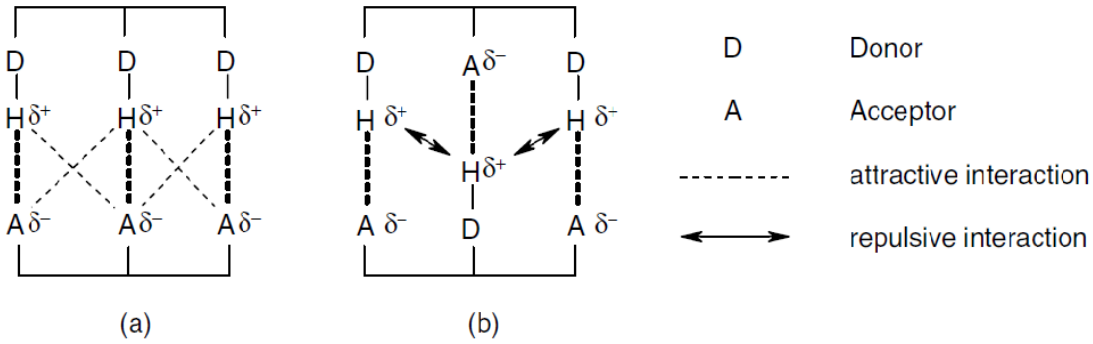

Figure 9. Secondary interactions: (a) attractions between neighboring groups between DDD and AAA arrays (primary interactions in bold); (b) repulsions from mixed donor/acceptor arrays (ADA and DAD).[8]

Hydrogen bonds may be intermolecular or intramolecular. Intramolecular hydrogen bonds occur within one single molecule, whereas hydrogen bonds are formed between two functional groups of the same molecule (Figure 10). One of these functional groups should possess donor properties whilst another should possess acceptor properties, and both groups should be located close enough to create a hydrogen bond. Intermolecular hydrogen bonds occur between separate molecules of the compound (Figure 10). This type of hydrogen bond can occur between any molecules, but the distance between hydrogen donors and acceptors should be small enough to interact.

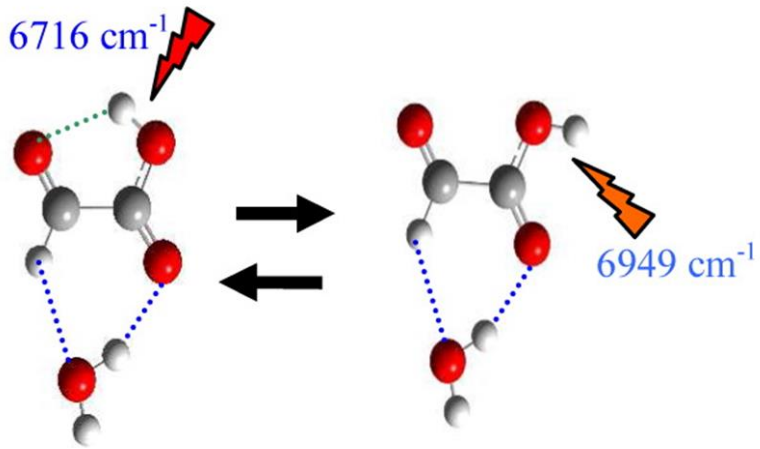

Figure 10. Hydrogen bond types in the example of the isomerization process of glyoxylic acid (GA) conformers and their complexes with a water molecule: intramolecular hydrogen bond within GA molecule (green dots); intermolecular hydrogen bonds between water molecule and GA (blue dots).[13]

There are some factors that could prevent hydrogen bonding such as electronegativity and atom size. The electronegativity differences could play a crucial role in the case of hydrogen bonding; if electronegativity differences between hydrogen and the atom it is bonded to are not big enough, there will be no hydrogen bonding. The best example is PH_3, which has a geometry that is similar to trigonal pyramidal molecular geometry, but due to the same 2.1 electronegativity of P and H atoms the bond between these atoms is not polar enough to form a first row (n = 2 valence shell) hydrogen bond.[14] Therefore the hydrogen atom does not have the partial positive charge which prevents hydrogen bonding with the lone electron pair of another molecule. The size of interacting atoms also plays a very important role in hydrogen bonding. If the nuclei of two interacting atoms cannot achieve close proximity then a weak interaction takes place. This can happen when the radii of two atoms differ greatly. A good example of this is the lower ability of iodine atoms to form hydrogen bonds compared to chlorine atoms.

6. Π-INTERACTIONS

π-interactions are very important for synthetic and coordination chemistry. They can be divided into three main groups: cation–π interactions, anion–π interactions, and π-π interactions.

1. Cation–π interactions

In a pioneering gas phase study of ion-molecule complexes Kebarle *et al.* found that a K^+-benzene complex has greater interaction energy than the K^+-water complex (79 and 75 kJ/mol respectively).[15] Further studies by other researchers have provided evidence for many other cation–π complexes.

The cation–π interaction is the electrostatic interaction of a cation with the face of a π-system; π-cation binds better to the system the more negative an electrostatic charge. A good illustration of this phenomenon is the experiment of complexation of the benzene with different alkali metals. It can be seen from the Table 1 the binding energy trend is $Li^+ > Na^+ > K^+ > Rb^+$ which substantiates that electrostatic forces have a dominant role in cation–π interactions.

Table 1. Free binding energy (in kJ/mol)a for $M^+(C_6H_6)$ at 298 K.

System	ΔG_{298}, kJ/mol
$Li^+(C_6H_6)$	132.2
$Na^+(C_6H_6)$	63.8
$K^+(C_6H_6)$	45.9
$Rb^+(C_6H_6)$	42.3
$Cs^+(C_6H_6)$	38.9

The reason for this electrostatic interaction occurs is the cation interacting with the arene quadropole moment when two dipoles are aligned such that there is no net dipole moment. The quadropole moment is topologically analogous to the dz^2 orbital (Figure 11).

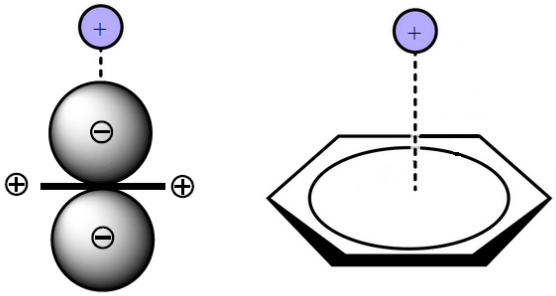

Figure 11. Cation binding of a negative dz^2 aromatic (benzene).

Cation–π interactions are often observed in transition metal complexes, for example ferrocene [$Fe(C_5H_5)_2$], where the strong bonding could not be considered as covalent due to intimate linkage with the partially occupied *d*-orbitals of the metals. However, this type of interaction also takes place between alkaline or alkaline earth metal cations and double C=C bonds, even though it is weak, and it is essential for some biological systems.[8]

This type of interaction is widely used in supramolecular chemistry. One of the pioneers in this area is Dougherty, who made a significant contribution to the study of a physical model of cation–π interaction.[16-17] Dougherty *et al.* had synthesized cyclophane

receptors, and it has been observed that cation–π interactions can be rationalized by an electrostatic model. Nevertheless, it has been found that the nature of the aromatic ring can influence electrostatics; for example, the electrostatic contribution is significant for Na^+-benzene complex, while there is no electrostatic contribution for the Na^+-1,3,5-trifluorobenzene complex. The synthesized cyclophane has been found to be a better receptor for quaternary ammonium and iminium ions than other neutral receptors (Figure 12). Replacing two of the benzene rings with cyclohexyl units significantly worsens the binding ability of the host. Therefore, it has been proved that cation–π interactions are responsible for binding of the cation.

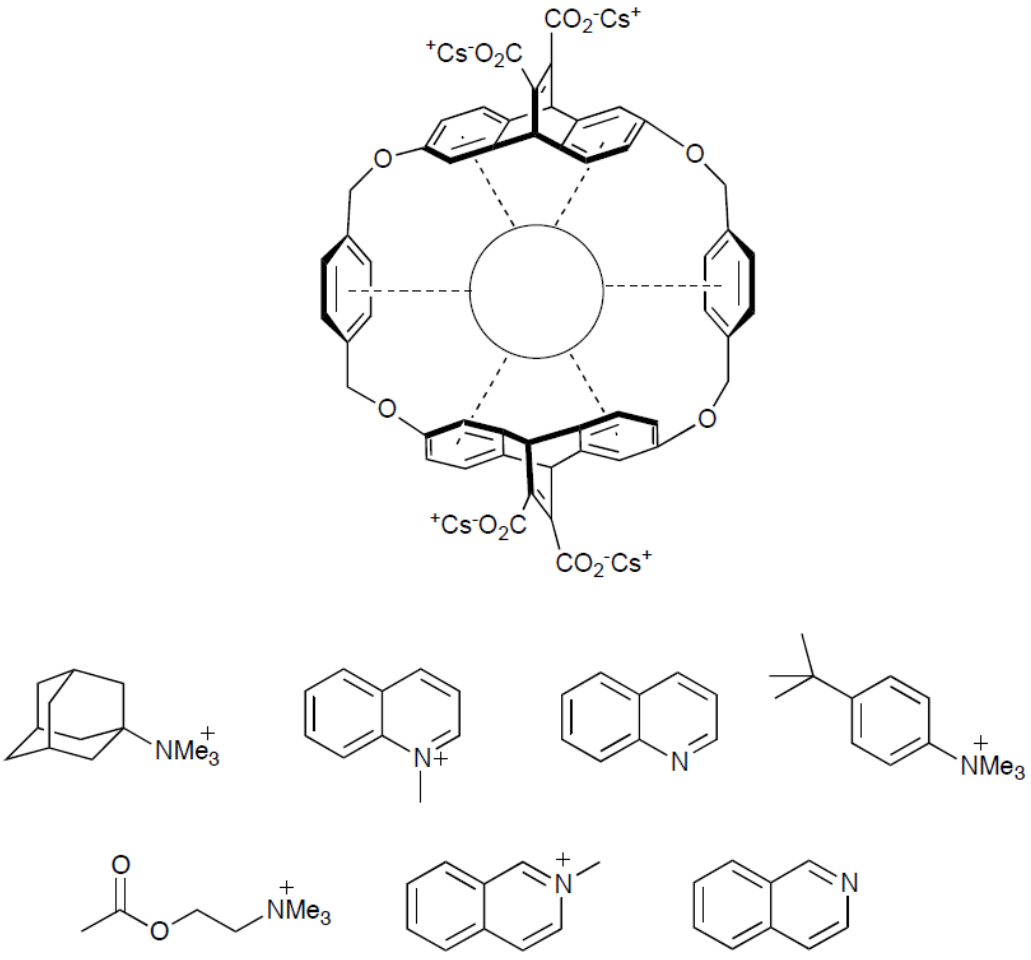

Figure 12. An example of cyclophane receptor and the substrates used for the cation–π complexation studies.[16]

Another study has been done by Yamada *et al.* who discussed the importance of cation–π interactions for asymmetric organocatalysis.[18] To have good enantioselectivity the catalyst with a cation–π interaction (Figure 13) was used for the reaction of Stetter cyclisation of aromatic aldehydes (Figure 14). During face-selective 1,4-addition

reaction charge separated zwitter ionic intermediate forms a cation–π complex with a catalyst to give chroman-4-one.

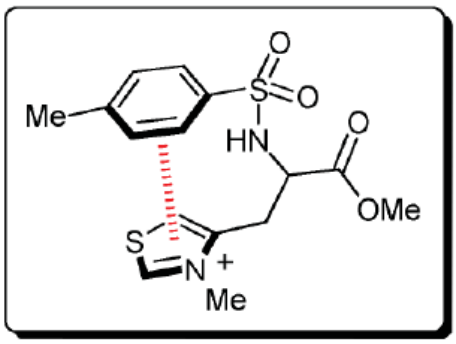

Figure 13. Catalyst with cation–π interaction.[18]

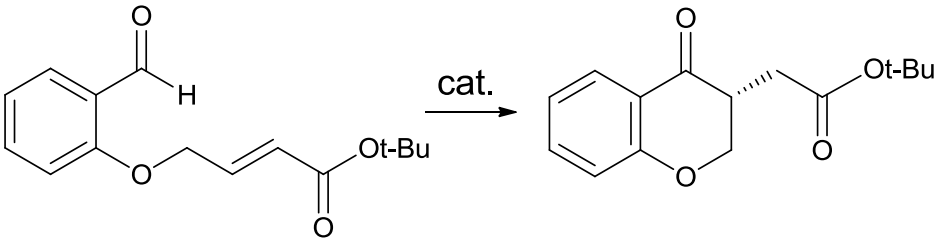

Figure 14. Stetter cyclisation of aromatic aldehydes with addition of cation–π interaction catalyst.[18]

2. Anion-π interactions

An anion-π interaction is the electrostatic interaction of an anion with the face of a π-system. Anion-π interactions are not as common as cation interactions due to the fact π-electron density repulses anions. For example, due to the anion repulsions, the aromatic ring affinity of the compound presented in the Figure 15 decreases according to the trend: F^- >> Cl^- > Br^- ~ I^-.[19] Nevertheless, there is a principle possibility for an electrostatic attraction to exist because of a charge difference between an overall neutral aromatic ring and an anion.

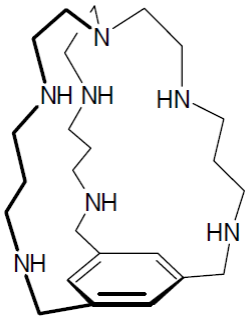

Figure 15. A macrobicyclic azaphane containing benzene ring.[19]

In 2004 Rosokha *et al.* presented curious results showing that anions and electron deficient aromatic compounds may form stable charge transfer complexes.[20] The results showed a linear correlation between the energy of the charge transfer band in the electronic spectrum and the formal reduction potential of the aromatic compound. According to X-ray crystallography investigations the anion sits in an offset fashion at the edge of the aromatic rings rather than above the centroid (Figure 16).

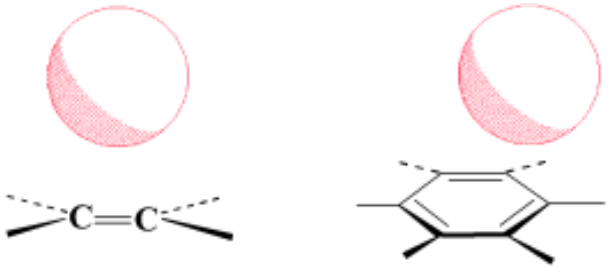

Figure 16. Schematic drawing of the anion–π interactions. The sphere representing the van der Waals radius of bromide is drawn to scale relative to the electron-deficient olefinic and aromatic centers.[20]

Organometallic calixarenes have also been reported to form anion-π complexes.[21] It was proposed that the aromatic ring that bears a significant positive charge can make anion-π complexation possible. Considering the size and shape compatibility between anion and organometallic host molecules based upon the calixarenes, several anion-π calixarene complexes have been synthesized. These may have the potential of being used in the detection and removal of unwanted environmental contaminants have been synthesized (Figure 17, Figure 18).

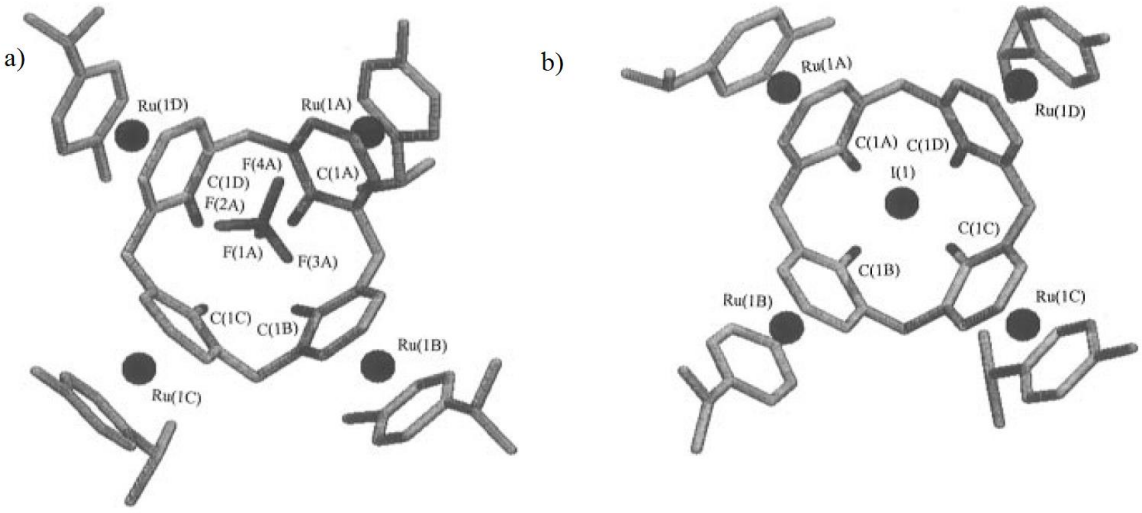

Figure 17. X-ray crystal structure of the ruthenium tetrametallic complex with: a) BF_4^- anion; b) I^- anion.[21]

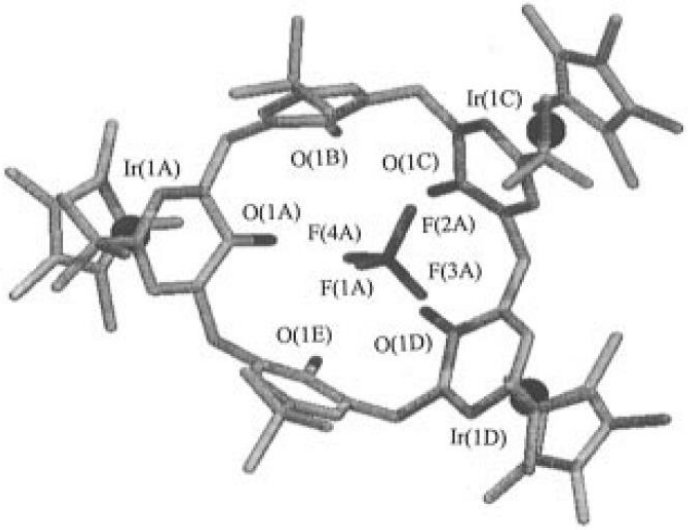

Figure 18. X-ray crystal structure of the ruthenium tetrametallic complex with BF_4^- anion.[21]

Another example of anion-π interactions was presented by Schottel *et al.*, who presented crystallographic and computational investigations of anion-π interactions on the preferred structural motifs of Ag(I) complexes containing π-acidic aromatic rings (for example Figure 19).[22]

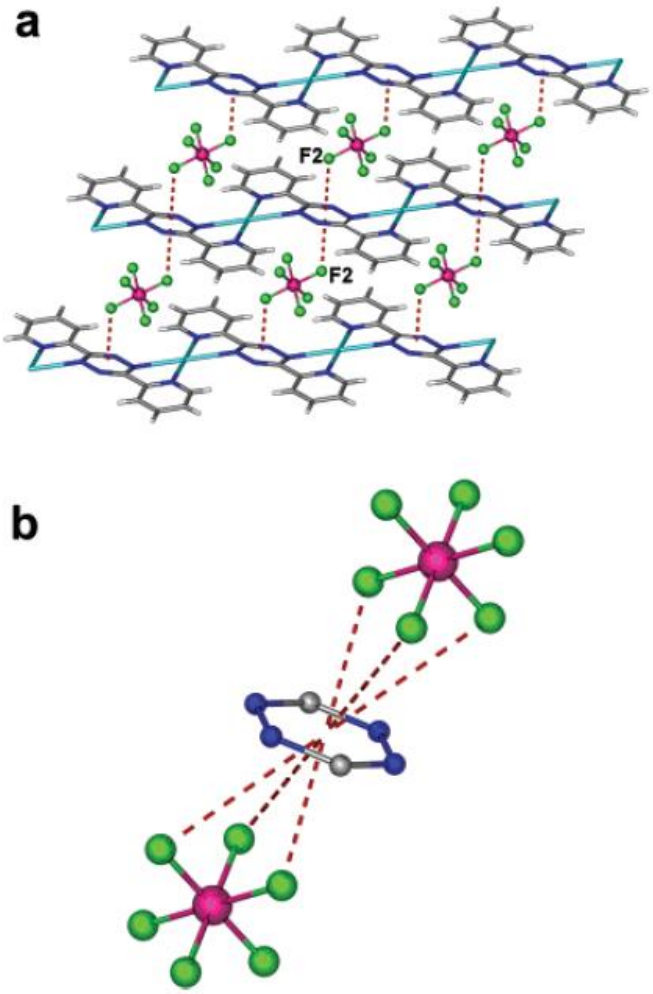

Figure 19. Anion-π interaction (dotted lines drawn to the ring centroid) : (a) In the packing diagram of $\{[Ag(bptz)][PF_6]\}_\infty$; (b) between tetrazine ring and two $[PF_6]^-$ anions.[22]

Electron-deficient anion-π hosts have the potential use as molecular receptors for the recognition of anions which may have important analytical, biological, and medicinal possible applications.

3. π-π interactions

Aromatic π-π or π-π stacking interactions are interactions between relatively electron rich and electron poor aromatic rings. To explain the π-π interactions, the quadrupole moment of an aromatic system, describing its' molecular charge distribution, is used. Ritchie *et al*. visualized the quadrupole moment of benzene and similar molecules as a delocalized negative charge above and below the plane of the ring (Figure 20).[23] Meanwhile the electronegativity of the ring substituents can affect the sign of the

quadrupole moment. For example, the sign of quadrupole moment of hexafluorobenzene is reversed and the positive charge is now delocalized above and below the ring (Figure 20).

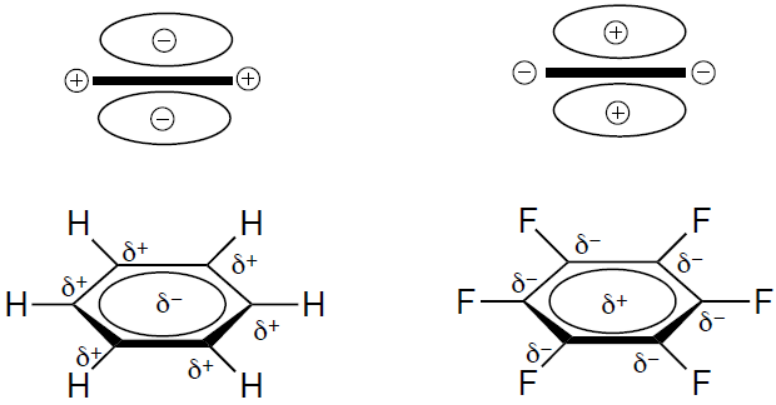

Figure 20. Schematic representation of the quadrupole moments of benzene and hexafluorobenzene.[23]

There are several types of geometries of π-π interactions described in the literature; the edge-face geometry, the offset stacked geometry, and the face-to-face stacked geometry.[24] The edge-face geometry (Figure 21, a) can be presented by a CH–π interaction, for example, in benzene in the solid state or between aromatic residues in proteins. In the offset stacked geometry (Figure 21, b), more surface area is buried, and the van der Waals and hydrophobic interactions are increased; this happens when the electron density on the face of one or both rings is reduced. It can also be observed in proteins or in the geometry of base stacking in DNA. In the face-to-face stacked orientation geometry donor–acceptor pairs and compounds have opposite quadrupole moments, and the interaction between the faces of the rings is attractive. The best example of this type of interaction is benzene–perfluorobenzene one (Figure 21, c).

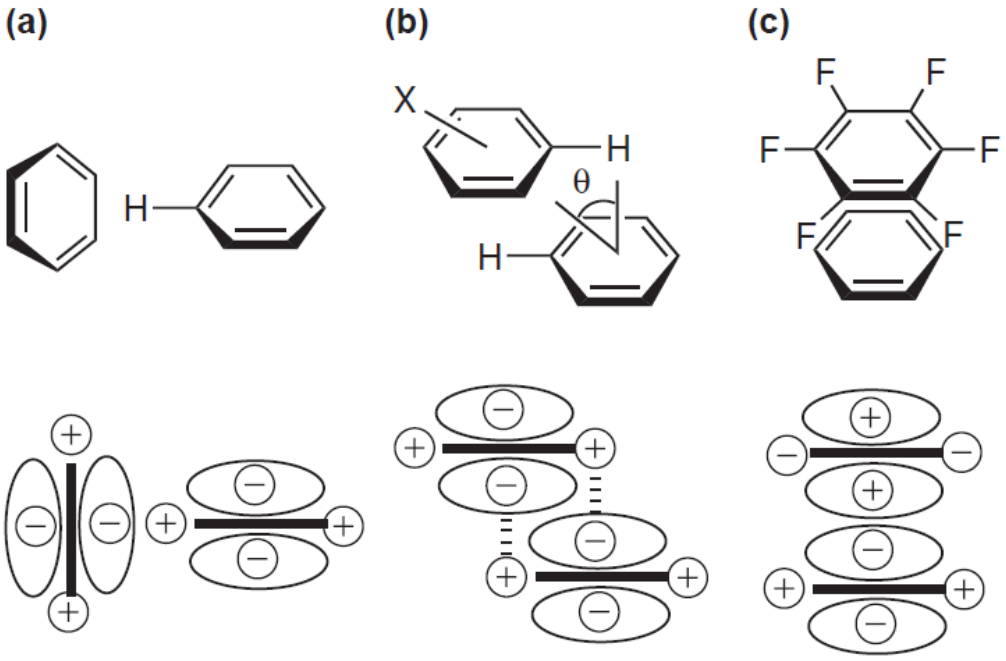

Figure 21. Geometries of aromatic interactions: (a) edge-face; (b) offset stacked; (c) face-to-face stacked.[24]

Hunter and Sanders were pioneers in the study of the nature of aromatic π-π interactions within supramolecular systems. To characterize the nature of π-π interactions they have been studied the host-guest chemistry of flexible macromolecules, especially two porphyrin molecules in solution (Figure 22).[25,26]

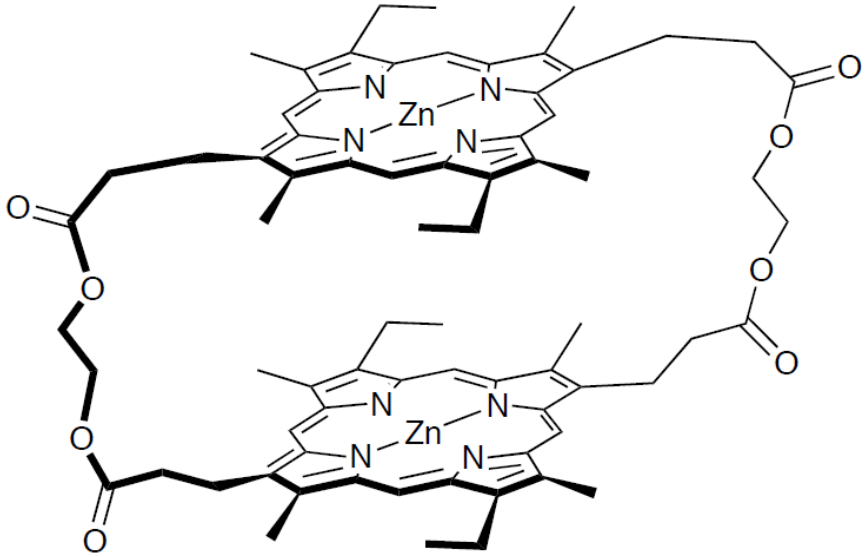

Figure 22. A porphyrin dimer studied by Hunter and Sanders.[41]

The information about the strength of the π-π interactions had been obtained by research of the effects of metallation and coordination of the central zinc ion and the kinetics and thermodynamics of binding with host molecules to the cavity between the porphyrins. It has been found that π-π interactions appear when attractive interactions between π-framework and π-electrons are bigger than π-π repulsive ones.[41]

However, the total energy of the aromatic interaction has been proposed to consist of several contributions such as van der Waals interactions, electrostatic forces, charge transfer and desolvation.[24] Van der Waals and electrostatic interactions contribute the most to the total energy. Van der Waals interaction between aromatic rings is proportional to the area of π-overlapping. This term is always attractive and it dominates the overall energy of the *π–π* interaction. Electrostatic forces between the two negatively charged *π*-systems define the relative orientation of the two interacting molecules (Figure 23).

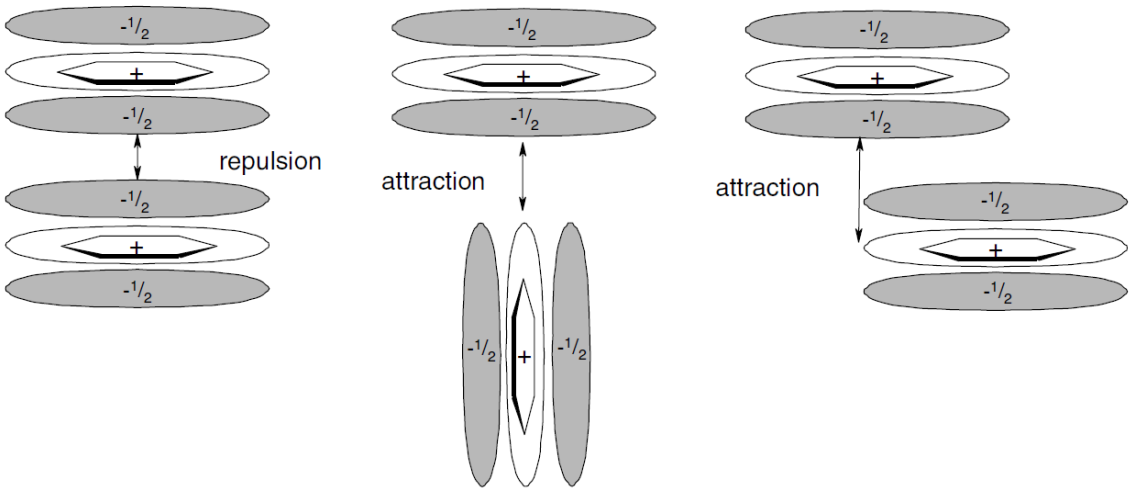

Figure 23. Interacting *π*-quadrupoles.[8]

Charge transfer stabilizes non-covalent interactions by mixing the ground state with an excited charge-separated state. Desolvation occurs between two molecules in solution that are firstly desolvated (Figure 24), then a non-covalent interaction destabilizes the molecules when the solvent interacts strongly with the substrate.

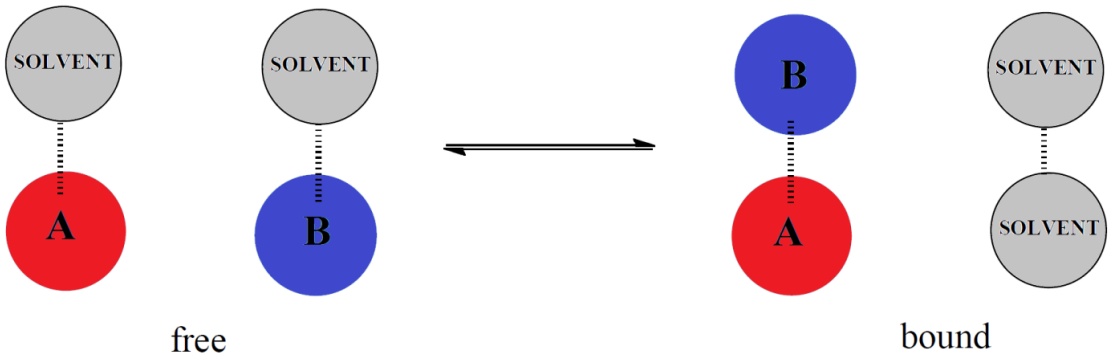

Figure 24. Scheme of desolvation.

7. IMIDAZOLE AND ITS DERIVATIVES

Imidazole is an organic molecule with a molecular formula $C_3H_4N_2$ (Figure 25).

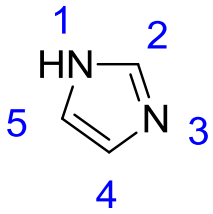

Figure 25. Structure of imidazole.

It is a heterocyclic compound and it is named according to its chemistry: numbering starts from the atom with the highest atomic number and continues to reach the next highest atomic number atom in the fastest way. The positions are specified by numbering from nitrogen atoms which are not multiply-bonded, but have an 'extra' hydrogen atom, and its written in italic capital '*1H*'. For nitrogen-containing heterocycles the prefix -aza- is used and for 5-membered cycles the suffix –ole is used. Therefore, the full name of imidazole is *1H*-imidazole.[27]

It has a molecular weight of 68.077 g/mol, a melting point 90 °C, a high boiling point of 256°C due to intermolecular H-bonding, it is highly soluble in water, and it appears as a white or light yellow solid.[28] Imidazole can be synthesized according to the Radziszewski reaction where glyoxal is condensed with formaldehyde and ammonia in a molar ratio of 1 : 1 : 2 (Figure 26).[29]

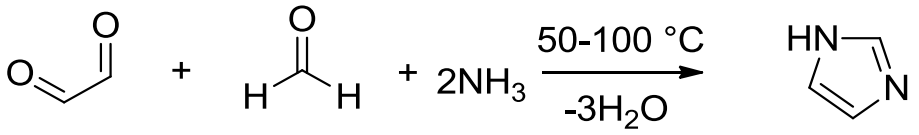

Figure 26. Synthesis of imidazole by the Radziszewski reaction. [29]

Imidazole is the amphoteric compound with p_{Kb}= 7.0, which makes it a stronger base than pyridine, and p_{Ka}= 14.9 which is weaker than carboxylic acids, but stronger then alcohols.[28]

Imidazole is an aromatic compound due to the sextet of π-electrons: one pair from the protonated nitrogen and 2 pairs from double bonds. The aromaticity of the compound determines its resonance stability (Figure 27) and its reactivity, for example, the possibilities of coordination.

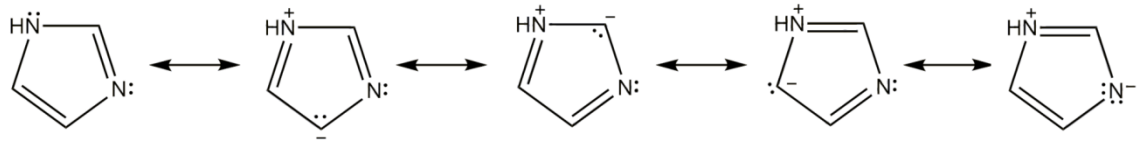

Figure 27. Resonance structures of imidazole.

Aromaticity of the compound also determines the varieties of electrophilic substitution reactions (S_E) that occur; coupling with aromatic diazonium salts, halogenation, nitration and sulfonation, hydroxymethylation, and carboxylation.[30]

In order to explain the regioselectivity of the electrophilic substitution reactions for imidazole, it is necessary to reflect on the different embodiments of the resonance structures in a reaction (Figure 28). It is clear that an electrophile attacks more efficiently at the 4th and 5th position in the imidazole ring (Figure 28 A,B) since attack at the 2nd position involves an extremely disadvantaged canonical form due to the positively charged N at the 3rd position (Figure 28 C).[30]

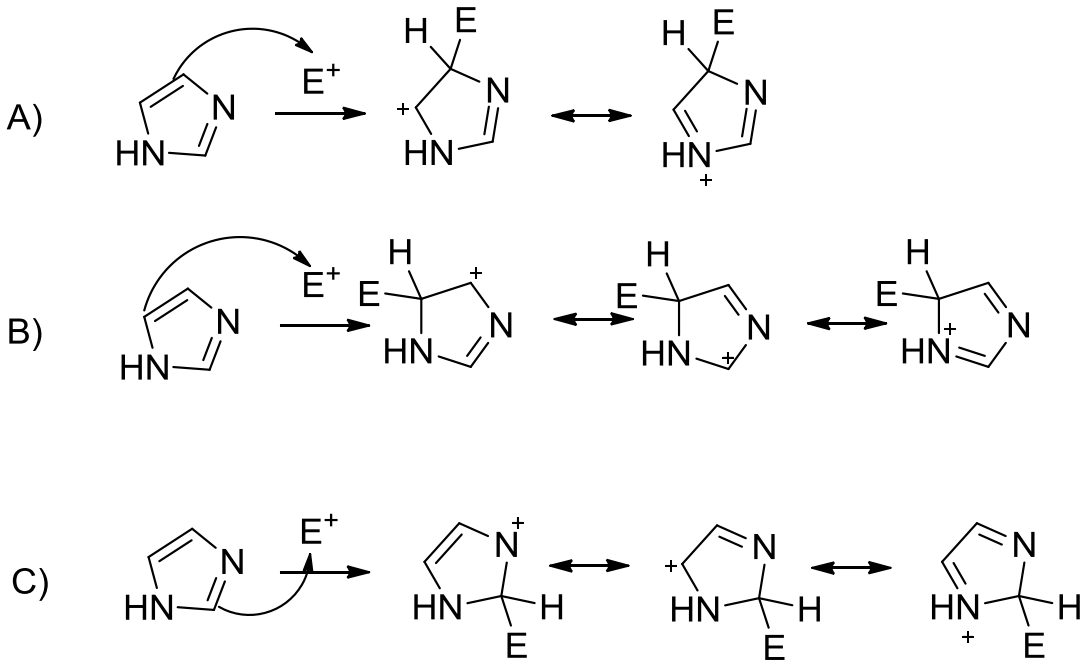

Figure 28. Resonance structures of imidazole in electrophilic substitution reactions.[30]

Reactivity of imidazole is more liable than oxazole or thiazole (Figure 29) and amplified towards electrophillic attack.

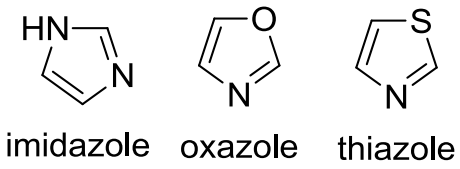

Figure 29. Structures of imidazole, oxazole, and thiazole.

The availability of the lone pair of electrons is a crucial factor in S_E reactions. Due to the resonance stability and symmetry of conjugated acid imidazole (p_{Ka}= 7.0), it is more basic than for oxazole (p_{Ka}= 0.8), or thiazole (p_{Ka}= 2.5).[31] Oxygen and sulfur atoms are, as a result, more electronegative than a nitrogen atom and, therefore, the inductive effect is stronger in the case of oxazole and thiazole then imidazole due to the fact that lone pair on nitrogen of these molecules is less available than of imidazole.

Derivatives of the imidazole have a wide range of application in synthesis and in pharmacology. Alkylimidazoles are used to make epoxy resins and polyurethanes harder; 1-vinylimidazole is used as a copolymer in the production of cationic polymers; alkyl- and arylimidazoles are used in photography and dyes.[28] Imidazole derivatives possess different kinds of bioactivity: anti-inflammatory, enzyme inhibition, analgesic, anti-neoplastic, anti-anthelmintic, anti-viral, anti-ulcer, anti-fungal, anti-filarial, anti-cancer, cardiovascular activity, and many others.[30]

Derivatives of imidazole are actively used in the synthesis of various coordination compounds.

For example, palladium complex with imidazole-based ligands have a possible use as molecular switcher (Figure 30).[32] Imidazole-based ligand can be isomerized by UV-light exhibiting photochromic activity (Figure 31).

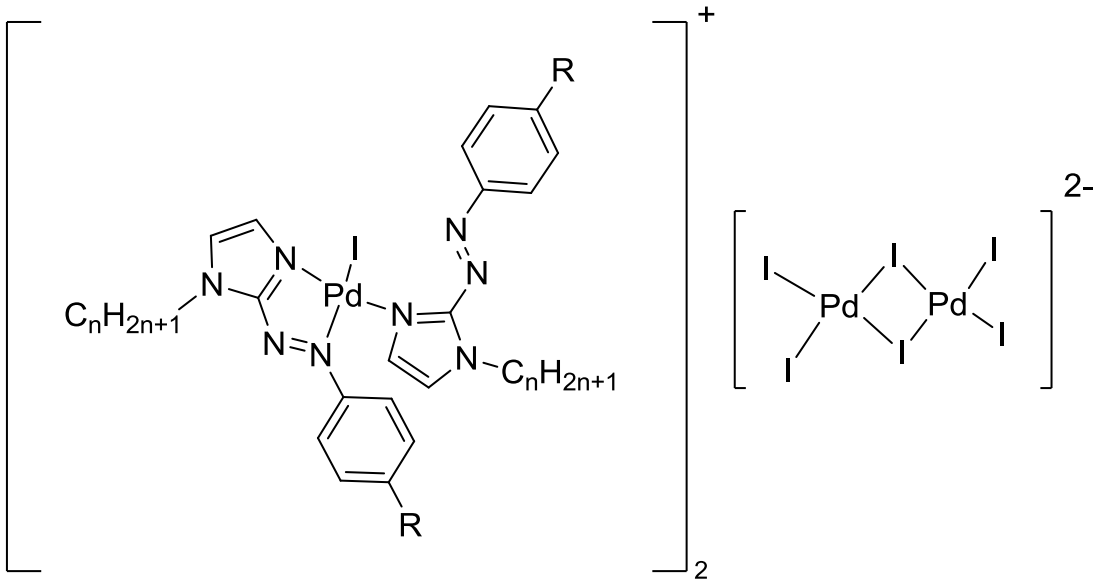

Figure 30. Structure of the palladium complex with imidazole-based ligands.[32]

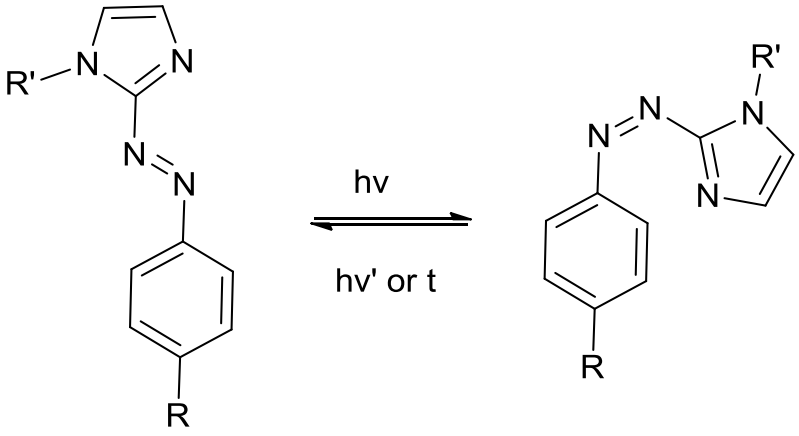

Figure 31. Cis-trans isomerization of imidazole-based ligand.[32]

The same imidazole-based ligands were also used to study photochromism of cadmium complexes (Figure 32).[32]

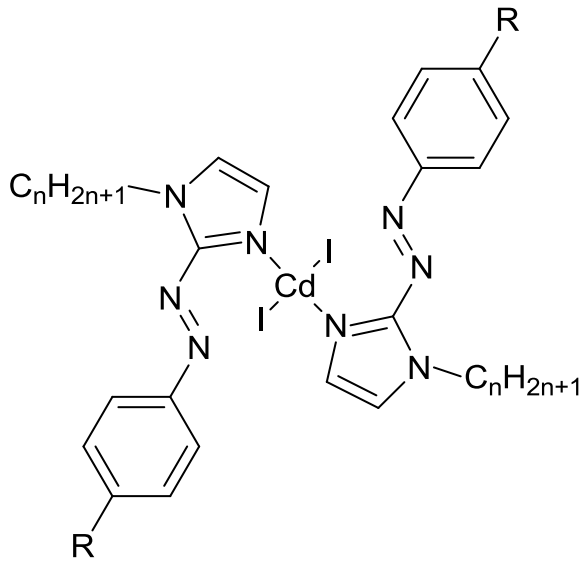

Figure 32. Structure of the cadmium complex with imidazole-based ligands.[32]

Another example is the iridium complex containing *1,1'*-diethyl-*1H,1'H-2,2'*-bibenzo[d]imidazole as the ligand[33], this has been effectively used as the luminescence conversional material in InGaN-based light-emitting devices (LED) (Figure 33).

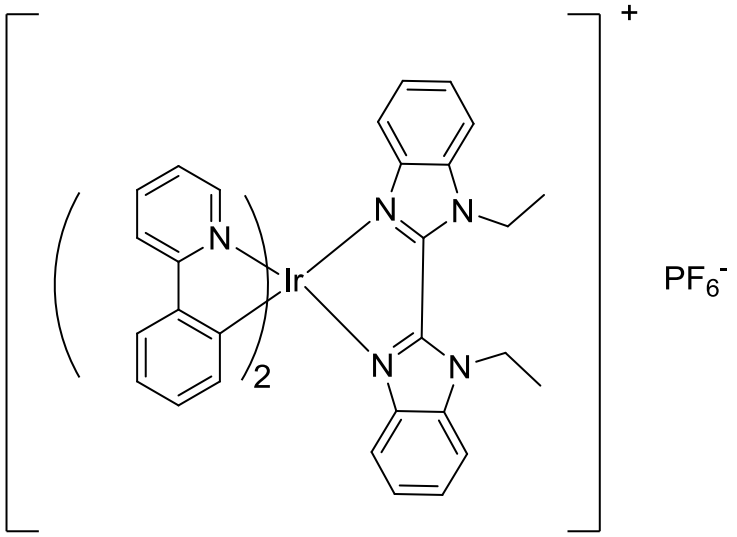

Figure 33. Iridium complex with imidazole-based ligand.[33]

The great possibilities for coordination reactions and its wide range of applications have attracted the attention of researchers to imidazole, and have, therefore, contributed to the development of imidazole derivatives, for example biimidazole and biimidazole-based compounds.

8. BIIMIDAZOLE

2,2'-biimidazole is an organic heterocycle with the molecular formula $C_6H_6N_4$, a molecular weight of 134.14 g/mol, and a melting point of 350 °C (Figure 34).[34]

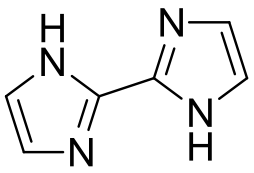

Figure 34. Structure of *2,2'*-biimidazole.

Biimidazole is named according to the same rules as imidazole with some additions. Biimidazole is assembled of two identical heterocycles, and is underlined by adding the prefix "bi-" to the name of the heterocyclic system. The assembly is then numbered according to the corresponding heterocyclic system; the first cycle is assigned to be unprimed and the second is primed (*2,2'*-biimidazole).

There are two methods to synthesize biimidazole. The most common method has been proposed by Fieselmann *et al.* where ammonia gas is bubbled through 20% glyoxal solution (Figure 35).[35]

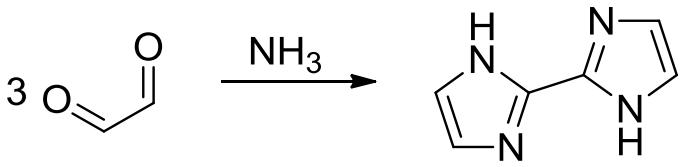

Figure 35. Scheme of biimidazole synthesis by Fieselmann method.

The yield of the reaction is 70%, but it is difficult to control the exact amount of ammonia gas which is toxic and it is always better to use safer methods of synthesis if possible. In 2003 Cho *at al.* proposed another method of synthesis of *2,2'*-biimidazole.[36] It has been proposed to use ammonia salts instead of ammonia gas (Figure 36). The temperature of the reaction should be kept in the range of 30-60°C, which produces the yield of 53.3%. This method is simple and safe and therefore is preferable to the first one.

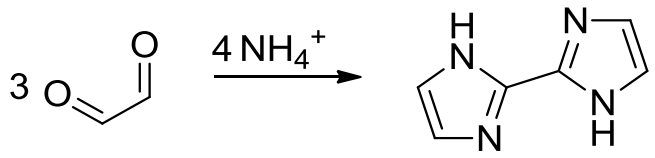

Figure 36. Scheme of biimidazole synthesis by Cho *at al.* method.

2,2'-biimidazole is a derivative of imidazole and therefore there are similarities in their chemical properties. Inherently, as imidazole-based compound biimidazole demonstrates aromaticity and results in substitution reactions. The ability to create hydrogen bonds gives the compound many possible uses, especially in coordination chemistry.[37]

Biimidazole has two isomers: *cis*- and *trans*-, which coordinate differently according to the structure (Figure 37). Murata *et al.* stated that 'the H-bond and coordination sites (nitrogen atoms) of 2,2'-H_2biim locate at the long sides of the molecular shape; therefore, interactions elongate along the molecular short axis, forming one-directional interactions'.[38]

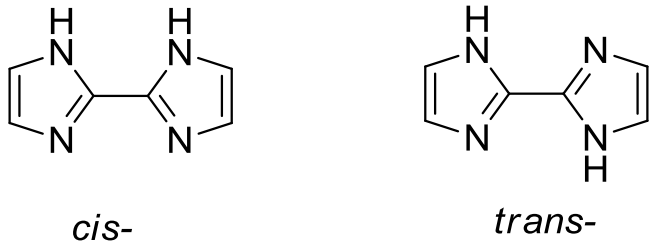

Figure 37. Biimidazole isomers.

In contrast to the nitrogen coordination sites the direction of H-bonding is determined by *cis/trans*-conformation of biimidazole, and by geometry of the coordination centre.[38] In *trans*-conformation biimidazole coordinates to two metal centers, forming one dimensional polymer in which hydrogen bonds are parallel to the direction of coordination, which connects complexes through counteranions (Figure 38, 1). In contrast, H-bonds in *cis*-conformation of biimidazole become antiparallel to the coordination direction and several types of coordination geometries are possible. When a linear coordination complex is formed, H-bonds are stretched parallel creating a one-dimensional structure (Figure 38, 2a). In a square-planar coordination complex two biimidazole molecules are chelating a metal center to form a one-dimensional structure, where polymer chains are connected to each other by bifurcated H-bonds with counteranions (Figure 38, 2b). In octahedral coordination complexes three biimidazole

molecules in cis-conformation chelating a metal center and three pairs of H-bonds form two-dimensional structure with D_{3h} symmetry (Figure 38, 2c).[38]

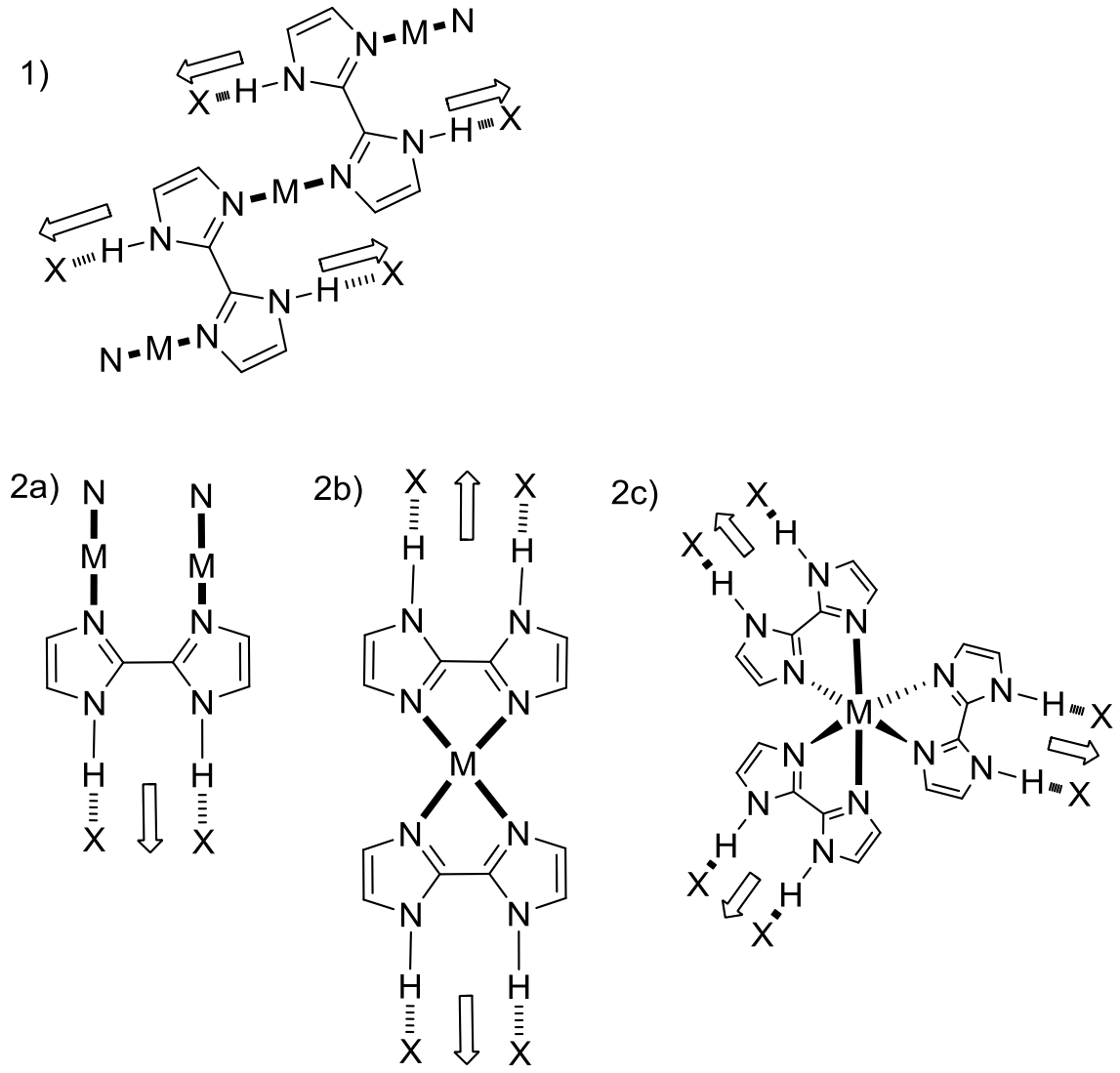

Figure 38. Geometry of biimidazole isomers: 1) *trans*-; 2a) *cis*- linear; 2b) *cis*- square-planar; 2c) *cis*- octahedral. M is metal, X is counteranion.[38]

9. APPLICATION OF BIIMIDAZOLE-BASED COMPOUNDS

Due to the possibility to form hydrogen- and π-bonds biimidazole-based coordination compounds have various applications.

1. In medicine

14.6% of all human deaths are caused by cancer. Nowadays there are more than 100 different known types of cancer and more than 500 genes involved in cancer formation.[39]

Cisplatin is now widely used as an anti-cancer agent (Figure 39). The mechanism of action of this agent is to violate the functions of DNA, causing chemical damage to DNA bases. DNA is damaged chemically by the formation of a coordination bond between the platinum atom and two DNA bases (preferably guanine), causing DNA to form intra- and inter-strand crosslinks. At the cellular level, cisplatin causes a disturbance of replication and transcription, leading to cell cycle delay and apoptosis.

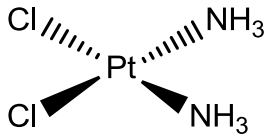

Figure 39. Cisplatin structure.

There are, however, a wide number of side-effects of cisplatin, such as nephrotoxicity, neurotoxicity, ototoxicity, myelosuppression, vomiting, and induction of nausea. Attempts to eliminate the side-effects of this drug led Casas *et al.* to synthesis $[PtCl_2(H_2bim)]$. This is a modification of the cisplatin: it is based on the platinum complex, but has biimidazole as a ligand instead of two ammonia ligands (Figure 40).[40] It has been found the complex interacts actively with DNA.[41] It has been also confirmed by Bloemink *et al.* that this complex is rather reactive with 5'-GMP or d(GpG), but it is not bioactive against L1210 leukemia and P388 leukemia.[41]

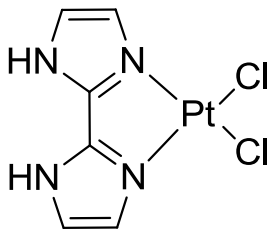

Figure 40. Structure of platinum complex with biimidazole ligand.[40]

However, it has been confirmed that $[PtCl_2(H_2bim)]$ modifies pBR322 plasmid DNA ditto cisplatin into possessing antiproliferative properties against the tumour cells.[42]

P. Alvarez Boo *et al.* used biimidazole derivative N-methyl-2,2'-bisimidazole as a ligand to synthesize $[SnR_2X_2(MBiim)]$ (MBiim=N-methyl-2,2'-bisimidazole; R=Me, Et, Bu, Ph;X=Cl or Br). This diorganotin(IV) are complexes of the type $SnR_2X_2(L—L)$, where L—L is a bidentate N-donor ligand, and possessed antitumour activity towards

P388 lymphocytic leukaemia cells. The activity has been caused by the low stability of the complexes of 2,2'-bisimidazole with certain transition metals.[43]

Tan *et al.* have also been searching for an agent with less toxicity and higher antitumor activity then cisplatin.[44] Attention has been paid to the ruthenium complexes due to their transferrin transportation, activation by reduction and targeting various biomolecules besides DNA. Biimidazole has been selected as a ligand since it has been used in the two important ruthenium anticancer complexes: NAMI-A ([ImH][trans-RuCl4(dmso-S)(Im)]) and ICR ([ImH][trans-$RuCl_4(Im)_2$]) (Figure 41). Therefore two biimidazole based complexes have been synthesized and characterized: *trans,cis,cis*-[$RuCl_2(DMSO)_2(H_2biim)$] (1) and *mer*-[$RuCl_3(DMSO)(H_2biim)$] (2) (Figure 42).

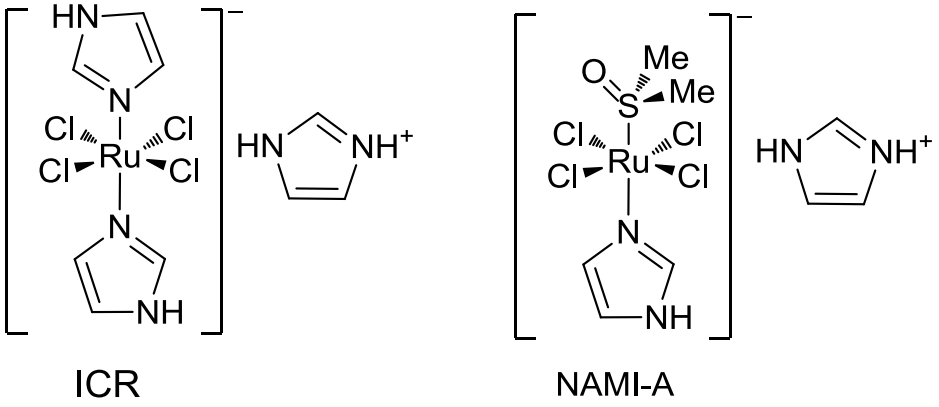

Figure 41. Structures of ICR and NAMI-A.[44]

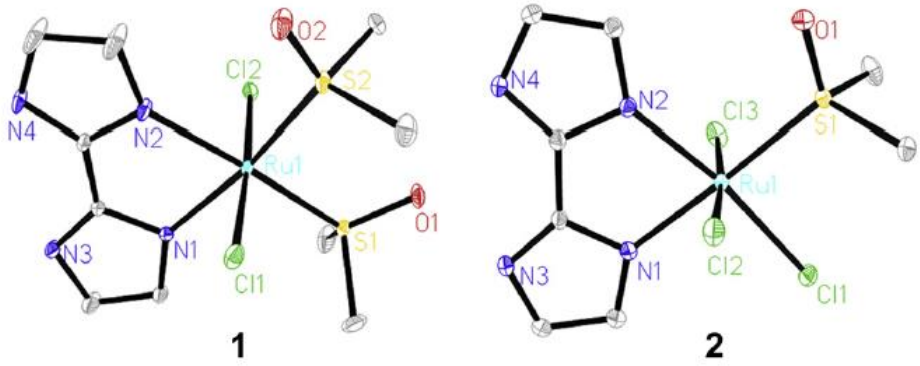

Figure 42. ORTEP drawings of structures of *trans,cis,cis*-[$RuCl_2(DMSO)_2(H_2biim)$] (1) and *mer*-[$RuCl_3(DMSO)(H_2biim)$] (2).[44]

According to cytotoxic potentialities cisplatin still possesses the highest cytotoxicity against four human tumor cell lines comparing to ICR, NAMI-A, and complexes 1 and 2, which is typical for ruthenium-based complexes compared to platinum-based. However, complex 1 had demonstrated higher cytotoxicity than NAMI-A, but lower

than ICR, and due to the low water solubility complex 2 exhibits higher cytotoxicity than ICR. Complexes 1 and 2 demonstrated induction of mitochondria-mediated apoptosis and G0/G1 phase cell cycle arrest. Complex 2 inhibits cell metastasis by reducing cancer cell migration and increasing cell adhesion, and therefore, coth Complex 2 and NAMI-A could be used as anti-metastatic drugs. DNA binding ability has been found to be almost equal for both 1 and 2 complexes; both 1 and 2 could be considered as potential CDK (cyclin-dependent kinase) inhibitors. The authors proposed the best target for complexes 1 and 2 are protein kinases.[44]

Another attempt to find anticarcinogen that can recognize and cleave DNA has been done by Yanping *et al.*[45] Copper has been known as a bioactive element, and copper complexes have been involved in important biological processes. Due to the possibility of different interactions biimidazole that inhibit tumor growth by interacting with DNA.[45] Therefore a novel binuclear copper(II) complex $[Cu_2(1,1'\text{-dimethyl-}2,2'\text{-biimidazole})_4(H_2O)_2](ClO_4)_4 * 6H_2O$ has been synthesized (Figure 43).

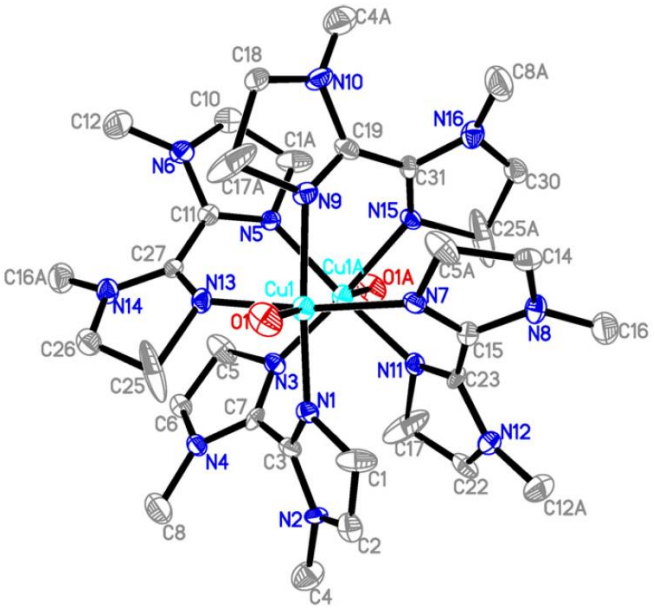

Figure 43. $[Cu_2(1,1'\text{-dimethyl-}2,2'\text{-biimidazole})_4(H_2O)_2]^{4+}$ crystal structure.[45]

Researchers have studied the interaction between DNA and copper(II) complex by electronic absorption spectroscopy, fluorescence spectroscopy, viscosity measurement, and voltammetry. It has been found that DNA interacts with copper(II) complex by minor groove binding, and in the presence of AH_2 (ascorbic acid) the complex can efficiently cleave DNA plasmids (Figure 44).

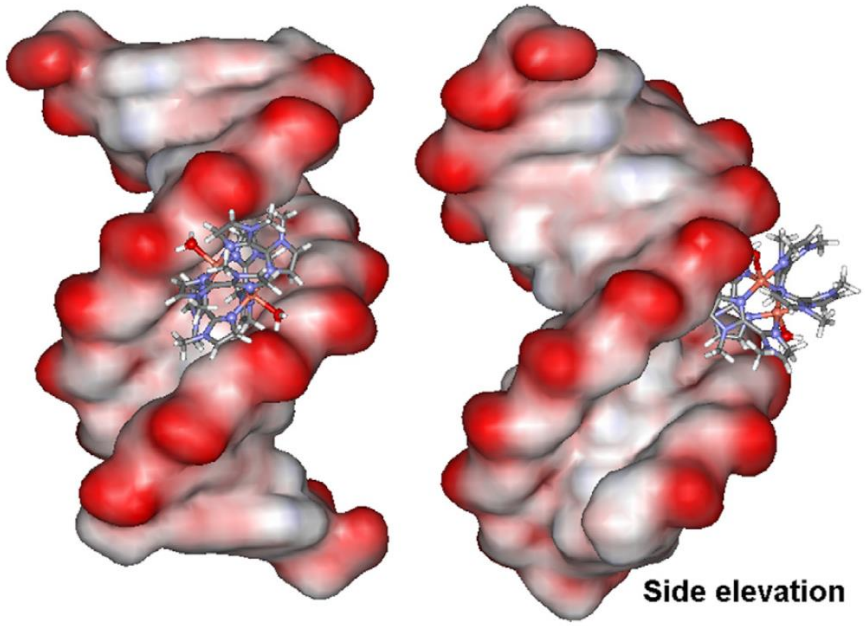

Figure 44. The binding model of copper(II) complex-DNA interactions (left picture) and its side elevation (right picture) showing the complex inserts and stays at the DNA minor groove.[45]

2. In supramolecular chemistry

M.Liu *et al.* studied metal-H_2Biim framework structures containing 4,4'-bipyridine or malonic acid as a co-ligand since these ligands are well known as promising bridging ligands for to synthesizing innovative functional supramolecular complexes.[33] Six new M(II)–H_2Biim complexes have been synthesized by the reactions of transition metal(II) salts with chelate 2,2'-biimidazole ligand and co-ligands in the mixed solvent of methanol/water: $[M(H_2Biim)_2(bipy)_2](NO_3)_2*2H_2O$ (1–3) (M= Co, Ni , Zn), $[Co(H_2Biim)_2(bipy)](ClO_4)_2*3H_2O$ (4), $\{[Cu(H_2Biim)_2]_3(\mu\text{-}C_3H_3O_4)_2, (C_3H_2O_4)_2\}*6H_2O$ (5), $[Co(H_2Biim)_2(H_2O)_2](C_3H_3O_4)_2$ (6) (Scheme 1).[33]

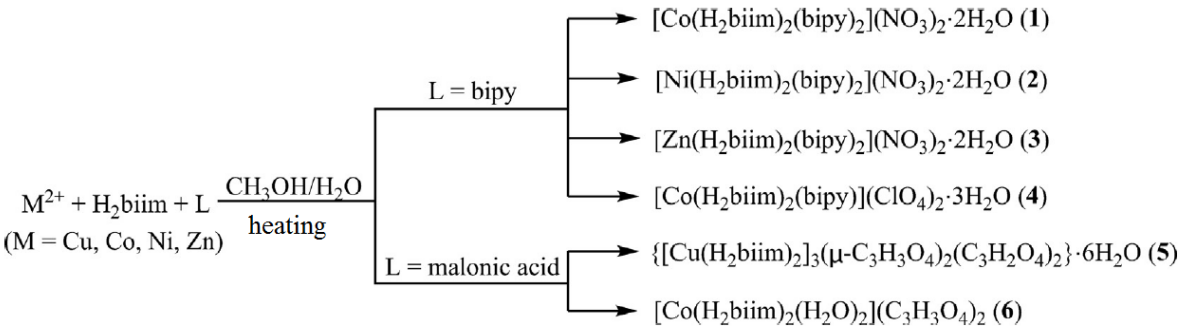

Scheme 1. The synthesis routine of M(II)–H_2Biim complexes.[33]

Complexes 1-3 have similar supramolecular architectures: through N–H···O and O–H···O hydrogen bonds NO_3^- and H_2O attached straight to the H_2Biim moiety $[M(H_2Biim)_2(bipy)_2]^{2+}$ (M = Co, Ni, Zn), forming a step-like chain from mononuclear fragments due to hydrogen bonding. Due to the pyridyl rings, π-π interactions 2D network forms from these chains, whilst 3D entanglement is formed by crossed (4,4) sheets (Figure 45).

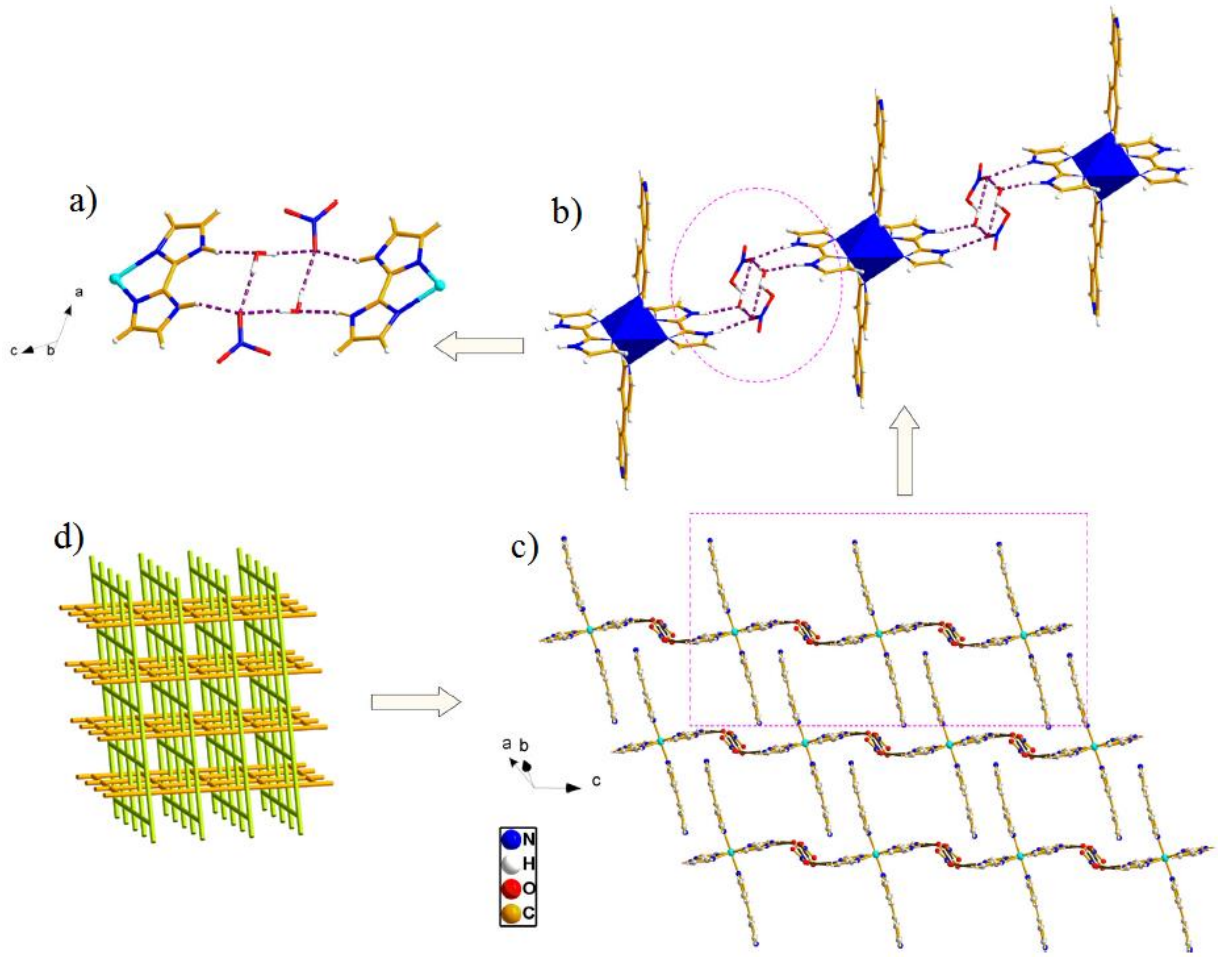

Figure 45. Structure of $[M(H_2Biim)_2(bipy)_2](NO_3)_2*2H_2O$ complexes: a) mononuclear fragment formed by hydrogen bonding between NO_3^- and H_2O ; b) mononuclear fragment linked together by hydrogen bonding to a step-like chain; c) 2D network formed by pyridyl rings π-π interactions; d) 3D entanglement.[33]

In complex 4 ($[Co(H_2Biim)_2(bipy)](ClO_4)_2*3H_2O$) two H_2Biim and two 4,4'-bipyridine ligands are coordinated through nitrogen atoms on Co(II) in a distorted octahedral geometry (Figure 46, a). Co(II) ions are linked together into the cationic chain by 4,4'-bipyridine ligands (Figure 46, c). Multiple hydrogen bonds N–H···O and O–H···O are

made between perchlorate anions/water molecules and H_2Biim N–H donors/H_2O O-H groups (Figure 46, b). The cationic chains of $([Co(H_2Biim)_2(bipy)]^{2+}$ connected by multiple hydrogen bonds create 3D porous framework that contains cavities of 23*23 Å (Figure 47, Figure 48).

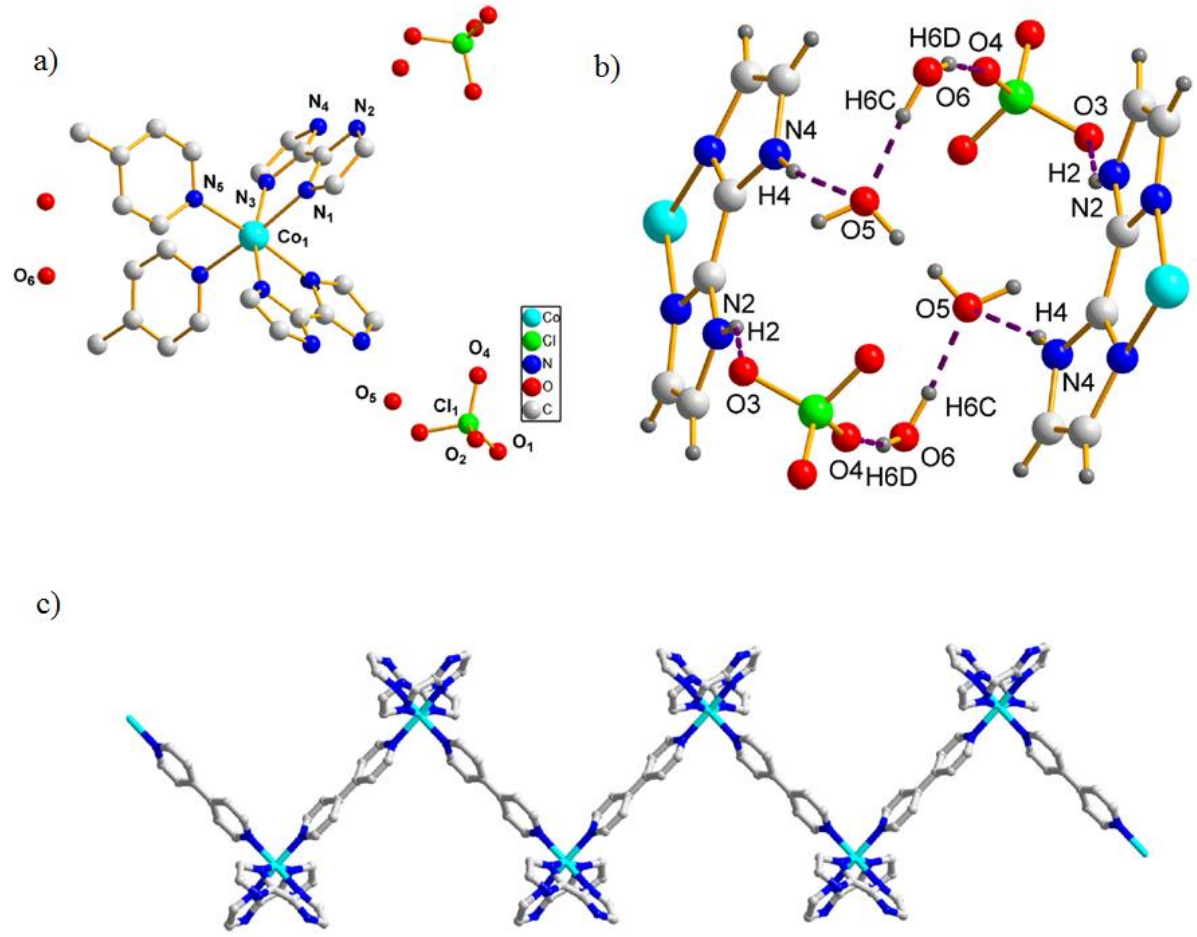

Figure 46. Structure of: a) $([Co(H_2Biim)_2(bipy)](ClO_4)_2*3H_2O)$; b) hydrogen bonds N–H···O and O–H···O connecting mononuclear fragments; c) Co(II) cationic chain.[33]

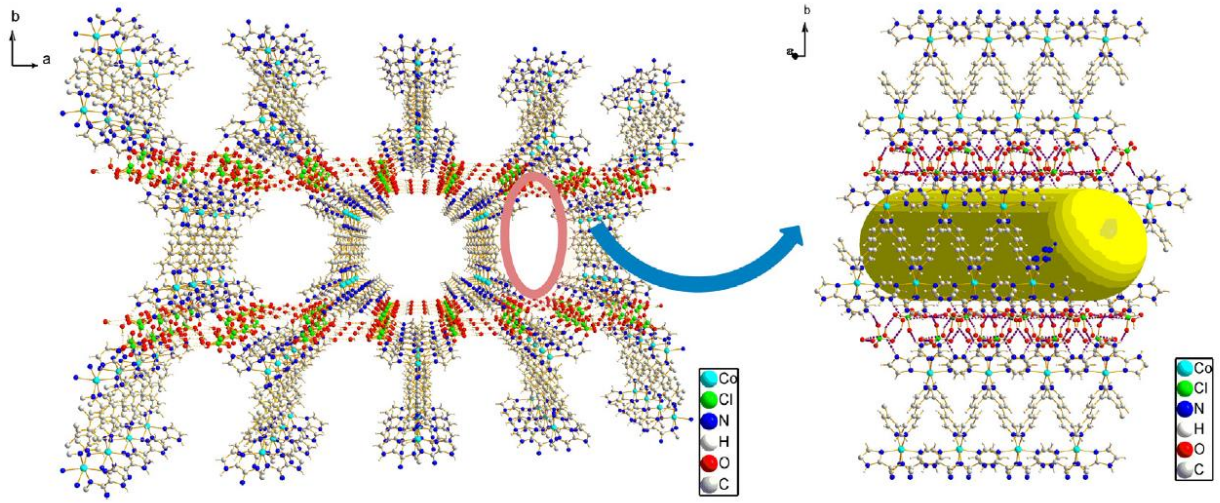

Figure 47. Perspective view of packing diagram along c-axis and view of the 3D porous network in complex 4.[33]

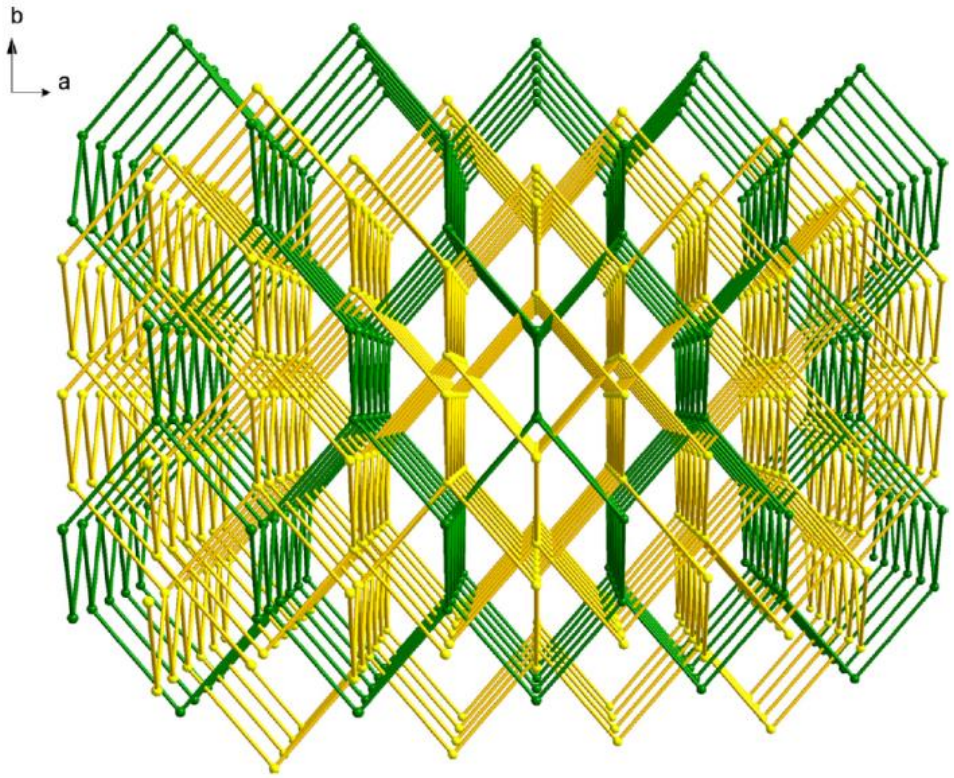

Figure 48. Complex 4 topology networks.[33]

In complex 5 ({[Cu(H_2Biim)$_2$]$_3$(μ-$C_3H_3O_4$)$_2$, ($C_3H_2O_4$)$_2$}*6H_2O) a trinuclear entity is created by the connection of the [Cu(H_2Biim)$_2$]$^{2+}$ with two units of [Cu(H_2Biim)$_2$($C_3H_2O_4$) by two malonate anions bridging in an end-to-end manner (Figure 49). Hydrogen bonds between N–H donors of [Cu(H_2Biim)$_2$]$^{2+}$ and the oxygen

atom of malonate anions/dianions creates a 3D network that fixes a water pipe, cyclic water hexamer, which is made up of six water molecules (Figure 50). Due to π-π interactions between parallel oriented imidazole rings 3D structures have been stabilized.

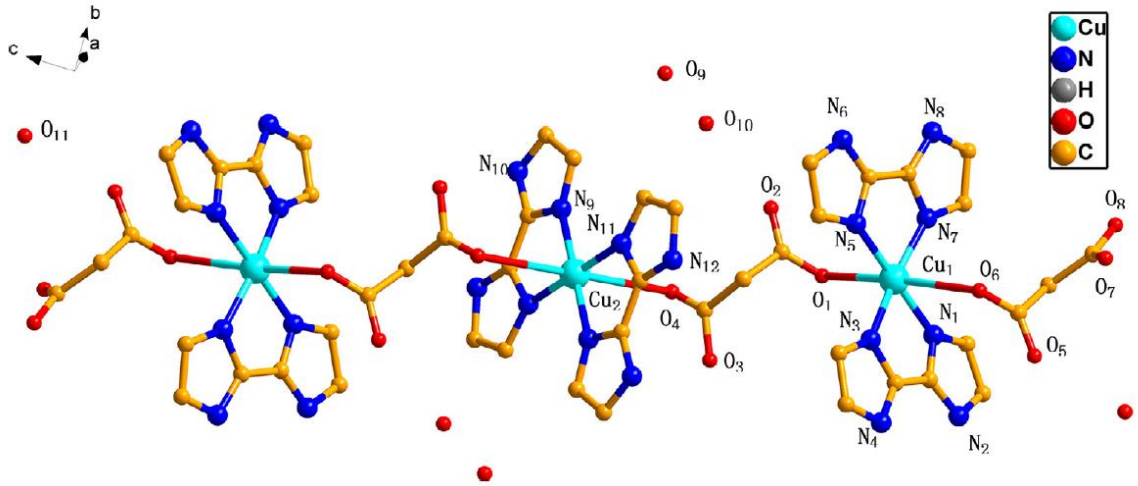

Figure 49. Structure of {[Cu(H_2Biim)$_2$]$_3$(μ-$C_3H_3O_4$)$_2$, ($C_3H_2O_4$)$_2$}*6H_2O (complex 5).[33]

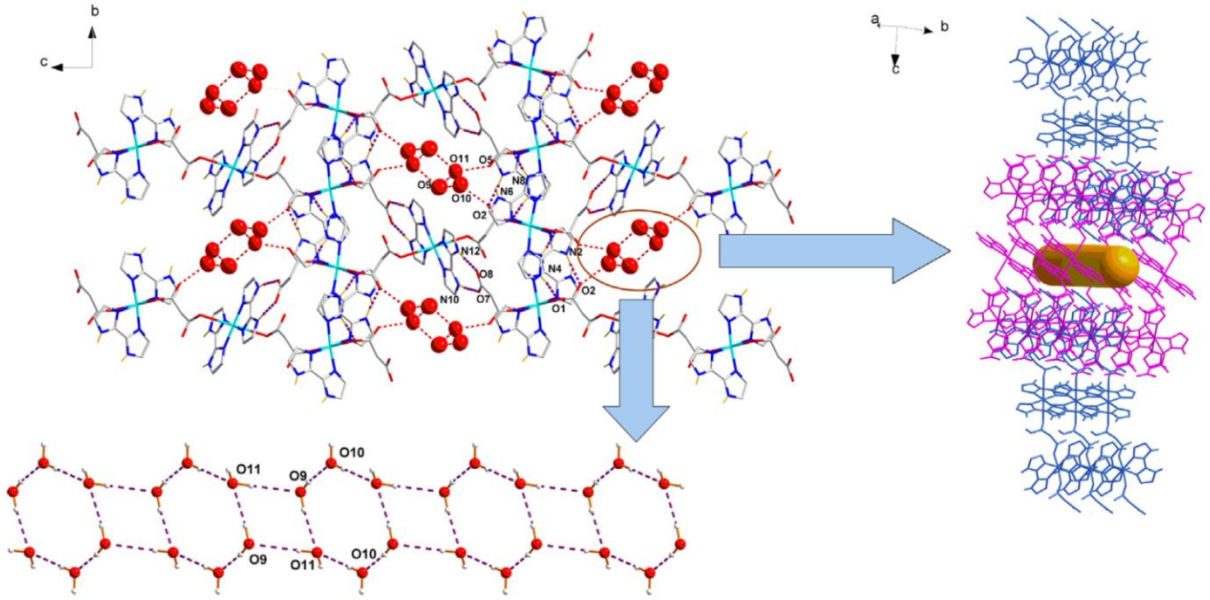

Figure 50. Perspective view of complex 5 and 3D porous network with water cluster pipe.[33]

In complex [Co(H_2Biim)$_2$(H_2O)$_2$]($C_3H_3O_4$)$_2$ (6) [Co(H_2Biim)$_2$(H_2O)$_2$]$^{2+}$ moiety is created by two bidentate H_2Biim ligands coordinated to Co(II) through N atoms being located in equatorial positions, whilst two water molecules are coordinated into axial positions through O atoms. This moiety results in malonate anions becoming attached

through N–H···O hydrogen bonds with H_2Biim and O–H···O hydrogen bonds with a water molecule, so an acid–water ring is formed (Figure 51). Therefore, a 2D (4,4) network structure is created by π-π interactions between parallel oriented imidazole rings, resulting in the formation of a 3D framework (Figure 52).

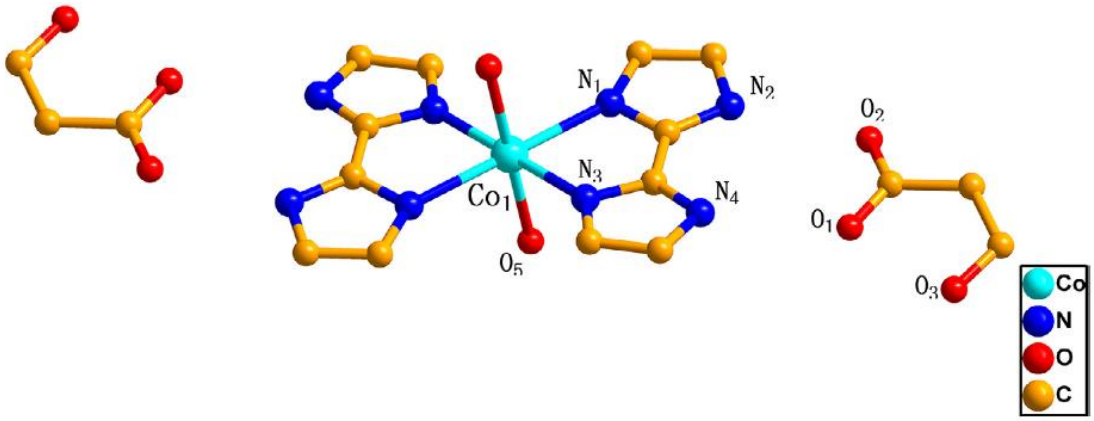

Figure 51. Structure of $[Co(H_2Biim)_2(H_2O)_2](C_3H_3O_4)_2$ (complex 5).[33]

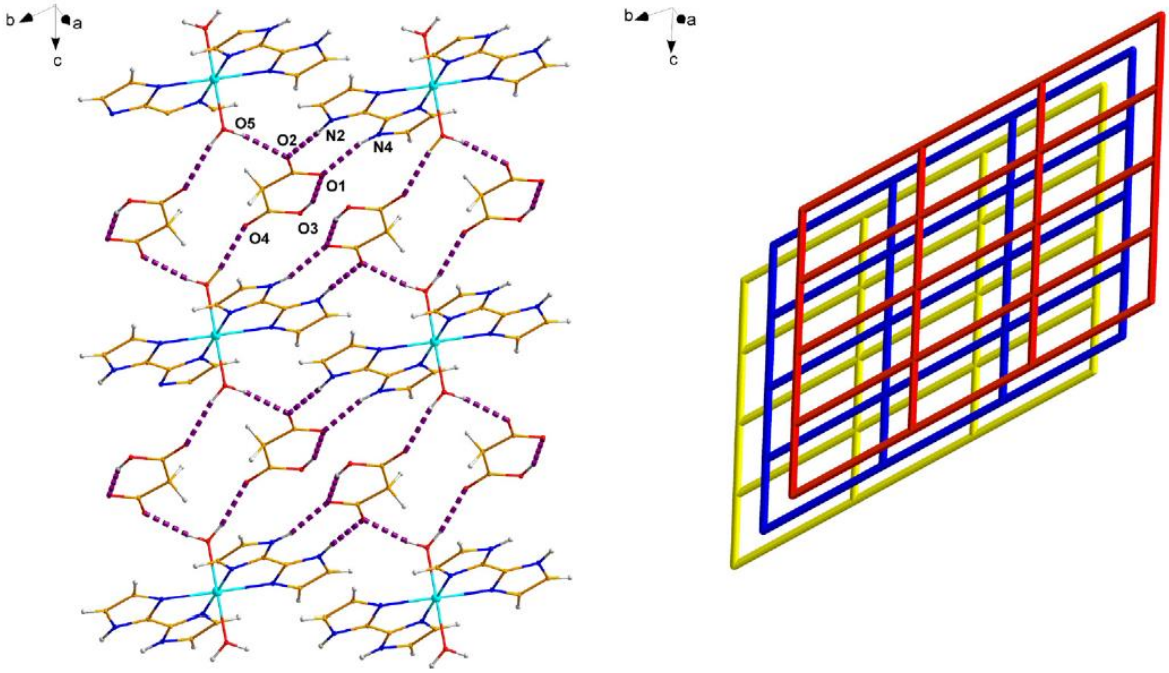

Figure 52. The 2-D hydrogen-bonded net and the (4,4) topology networks of complex 6.[33]

Because of the H_2Biim intraligand π-π' transition described, the complexes possessed luminescent properties.

Fitchett *et al.* had been cattying out research to find a ligand similar to the carboxylate group, which has a binding mode, that permits the bridging of metals in close proximity, depending on the anions.[46] A derivative of biimidazole N,N′-dimethylene-2,2′-biimidazole has been found to be an analogue of carboxylate ligand (Figure 53).

a) carboxylate ligand b) N,N'-dimethylene-2,2'-biimidazole

Figure 53. Structure of carboxylate (a) and N,N′-dimethylene-2,2′-biimidazole (b) ligands.[46]

It has been used as a building block for the formation of supramolecular complex with weakly coordinated metals, particularly in silver and copper. It was found that the ligand is a nearly coplanar biheterocycle that bridges two silver atoms and, due to the narrow chelating angle, potential chelation is restricted while twisting is allowed.[46] Due to the fact that structures of complexes of Cu(I) carboxylates have not been widely investigated, authors decided to investigate N,N′-dimethylene-2,2′-biimidazole ligand complexation with Cu(I) as an analogue of carboxylate. After the reaction of the ligand and $Cu(CH_3CN)_4BF_4$ in hot acetonitrile, ligand bridging complex was obtained (Figure 54).

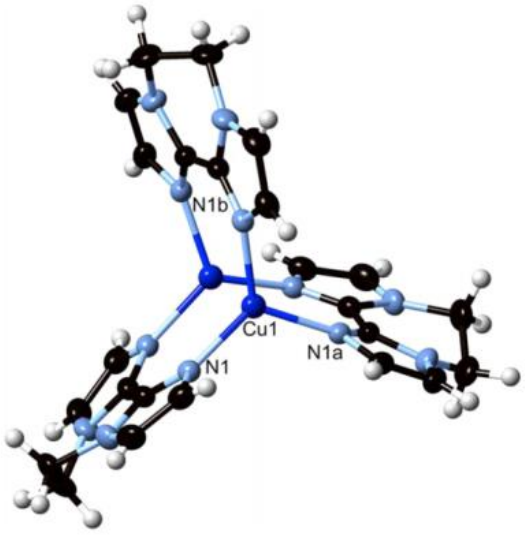

Figure 54. Structure of Cu(I) complex with N,N′-dimethylene-2,2′-biimidazole ligands.[46]

Furthermore, $Cu(PPh_3)_2NO_3$ and N,N′-dimethylene-2,2′-biimidazole have been used to synthesize supramolecular pockets made of three triple helicate subunits (Figure 54) that efficiently capture benzene through edge-to-face π–π interactions (Figure 55). It was found that in order to produce supramolecular pockets, a properly sized aromatic guest is needed (benzene or fluorobenzene) as well as an anion with a three-fold axis (BF^{4-}, ClO^{4-}, or NO^{3-}).[46]

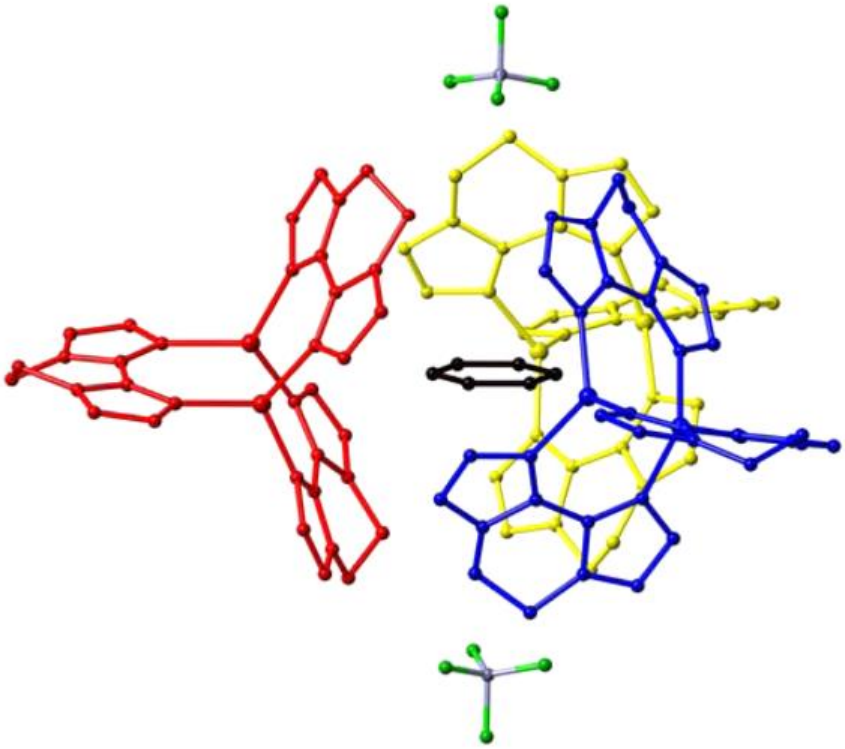

Figure 55. Supramolecular pocket surrounding a molecule of benzene.[46]

$\{P_5W_{30}\}$-based organic–inorganic hybrid compounds have interested researchers due to their potential use as efficient and eco-friendly catalysts.[47] This type of compounds have been used as catalysts in the air oxidation of thiols to disulfides, esterification of organic acids, and the oxidation of pyridine carboxylic acids or aromatic aldehydes. $[P_5W_{30}O_{110}]^{15-}$ is a Preyssler-type polyoxometalate (POM) anion which has a crown ether-like structure, and is able to capture the cations of appropriate-size cations (alkali and alkaline-earth metal cations, lanthanide and actinide cations). Further study of the interactions between organic molecules and the surface of oxides has aimed to obtain recyclable multifunctional catalysts. Polyoxometalate clusters modified by 2,2′-biimidazole have been synthesized and investigated by Yang *et al.*[47] Being a nitrogen donor ligand, 2,2′-biimidazole has been used to prepare new Preyssler-type polyoxotungstophosphates:

$[Mn(H_2biim)_3]_5H_2[\{Mn(H_2biim)_2(H_2O)\}(NaP_5W_{30}O_{110})]*39H_2O$ (1), $[\{(H_2biim)_2Zn(\mu\text{-}OH)Zn(H_2biim)(\mu\text{-}H_2biim)Zn(H_2biim)(H_2O)\}_2H_4(NaP_5W_{30}O_{110})]*22H_2O$ (2), and $\{(H_4biim)_{18}NaH_5[\{\mu\text{-}Fe(H_3biim)(H_2O)_3\}\{\mu\text{-}Fe(H_2O)_4\}(NaP_5W_{30}O_{110})_2]_2*78H_2O\}_n$ (3). It was shown that various electrophilic metal ions (e.g., Mn^{2+}, Zn^{2+} or Fe^{3+} ions) can be coordinated to Preyssler-type $\{P_5W_{30}\}$-based anions. In these complexes H_2biim displays three different types of coordination modes.

Compounds 1 and 2 have an 0-D structure and are constructed by mono- and bi-supporting Preyssler-type anions respectively. Compound 1 has different coordination environments of manganese centers: Mn1 is six-coordinated by four nitrogen atoms from two H_2biim molecules, one terminal oxygen atom from a $\{P_5W_{30}\}$ unit, and one water ligand, while Mn2 and all other Mn centers are six-coordinated by the six nitrogen atoms from three H_2biim molecules (Figure 56). Compound 3 has 1-D structure; it represents infinite 1-D zigzag chains (Figure 58). Compound 2 has two symmetrical trinuclear zinc-H_2biim complex cations (Figure 57).

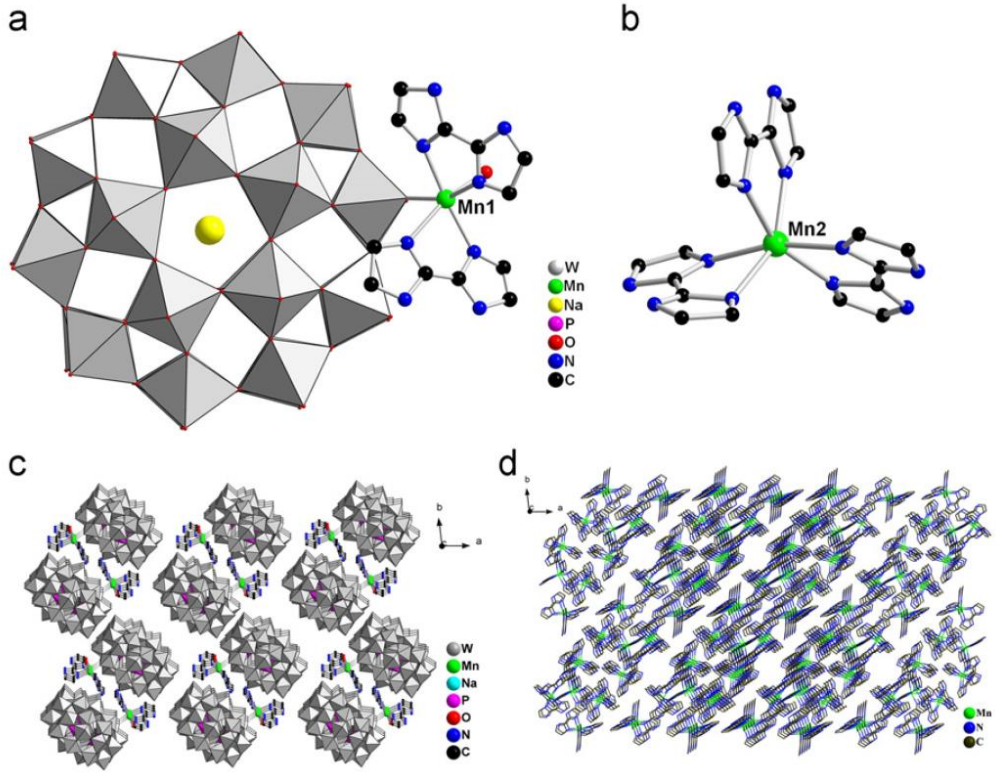

Figure 56. The structure of compound (1): (a) ball-and-stick/polyhedral view of the mono-supporting $[Mn(H_2biim)_2(H_2O)(NaP_5W_{30}O_{110})]^{12-}$ anion; (b) ball-and-stick view of the isolated $[Mn(H_2biim)_3]^{2+}$ cation; (c) packing arrangements of the $[Mn(H_2biim)_2(H_2O)(NaP_5W_{30}O_{110})]^{12-}$ anions; (d) packing arrangements of the $[Mn(H_2biim)_3]^{2+}$cations in the same direction.[47]

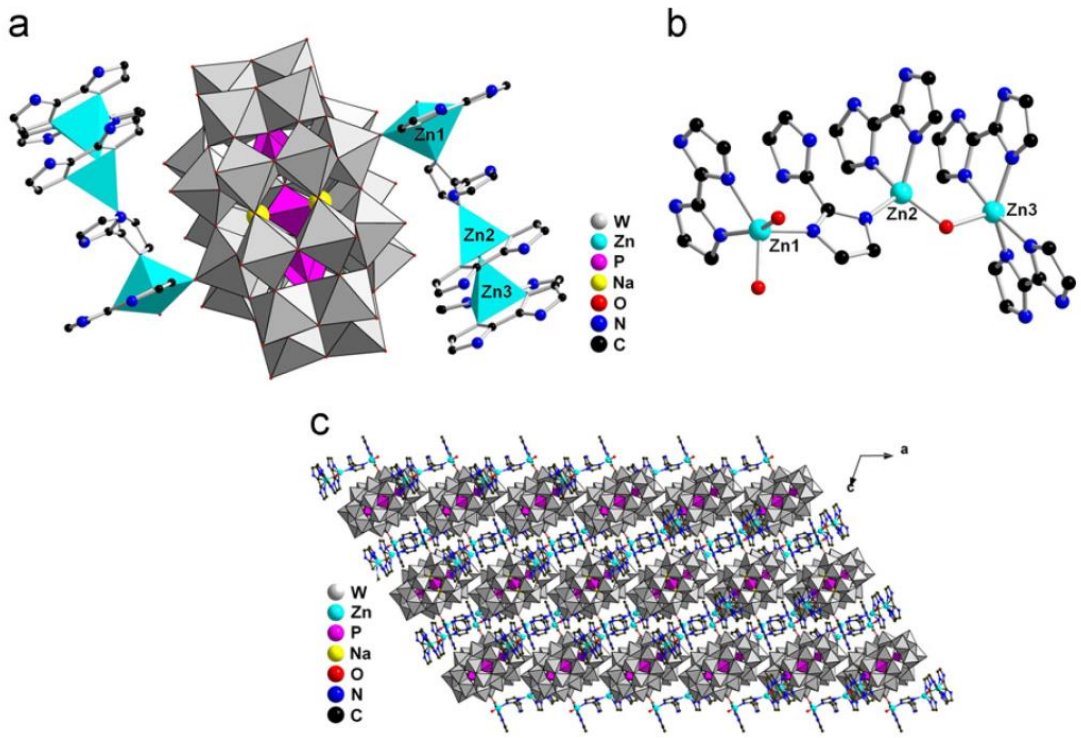

Figure 57. The structure of compound (2): (a) ball-and-stick/polyhedral view of the asymmetric unit; (b) ball-and-stick view of the trinuclear zinc complex unit; (c) polyhedral and ball-and-stick view of the 3-D supramolecular framework.[47]

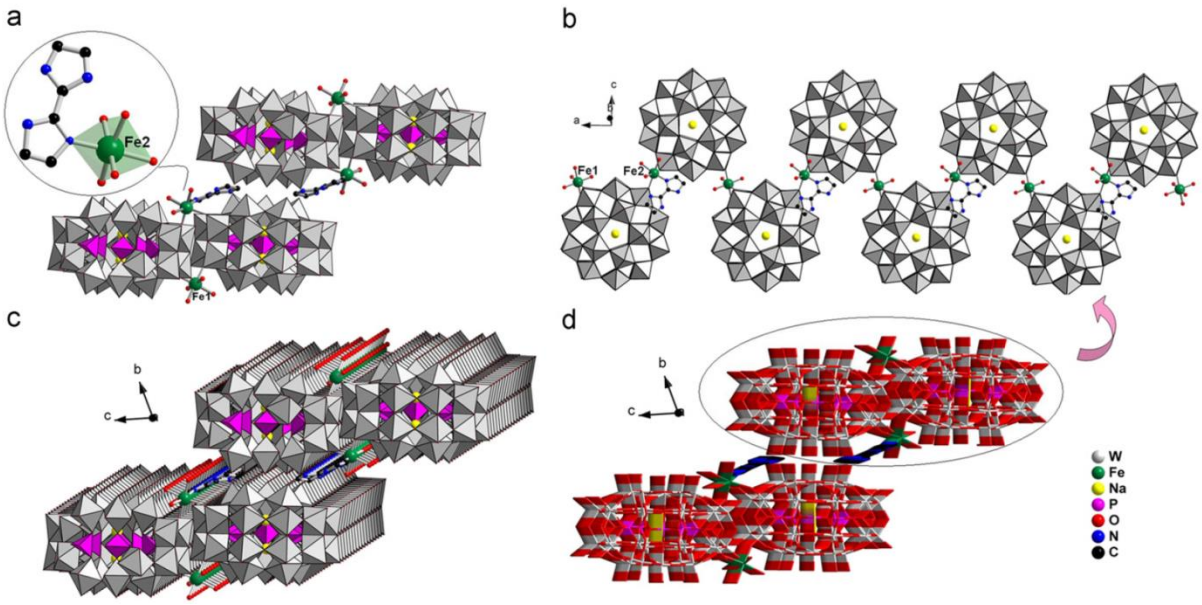

Figure 58. The structure of compound (3): (a) ball-and-stick/polyhedral view of the asymmetric unit and the coordination site of the Fe^{3+} ion; (b) the1-D zigzag chain; (c) polyhedral and ball-and-stick view of the 3-D supramolecular framework; (d) wire/stick representation of the packing arrangements.[47]

Transition metal-H_2biim complexes stabilize compounds through strong hydrogen bond interactions. Obtained compounds display higher thermal stabilities, and great electrocatalytic activities toward the reduction of H_2O_2. It has been found that compound 3 has better catalytic activity compared to compounds 1 and 2 for the oxidation of cyclohexanol to cyclohexanone. In conclusion, obtained compounds could be used as novel catalysts which could be recycled and reused without loss of their catalytic activities.

Due to the ability to produce organometallic complexes and supramolecular ensembles 2,2' -biimidazole moiety was used in a five-steps synthesis to prepare a novel crown ether-based structure, with the possible application as an anion sensor.[48] This macrocyclic structure has been investigated by X-ray diffraction (Figure 59) and supramolecular channels (Figure 60) have been found.

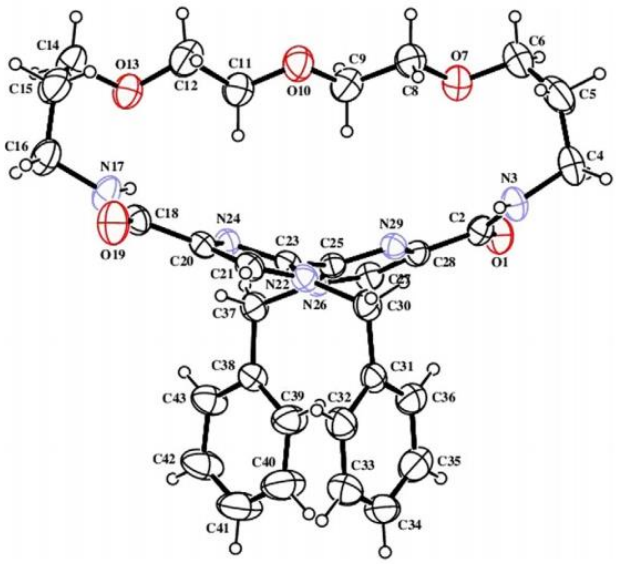

Figure 59. Molecular structure of crown ether incorporating 2,2′-biimidazole.[48]

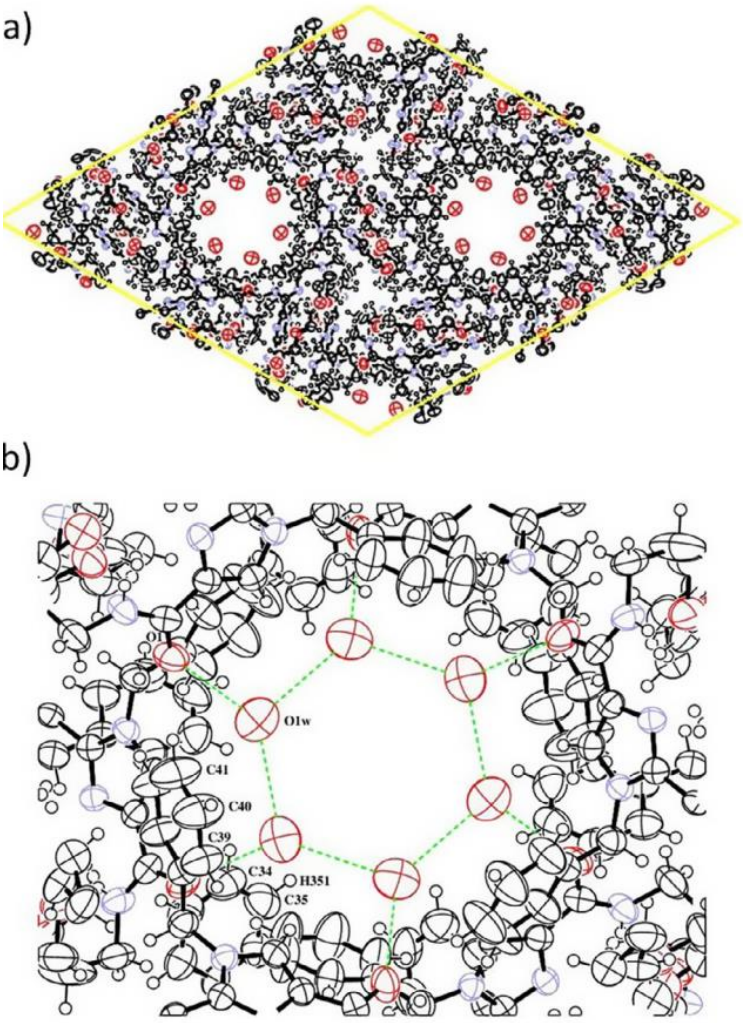

Figure 60. Supramolecular channels: a) view of the unit cell contents down the *c* axis. b) detailed view of a channel down the *c* axis. Dashed lines indicate possible hydrogen bonds.[48]

Through a minimal reorganization of the receptor *syn*- geometry, the anion affinities and selectivity are improved (Figure 61). Anion receptor properties of N-dibenzylated derivative receptor have also been studied, and binding constants for 1:1 biimidazole–anion complexation (Kassoc) have been found on the order of 10^5 M^{-1} for $H_2PO_4^-$ and Cl^-. Therefore, the complexing capacity of the receptor is improved by inducing of *syn*-conformation of the macrocycle.

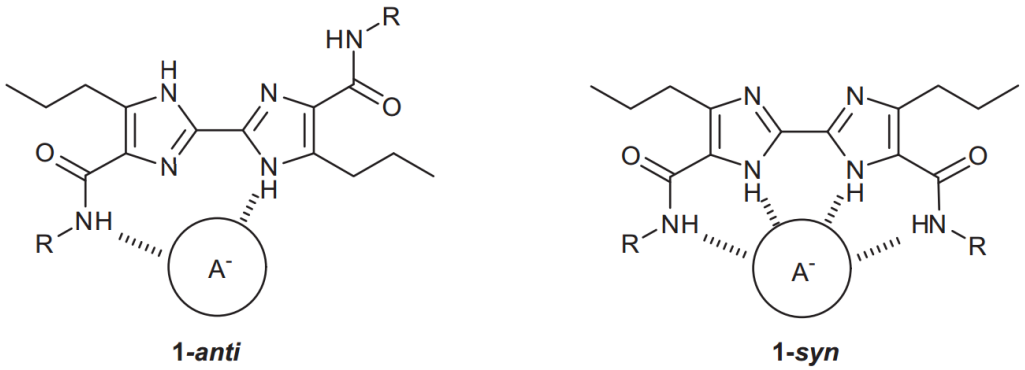

Figure 61. *Anti*- and *syn*- conformers of biimidazole–anion complexes.[48]

3. In coordination chemistry

Fortin *et al.* have chosen biimidazole as a ligand for a coordination reaction with previously synthesized precursors $ReOX_3(PPh_3)_2$ and $ReO(OEt)X_2(PPh_3)_2$.[49] H_2Biim has interested researchers because it could be used as a building block for polymetallic complexes due to the fact of being a bis-bidentate ligand when deprotonated. Therefore, *cis*-/*trans*- cationic complexes of Re (III) were synthesized to give $[ReX_2(PPh_3)_2(H_2Biim)]X$ (where X = Cl, Br, and I). However, the complexes behaved differently to N,N'-dimethyl analog (Me_2biim). The reason for this is that N-H groups in H_2Biim complexes form hydrogen bonds and fix anion by it, whilst the monodentate H_2Biim intermediate anion has been expected to be displaced from the coordination sphere (Figure 62).

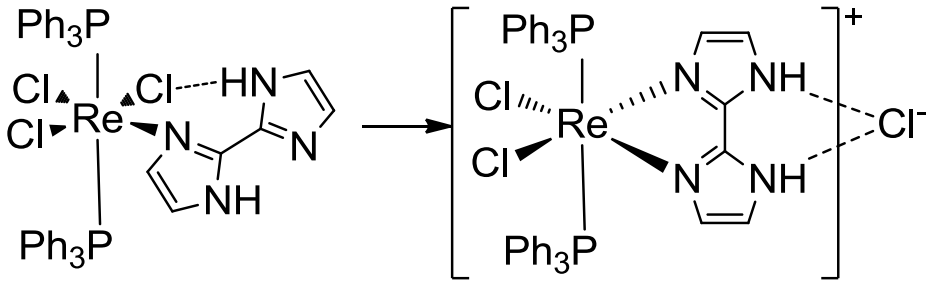

Figure 62. Displacement of an anion by H_2Biim.[49]

This assumption was further supported by an experiment in which a complicated mixture of different unidentified Re(V) (diamagnetic) and Re(III) (paramagnetic) compounds was obtained and investigated by NMR spectroscopy. It was found H_2Biim had been stabilized by the intramolecular N-H···Cl hydrogen bond, and the metal-

chloride bond had been breaking down releasing chloride, and bringing H_2Biim nitrogen donor to the coordination position.

During the experiment, ion pairing in solid and liquid states has been studied for the complexes obtained. It is important to study this since ion pairing could influence physical or chemical properties of both solutions or solid state of compound. According to the crystal structures, ion pairing has been confirmed for the solid state (Figure 63 and Figure 64). According to the variable-temperature ^{1}H NMR experiment it has been confirmed for the solution: at room temperature, the fast exchange between the two kinds of ion pairs has been shown by one set of H_2Biim signals at averaged positions. When lowering temperature exchange inhibits, these signals increasingly broaden, and around 225 K coalescence has been detected. At the temperature lower than 225 K two sets of H_2Biim signals has been detected, showing the ion pairs last as two separate entities for a long time on the NMR time scale. [49]

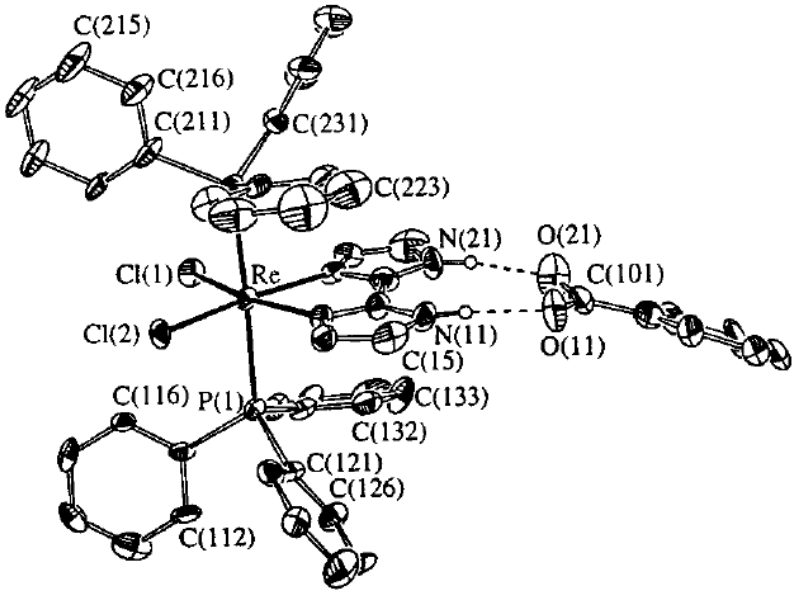

Figure 63. Crystal structure of [$ReCl_2(PPh_3)_2(H_2Biim)$](benzoate).[49]

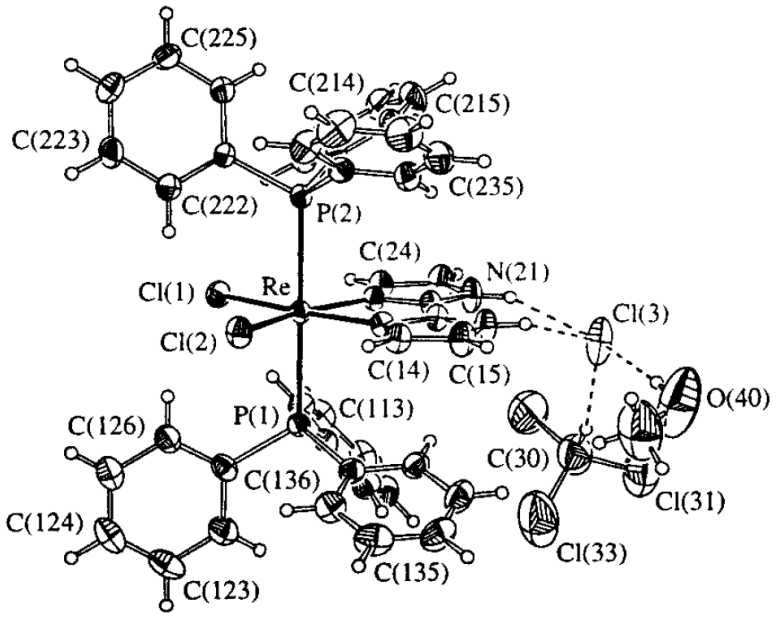

Figure 64. Crystal structure of $[ReX_2(PPh_3)_2(H_2Biim)]Cl*CH_3OH*CHCl_3$.[49]

However, for the $[ReCl_2(PPh_3)_2(H_2Biim)]$(benzoate) it is not clear whether carboxylate remains ionic (Figure 65, 1) or stays neutral (Figure 65, 2). Neither NMR nor X-Ray methods could solve this problem since the exchange between tautomeric forms is fast. The problem has, however, been solved by UV-visible spectroscopy: the spectra of $[ReX_2(PPh_3)_2(H_2Biim)]^+$ and its derivatives $[ReX_2(PPh_3)_2(HBiim)]$ and $[ReX_2(PPh_3)_2(Biim)]^-$ are different.

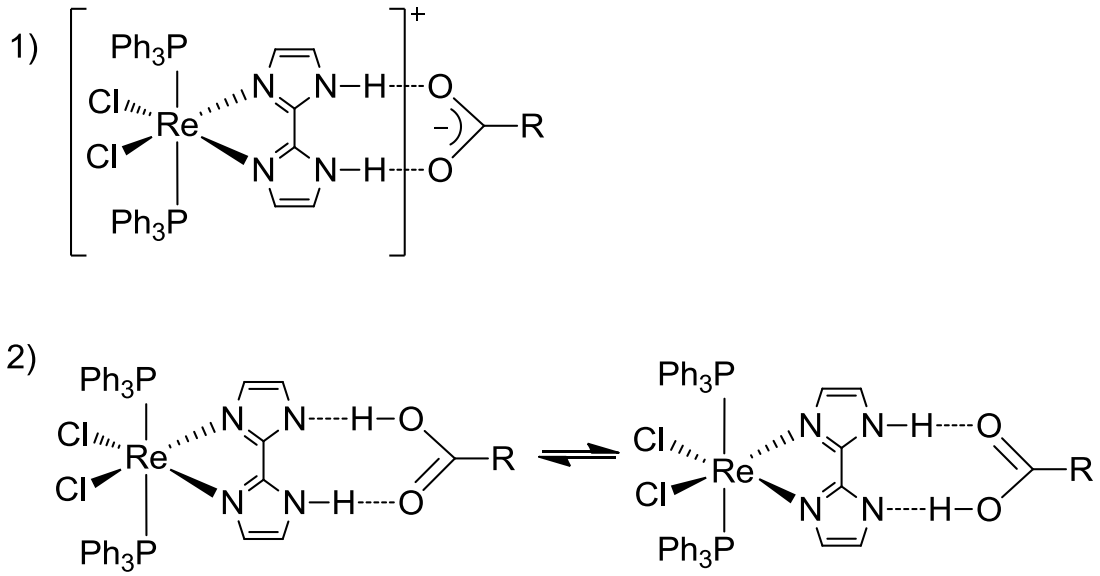

Figure 65. $[ReCl_2(PPh_3)_2(H_2Biim)]$(benzoate) possible structures: 1) ionic; 2) neutral.[49]

It was established, that if the carboxylic acid is weaker than H_2Biim, N-H proton association includes complementary N···H-O and N-H···O hydrogen bonds (Figure 65,

2). Both H_2Biim N-H groups could be deprotonated if treated with moderately strong base, for example $NaOCH_3$, and when deprotonated they could be used as a great building block for biimidazole-bridged bimetallic systems.

Due to the remarkable properties of N,N′-bis(ethylacetate)biimidazole a derivative of H_2Biim has been chosen as a ligand for the terbium complex.[50] Tb^{3+}-based complexes have attracted scientists as a promising visible luminescence material with a strong green emission. The fact is a low molar absorption coefficient for forbidden f–f transitions makes unfavorable direct excitation of the terbium ions. To overcome this fact, energy transfer from Tb^{3+} centers could be done by π-conjugated organic chromophores, for example, imidazole-based and multicarboxylate-based. Therefore N,N′-bis(ethylacetate)biimidazole is a perfect candidate for the aims described above. Nitrogen and oxygen atoms in this molecule can form coordination polymers by coordinating to metal ions, and according to coordination orientation steric hindrance could be lessened by the rotation of the $–CH_2–$ group.

Zhang *et al.* have synthesized novel 2D lanthanide–organic framework $\{[Tb_3(L)(\mu_3\text{-}OH)_7]\cdot H_2O\}_n$ with promising luminescence properties, which could have application as new green light emitting material.[50] $\{[Tb_3(L)(\mu_3\text{-}OH)_7]\cdot H_2O\}_n$ crystallized in the monoclinic space group, $P2_1/c$ and an asymmetric unit of it contains three independent Tb^{3+} ions, coordinated ligand, eleven μ_3-OH groups, and one free water molecule.[50] Tb1 center is eight-coordinated in a distorted bi-capped trigonal prismatic geometry arrangement by seven hydroxyl oxygen atoms and one carboxylic oxygen atom from the ligand. Tb2 and Tb3 metal centers form a distorted bi-capped trigonal prismatic [TbO8] as a result of the coordination of seven oxygen atoms from μ_3-OH groups and one carboxylic oxygen atom. The Tb1 atom is linked to two other terbium atoms (Tb3, Tb2) into a triangular [Tb3O19] unit by oxygen atoms from μ_3-OH groups (Figure 66).

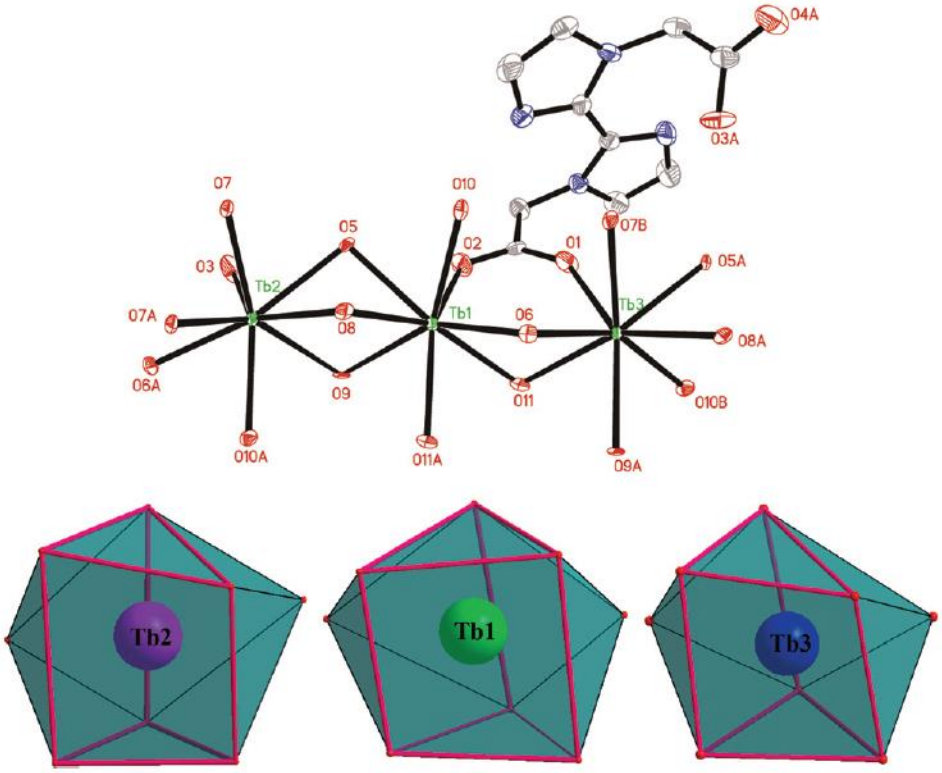

Figure 66. The coordination environment of Tb^{3+} ion in the coordination polymer 1 and the corresponding coordination polyhedron of Tb^{3+} ions in coordination polymer 1 (Tb1 for green spheres; Tb2 for pink spheres, and Tb3 for blue spheres).[50]

Furthermore, –M–O–M– infinite one-dimensional chains are formed by the connection of Tb^{3+} ions and hydroxyl groups, and a six-membered ring has formed when hydroxyl groups connect each Tb3 metal center with three Tb1 and three Tb2 metal centers in different directions (Figure 67). In addition, every Tb1 and Tb2 has been connected via hydroxyl groups with the surrounding six metal centers, prolonging the structure into a 2D layer along the bc plane. This framework has a distorted $CdCl_2$ type structure whereas Tb^{3+} ions and hydroxyl groups being decorated with ligand presented a rare 2D connectivity - N-heterocyclic coordination polymers.

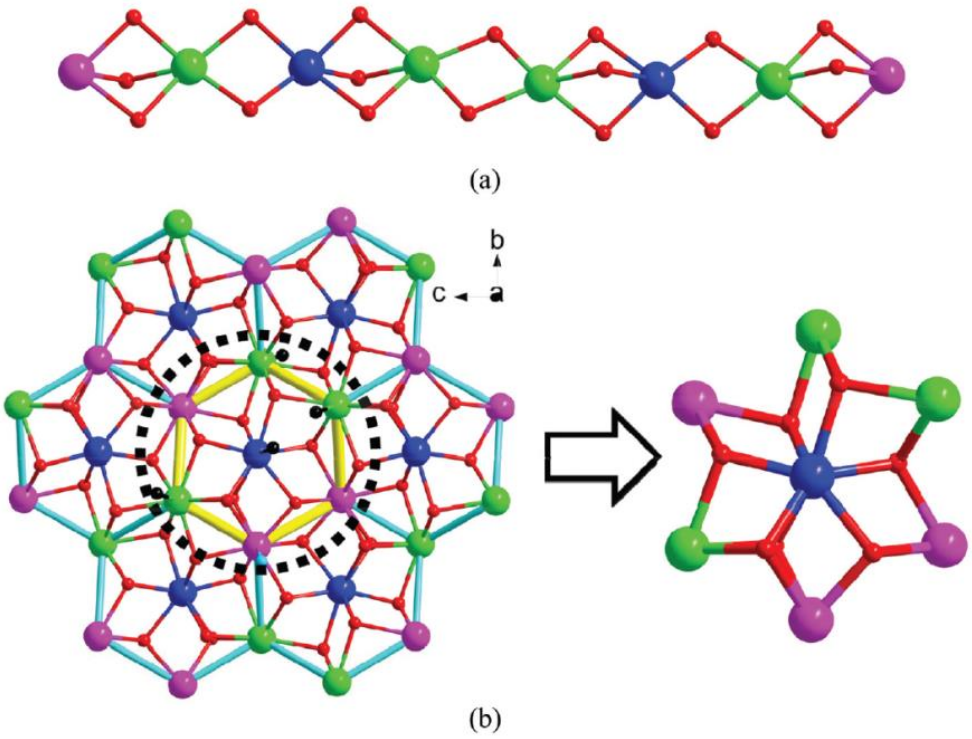

Figure 67. (a) The one-dimensional chains of coordination polymer 1; (b) $CdCl_2$ type two-dimensional structure formed by connection between the six connected Tb^{3+} ions and the three connected hydroxyl groups moieties (red spheres).[50]

2,2'-biimidazole had been used as an anion receptor in a new anion sensor $[Ru(bpy)_2(H_2biim)](PF_6)_2$, because it has protons that can be involved in hydrogen bonding with anions.[37] Anions play a crucial role in chemical, biological, and environmental processes and therefore the development of anion sensors have interested scientists long time. For analytical chemistry, chromogenic moieties have been considered to be a good anion receptor due to their ability to have a visual change of the color when a binding takes a place. For this purpose, metal-organic complexes are ideal candidates due to the many options available for capturing an anion, for example, by hydrogen bonding. Ru(II) polypyridyl complexes which have absorption and emission spectra within the visible range have been broadly employed as chromophores because of good redox and photo properties. In the Ru(II)-bpy complex, containing 2,2'-biimidazole, Ru(II)-bpy moiety acts as a chromophore and has absorption and emission spectra in a visible range, while imino moieties of H_2biim ligand have been coordinated to a Ru(II)-bpy fragment, where amino groups capture anions through hydrogen bonding. Hence, the solubility of the sensor is improved; *syn*-conformation is forced by the chelating coordination type, and the acidity of the metal-H_2biim complex is also increased by the chelating coordination. The different basicities and hydrogen bonding

capabilities of various anions such as Cl^-, Br^-, I^-, NO_3^-, HSO_4^-, $H_2PO_4^-$, OAc^-, and F^- the interactions with $[Ru(bpy)_2(H_2biim)](PF_6)_2$ result in a variety of different color outputs (Scheme 2, Figure 68).[37]

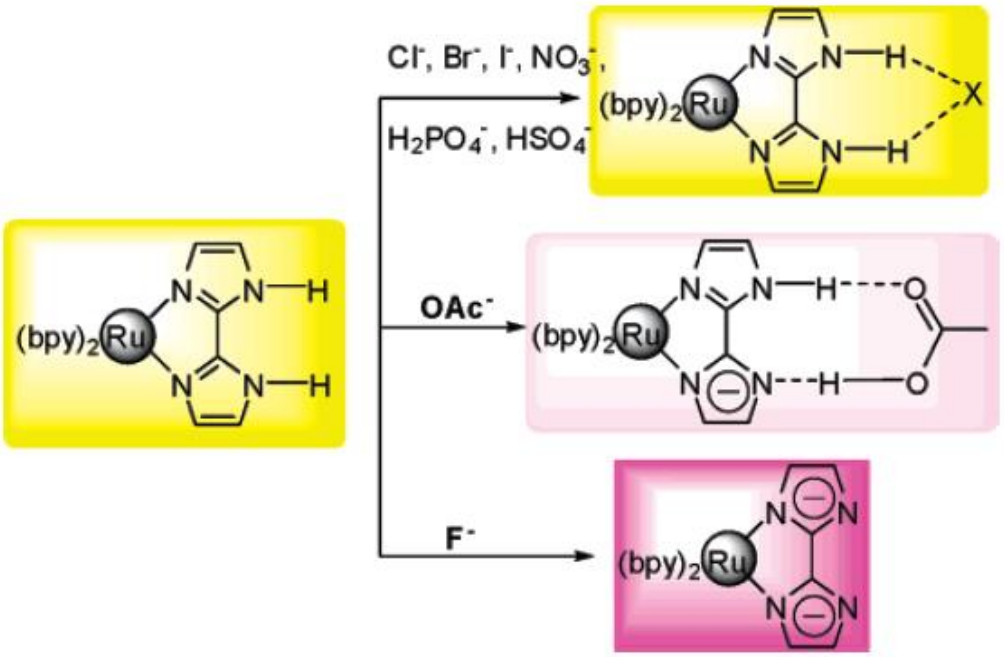

Scheme 2. The interaction of $[Ru(bpy)_2(H_2biim)](PF_6)_2$ with different anions.[37]

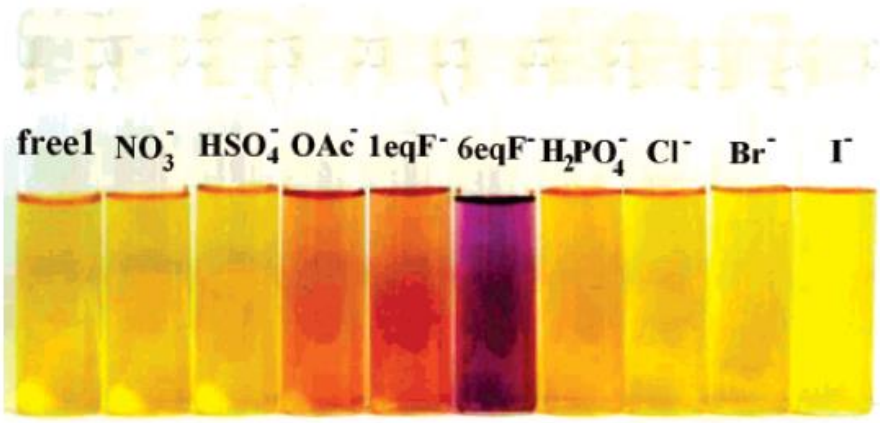

Figure 68. Color change of $[Ru(bpy)_2(H_2biim)](PF_6)_2$ observed in MeCN solution after the addition of 1 eq. of the corresponding anions as tetrabutylammonium salts (6 eq. for tetrabutylammonium fluoride).[37]

It was found that instead of forming hydrogen bond with the receptor, fluoride has a high affinity toward the N-H group possibly due to the formation of a highly stable HF_2^- complex, which allows N-H deprotonation. Thus stepwise deprotonation of the metal-

H_2biim complexes takes place. Next these deprotonated complexes, when in the presence of an appropriate anion, assemble into a polynuclear cluster bridged by $Hbiim^-$ or $biim^{2-}$. Therefore, a $[Ru(bpy)_2(H_2biim)](PF_6)_2$ anion sensor with incredible photophysical properties has been successfully designed, and its further modifications could help in developing of anion sensors. [37]

10. SUMMARY

Nowadays coordination compounds have been involved in essential areas of chemistry and industry such as catalysis, different types of sensors, and pharmacology. Noncovalent interactions play a central role in many forefront areas of modern chemistry such as coordination chemistry, supramolecular chemistry, biochemistry, synthetic organic chemistry. Investigation into the wide range of existing ligands and coordination centers interacting through different noncovalent types of interactions has resulted in the discovery of many interesting research topics for scientists who work in a variety of areas in chemistry.

2,2'-biimidazole has several potential binding sides to attach to the coordination center. Different complexes could be synthesized and the options of ligand binding could be investigated, depending on the coordination center. It was shown that due to the ability to interact through hydrogen or π-bonding, biimidazole-based compounds are widely used across modern research. Attempts to synthesize a drug with fewer side effects and toxicological properties lead scientist to use H_2biim-based complexes in medicine. H_2biim-based complexes are also widely used in coordination chemistry to produce novel ion sensors, light emitting materials, and building blocks for biimidazole-bridged bimetallic systems. Due to its ability to form hydrogen bonds, H_2biim is actively used in the field of supramolecular chemistry in, for example, the formation of self-assembly systems, 3D porous frameworks capable of catching molecules, POMs with catalytic properties, and other systems with luminescence, catalytic, or conductivity properties.

All applications explore a great possibility for further studies of biimidazole-based coordination compounds.

EXPERIMENTAL PART

11. OBJECTIVES

The main idea of this thesis was to synthesize and investigate the coordinative properties of 2,2'-biimidazole derived ligands which could form coordination compounds and supramolecular ensembles. H_2Biim was chosen as a promising ligand for complexation reactions because its variety of interesting properties; several potential binding sides, the ability to interact through hydrogen and/or π-bonding. After playing around with potential binding sides it was decided that a modified version of H_2Biim would be used.

The first option was a molecule presented by Aakeröy *et al.* - 1,1'-bis(pyridin-4-ylmethyl)-1H,1'H-2,2'-biimidazole (L1, Figure 69), a molecule with halogen bonding properties and possible application in supramolecular chemistry.[51] The second option was a molecule presented by Zhang *et al.* - diethyl 2,2'-(1H,1'H-[2,2'-biimidazole]-1,1'-diyl)diacetate (L2, Figure 69).[50] This molecule has two incredible features, the first being the ability for N and O atoms to coordinate with metal ions to form coordination polymers, and, secondly, the ability for the $–CH_2–$ group to be rotated to satisfy the coordination orientation of the carboxylate group in order to ease steric hindrance. The third option was a hydrolyzed version of L2 - 2,2'-(1H,1'H-[2,2'-biimidazole]-1,1'-diyl)diacetic acid which has two inflexible imidazole rings linked by a rotatable C–C bond allowing ligand, giving it subtle conformational adaptations. It also has a further strong coordinating ability of carboxylate arms (L3, Figure 69).[52] For the complexation reactions d-block transition metals (Fe(II), Zn(II), Ru(II), Ag(I), Re(III), Pt(II), Au(I)) were chosen in order to obtain a variety of coordinating patterns for constructing coordination frameworks.

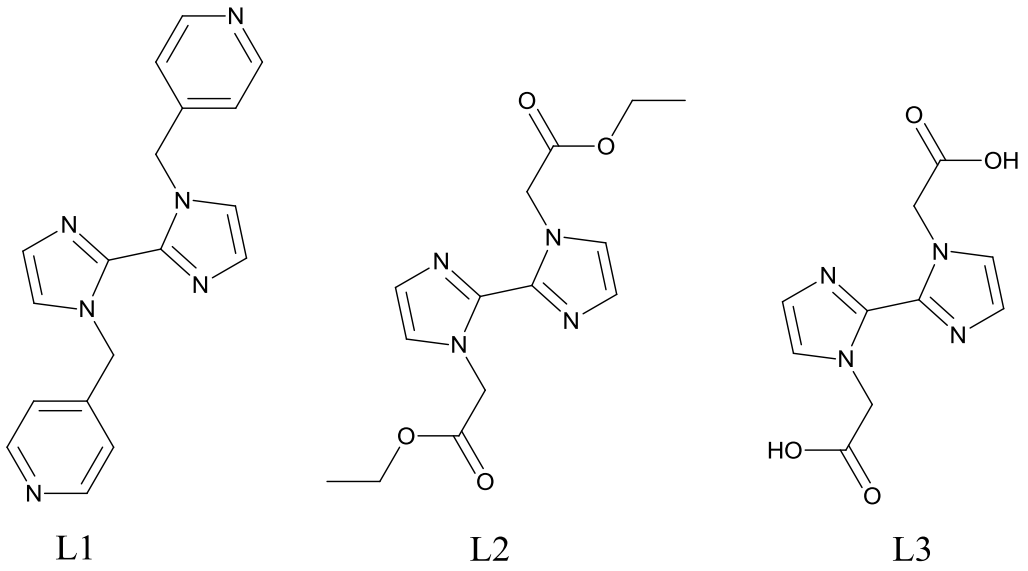

Figure 69. Structure of L1, L2, and L3.

It was, therefore, decided to investigate coordination properties of L1, L2, and L3 biimidazole based ligands. The experiment was divided into two stages: the synthesis and characterization of ligands, and the synthesis and characterization of appropriate complexes. The experimental part was done at the laboratory E501 of the Chemistry Department, University of Jyväskylä.

12. REAGENTS AND SOLVENTS

Reagents and solvents used in the experimental part are listed in the Table 2.

Table 2. Reagents and solvents used in experimental part.

Name	Manufacturer	Purity grade (%)
4-(bromomethyl)pyridine hydrobromide	ALDRICH	97
acetone	ALDRICH	≥ 99.5
acetonitrile	VWR	
ammonium acetate	ALDRICH	≥ 98
chloro(dimethylsulfide)gold(I)	ALDRICH	
dichloromethane	ALDRICH	≥ 99.9
dichlorotetrakis(dimethylsulfoxide) ruthenium(II)	ALDRICH	96
diethyl ether	ALDRICH	≥ 99.8
ethanol	ETAX	≥ 99.5
ethylchloroacetate	ALDRICH	99
glyoxal	ALDRICH	
hydrochloric acid	ALDRICH	
iron(II) chloride tetrahydrate	ALDRICH	≥ 99.0
methanol	J.T.BAKER	
potassium tert-butoxide	ALDRICH	≥ 98
potassium tetrachloroplatinate(II)	Alfa Aesar	99.9
rhenium(III) iodide	ALDRICH	97
sodium hydroxide	ALDRICH	≥ 98
tetrahydrofuran	ALDRICH	≥ 99.9

13.SYNTHESIS

All the reagents and solvents were purchased from commercial sources (Sigma-Aldrich, Alfa Aesar, J.T.BAKER, ETAX) and used as received without further purification. 2,2′-biimidazole and ligand L1 were synthesized according to previously reported methods.[36,51]

^{1}H NMR spectra were recorded using a Bruker AV 400 Ultrashield spectrometer, and commercial NMR solvents (methanol-d_4 and DMSO-d_6) were used.

Elemental analysis for carbon, hydrogen, and nitrogen was performed on the instrument Elementar Vario EV III by Elina Hautakangas. X-ray crystal structure determination was performed by PhD student Rajendhraprasad Tatikonda.

NMR signal assignments for the target compounds, crystal structures and unit cell parameters are presented in the Appendices.

1. Synthesis and structure determination of ligands

1. Synthesis of 1H,1H'-2,2'-biimidazole (H_2Biim)

The procedure known in the literature was used for the preparation of H_2Biim with slight modifications.[36] To obtain H_2Biim ammonium acetate and 40 % glyoxal were used as starting materials. The water solution of the reaction mixture was heated at 40 ^{o}C for 1 h, and then additionally stirred 5 h at r.t (Figure 70).

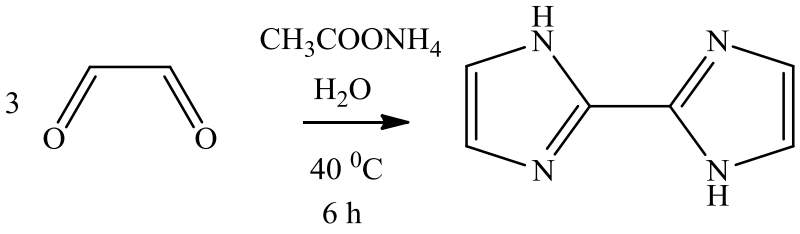

Figure 70. Scheme of H_2Biim synthesis.

2. Synthesis of L1

The procedure known in the literature was used for the preparation of L1 with slight modifications.[51] Firstly, in an inert atmosphere, an acetonitrile solution of H_2Biim was stirred for 1 h with NaOH. Next, 4-(bromomethyl)pyridine*HBr was added to the solution and the resultant mixture was stirred overnight to give the desired disubstituted compound as the product (Figure 71).

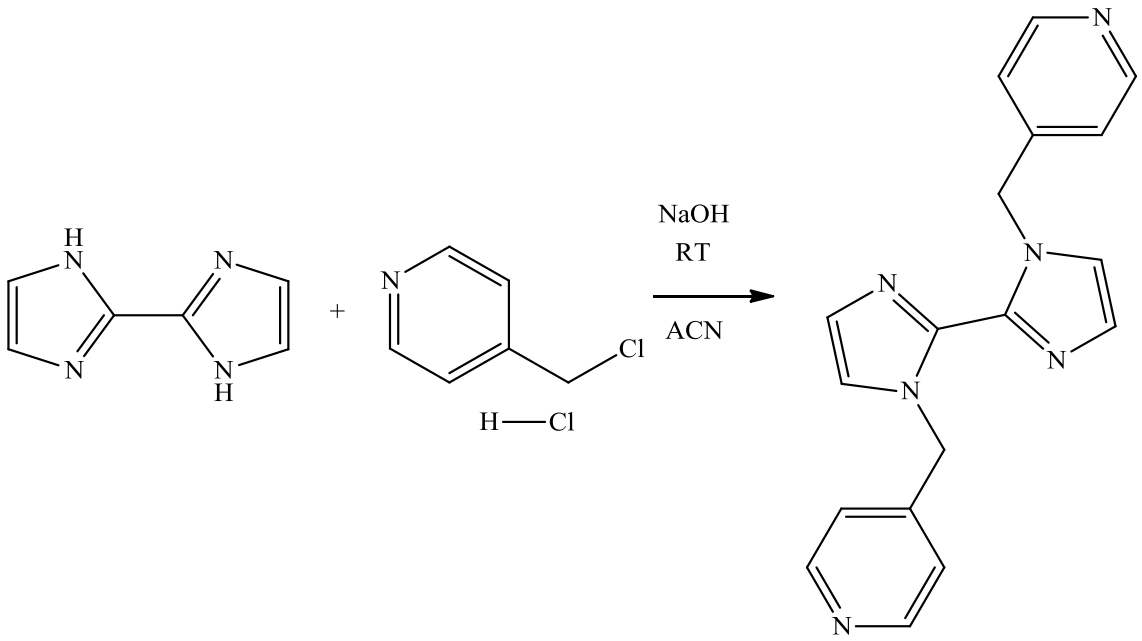

Figure 71. Scheme of L1 synthesis

3. Synthesis of L2

To obtain L2 , an acetonitrile solution of H_2Biim was, firstly, stirred in an inert atmosphere for 1 h with NaOH. An acetonitrile solution of ethylchloroacetate was then added to the reaction mixture and refluxed for 1 d to give the desired disubstituted compound as the product (Figure 72).

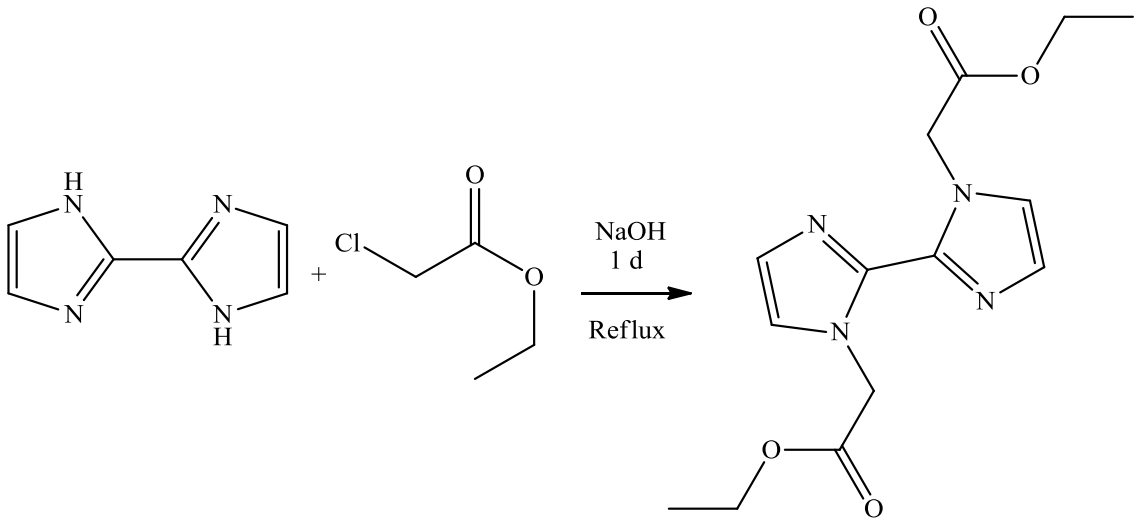

Figure 72. Scheme of L2 synthesis.

4. Synthesis of L3

To obtain L3 ice-cold potassium tert-butoxide in dry ether was stirred for 5 min with H_2O. L2 was then added and the reaction mixture was stirred at RT overnight to give disubstituted compound in a very low yield (Figure 73).

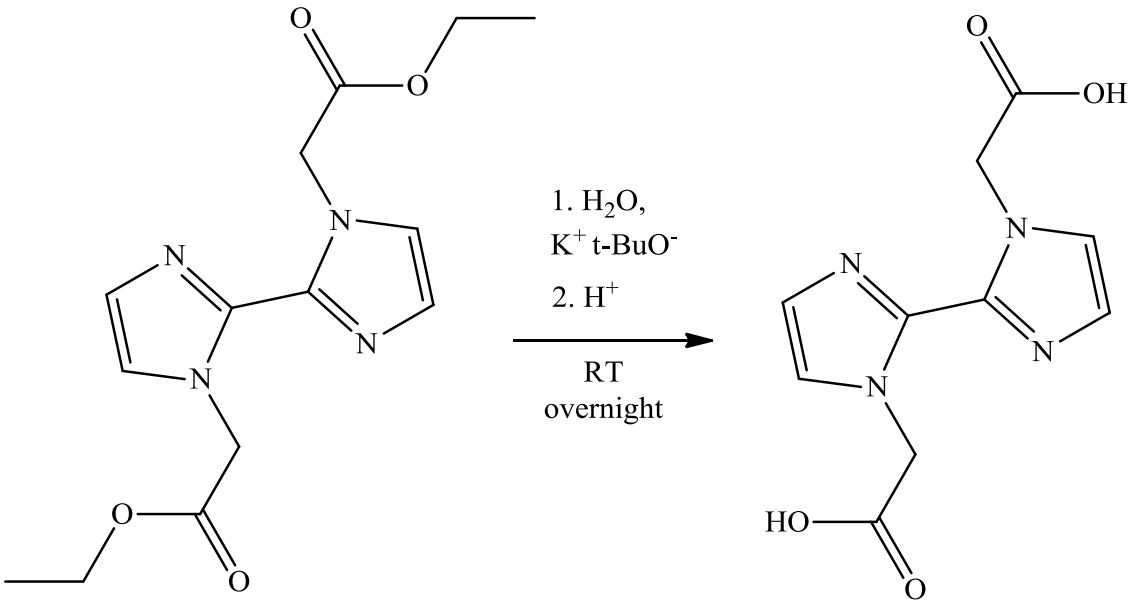

Figure 73. Scheme of L3 synthesis.

2. Synthesis and structure determination of complexes with L1

1. Synthesis of Fe(II) complex with L1

To obtain the Fe(II) complex with L1 an ethanol solution of $FeCl_2*4H_2O$ was degassed and L1 fully dissolved in EtOH was added to the reaction mixture which was then refluxed overnight. The reddish-brown product was obtained after purification.

2. Synthesis of Pt(II) complex with L1

To obtain Pt(II) complex with L1 K_2PtCl_4 and KI were stirred in MeOH. This was done because the chloride anions substitution is a slow process. Iodide anions, due to the bigger size and polarizability, result in higher kinetic lability. L1 dissolved in MeOH was added to the resulting mixture and stirred overnight at reflux. The yellowish product was obtained after purification.

3. Synthesis of Au(I) complex with L1

To obtain the Au(I) complex with L1, a mixture of L1 and $Au(SMe_2)Cl$ in 3 ml of DCM was stirred overnight in darkness for 1 d, and the light beige product was obtained.

4. Attempt of synthesis of Ru (II) complex with L1

To obtain the Ru (II) complex with L1, dichlorotetrakis(dimethylsulfoxide) ruthenium(II) in EtOH and L1 were stirred at reflux overnight in THF. The product was determined to be the starting material.

5. Attempt of synthesis of Re (III) complex with L1

To obtain the Re (III) complex with L1, ReI_3 and L1 in EtOH were stirred at reflux overnight. The product was determined to be the starting material.

3. Synthesis and structure determination of complexes with L2

1. Synthesis of Fe(II) complex with L2

To obtain the Fe(II) complex with L2 an ethanol solution of $FeCl_2*4H_2O$ was degassed and L2 fully dissolved in EtOH was added to the reaction mixture which was then refluxed overnight. The dark-orange product was obtained after purification.

2. Synthesis of Pt(II) complex with L2

To obtain the Pt(II) complex with L2 K_2PtCl_4 and KI were stirred in MeOH for 1 h. L2 dissolved in MeOH was added to the resulting mixture, which was then stirred overnight at reflux. The light-yellow product was obtained after purification.

3. Synthesis of Au(I) complex with L2

To obtain the Au(I) complex with L2 a mixture of L2 and $Au(SMe_2)Cl$ in 3 ml of DCM was stirred in darkness for 3 d. The greenish product was obtained after purification.

4. Attempt of synthesis of Ru (II) complex with L2

To obtain the Ru (II) complex with L2 dichlorotetrakis(dimethylsulfoxide) ruthenium(II) and L2 in acetonitrile were stirred at reflux for 2 d. The dark green solid product was determined to be the starting material.

5. Attempt of synthesis of Re (III) complex with L2

To obtain the Re (III) complex with L2 ReI_3 and L2 in chloroform were stirred at reflux 1 d. The black solid product was determined to be the starting material.

14.RESULTS AND DISCUSSION

Analysis of X-ray structures

The presented solid state structures were obtained by single crystal X-ray diffraction by Rajendraprasad Tatikonda, and the parameters are presented in the Appendices.

The crystal structure of L1 is presented in Figure 74.

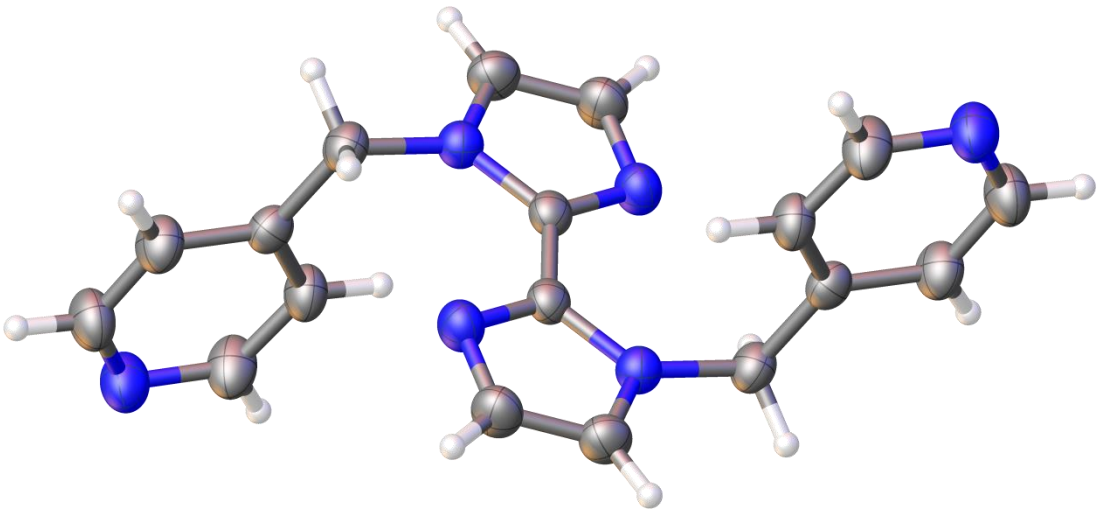

Figure 74. L1 structure

In this molecule, the imidazole rings align in one plane, creating an aromatic system, while pyridin-4-ylmethyl parts are directed opposite to each other and align at an angle to the biimidazole plane. Therefore, the molecule has a *trans*- conformation which is favored, due to less sterical hindrance.

The crystal structure of L2 is presented in Figure 75.

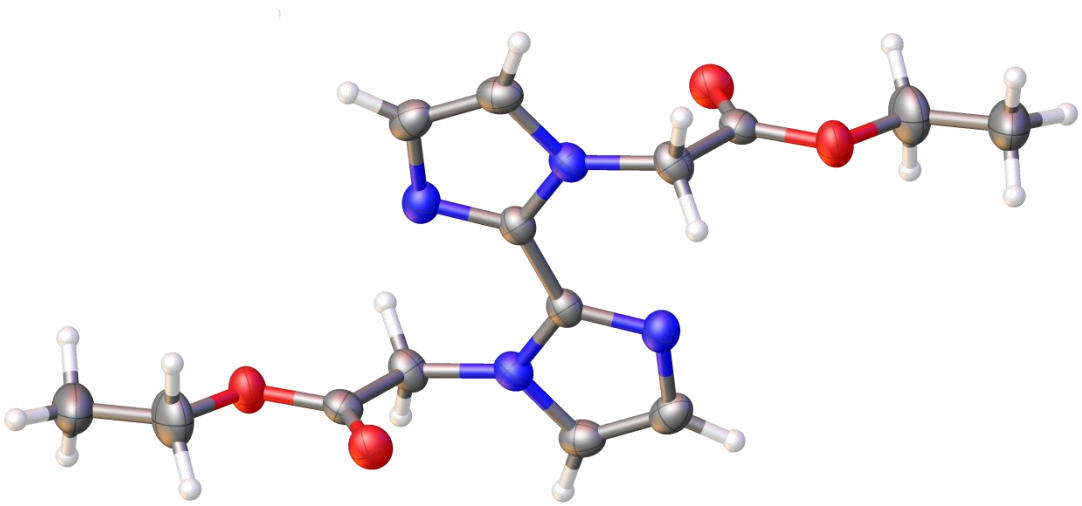

Figure 75. L2 structure

Similarly to the L1 molecule, the L2 molecule has a *trans*- conformation that is favored due to less sterical hindrance.

Crystal structures, of mentioned above complexes of transitional metals with L1 and L2 ligands, had not yet been obtained at this stage. However, PhD student Tatikonda received 2 single crystal structures of metal complexes with L1 ligand, which can provide a clue on the structures of the mentioned above complexes.

The first structure presented in Figure 76 is that of the polymeric Ag(I) complex with L1 that was crystallized from a water/chloroform mixture. One L1 molecule bridges two Ag(I) atoms to form a helical polymer which has inclusions of counter-anions. Being in a *trans*- conformation L1 is coordinated to Ag through the nitrogen on the pyridine ring.

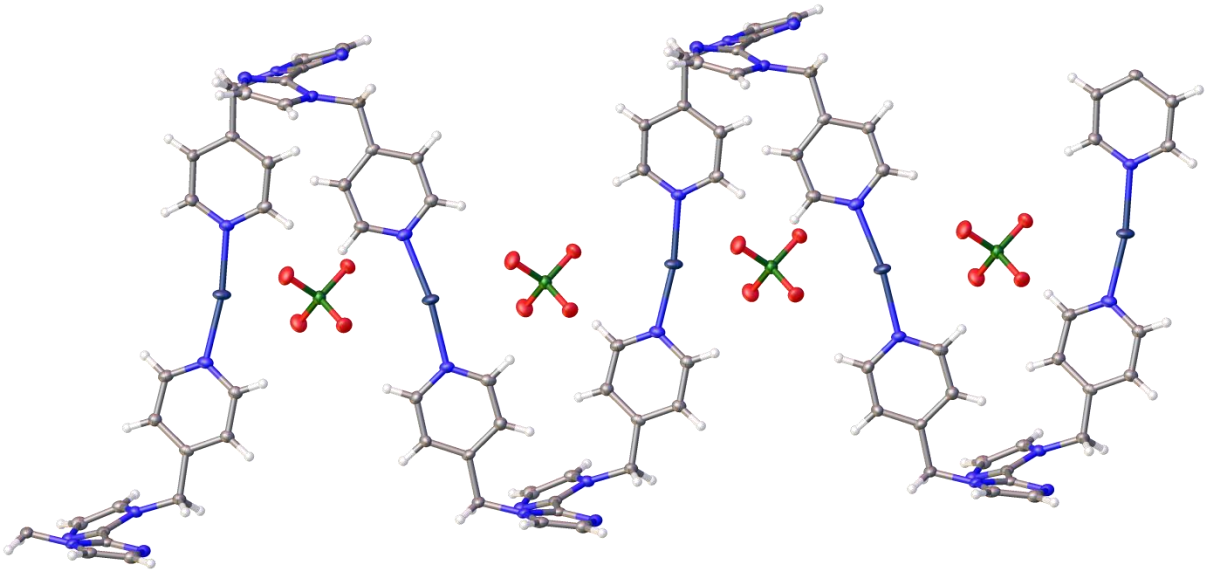

Figure 76. Structure 1 of the Ag(I) complex with L1.

The second structure presented in Figure 77 is that of the polymeric Ag(I) complex with L1 and inclusions of counter-anions, but crystallized from the acetonitrile solution. L1 has two conformations in the structure. In the first, L1 is bridging two Ag(I) atoms through nitrogen atoms of pyridine rings and biimidazole fragment is in the *trans*- form and not coordinated. In the second, L1 is coordinated to three different Ag(I): *cis*- form biimidazole is bridging two connected to each other Ag(I) atoms through two nitrogen atoms; the nitrogen atom of one of the pyridine rings coordinating to the third Ag(I) atom, the other pyridine ring nitrogen stays uncoordinated. This may be caused by the steric hindrance of the polymer and the fact that there is no space for extra Ag to be coordinated by the second pyridine ring. This may also be caused by the tensity of the structure in the *cis*- form of L1.

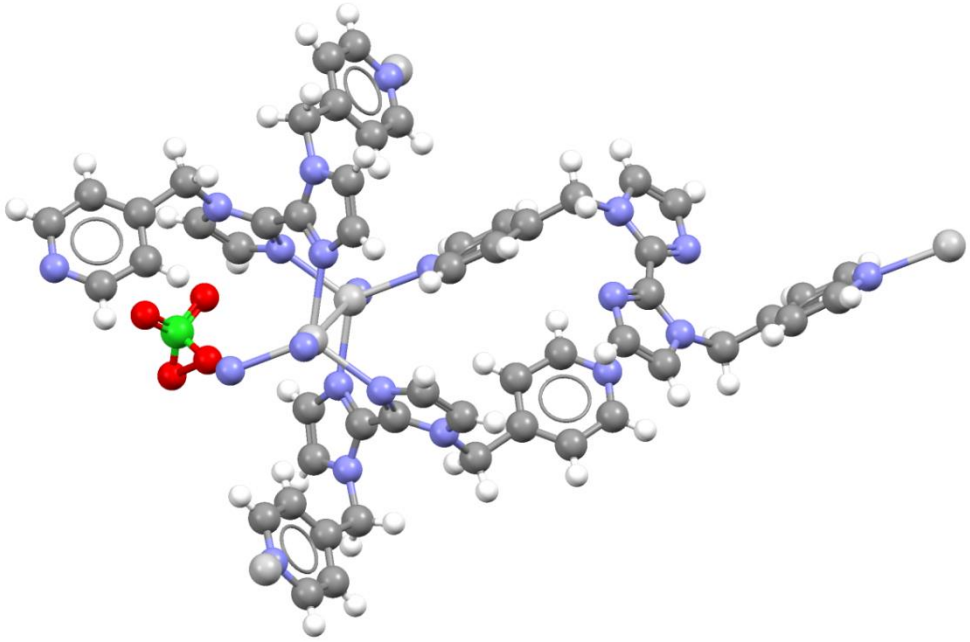

Figure 77. Structure 2 of the Ag(I) complex with L1

The third structure presented in Figure 78 is the structure of polymeric Zn(II) complex with L1. The L1 molecule is bridging two Zn(II) atoms to form a polymer which has inclusions of solvent molecules. Being in a *trans*-conformation L1 is coordinated to Zn(II) through the nitrogen on the pyridine ring.

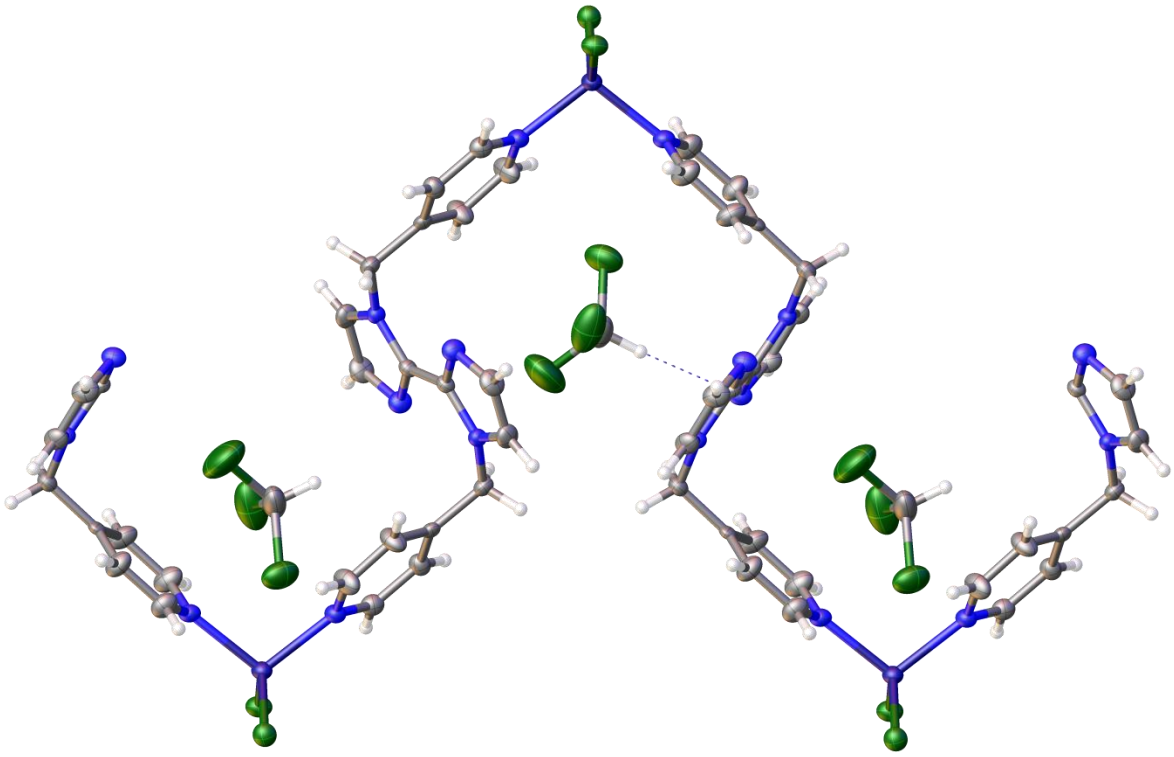

Figure 78. Structure of the Zn(II) complex with L1.

In conclusion, considering the observed structures, one may predict possible ways of the coordination of L1. If the biimidazole of the ligand remains in *trans*-conformation then it will be bridging metal atoms in complexes, but if biimidazole is in the *cis*-form then L1 could coordinate to a metal atom through a nitrogen atom of one of the pyridine rings, while the other stays uncoordinated to prevent torsion.

Analysis of NMR spectra

^{1}H NMR for L3 was not found within the literature, however, it was still obtained and the desired structure confirmed (Appendix 5).

Comparing the ^{1}H NMR spectra of the Fe(II)-L1 complex (Appendix 6) and pure L1 (Appendix 1) one can mention that in the complex NMR spectra all the peaks are broadened. The broadening of peaks could be caused by an exchange process between *cis*-/*trans*- forms of biimidazole and paramagnetic properties of Fe(II). Moreover, peaks of H1 and H6 in complex are broadened the most, meaning that these protons are also influenced the most by paramagnetic Fe(II), probably because of coordination of biimidazole and pyridine nitrogen.

Several differences were found between the ^{1}H NMR spectra of Pt(II)-L1 complex (Appendix 7) and pure L1(Appendix 1). All of the peaks were shifted to the downfield region. The peak from H1&H1' (pyridine ring hydrogens) was divided into two multiplets in the NMR, which may happen when the environment of these hydrogens is different. If biimidazole is in the *cis*-form then, as it was shown on the 2nd X-ray structure of Ag(I) complex with L1 (Figure 77), L1 is coordinated to Ag(I) through nitrogen atom of one of the pyridine rings, while the other one stays uncoordinated, then a different environment is created for each pyridine ring. This also influenced the peak of H2&H2', so that the complex spectrum was divided into two broad singlets.

Several differences between the ^{1}H NMR spectra of Au(I)-L1 complex (Appendix 8) and pure L1(Appendix 1) were found. All of the peaks were shifted to the downfield region. The peak from H1&H1' (pyridine ring hydrogens) was divided into two broad singlets in the NMR of complex which may happen if the environment of these hydrogens is different. It is most likely that, as mentioned in the discussion of the Pt(II)-L1 complex, one of the pyridine rings coordinated to Au(I), while other stayed uncoordinated. The peak from H6&H6'seems to also be influenced by the electron

environment due to the observation that it broadened and shifted to the downfield region more than other peaks. Therefore L1 probably coordinates to Au(I) through both biimidazole nitrogen and pyridine nitrogen.

Several proposals about the structure of ^{1}H NMR spectra of Pt(II)-L2 complex (Appendix 9) and pure L2 (Appendix 3) have been made. It has been shown[52] that L2 type of ligand can coordinate through nitrogen atoms of biimidazole or oxygen atoms of the ester group within same complex. For these two coordination structures ^{1}H NMR spectrum would vary due to the different environments. If coordination took place through the nitrogen atom of the biimidazole part of L2 then 5H, 5H', 6H, and 6H' peaks would be influenced the most. If the coordination took place through the oxygen atom of the ester group of L2 then 4H, and 4H' would be influenced the most. Due to the different electron environments, both structures would appear differently on the same NMR spectrum. This effect can be seen in Appendix 9. Therefore the structure analogous to the one published by Xu *et al.*[52] could be proposed.

Even though NMR is one of the most powerful and helpful instruments in the determination of structure, further investigations are needed to confirm the coordination of the ligands.

Further discussions

Elemental analysis of the complexes of Au(I) with L1 and L2 showed that the complexes have the formula $Au_2(L1)Cl_2$ and $Au_2(L2)Cl_2*CHCl_3$ correspondingly.

A by-product of the experiment is that a novel coordination compound was synthesized and characterized by X-ray diffraction (Figure 79). In this structure biimidazole has *cis*-conformation and L1 is coordinated to the I of the KI salt through nitrogen atoms of the pyridine ends of L1. Expanding the structure, one can see infinite KI chains. This type of structure was synthesized for the first time, and it is planned to try other alkali metal halogenides for complexation with L1.

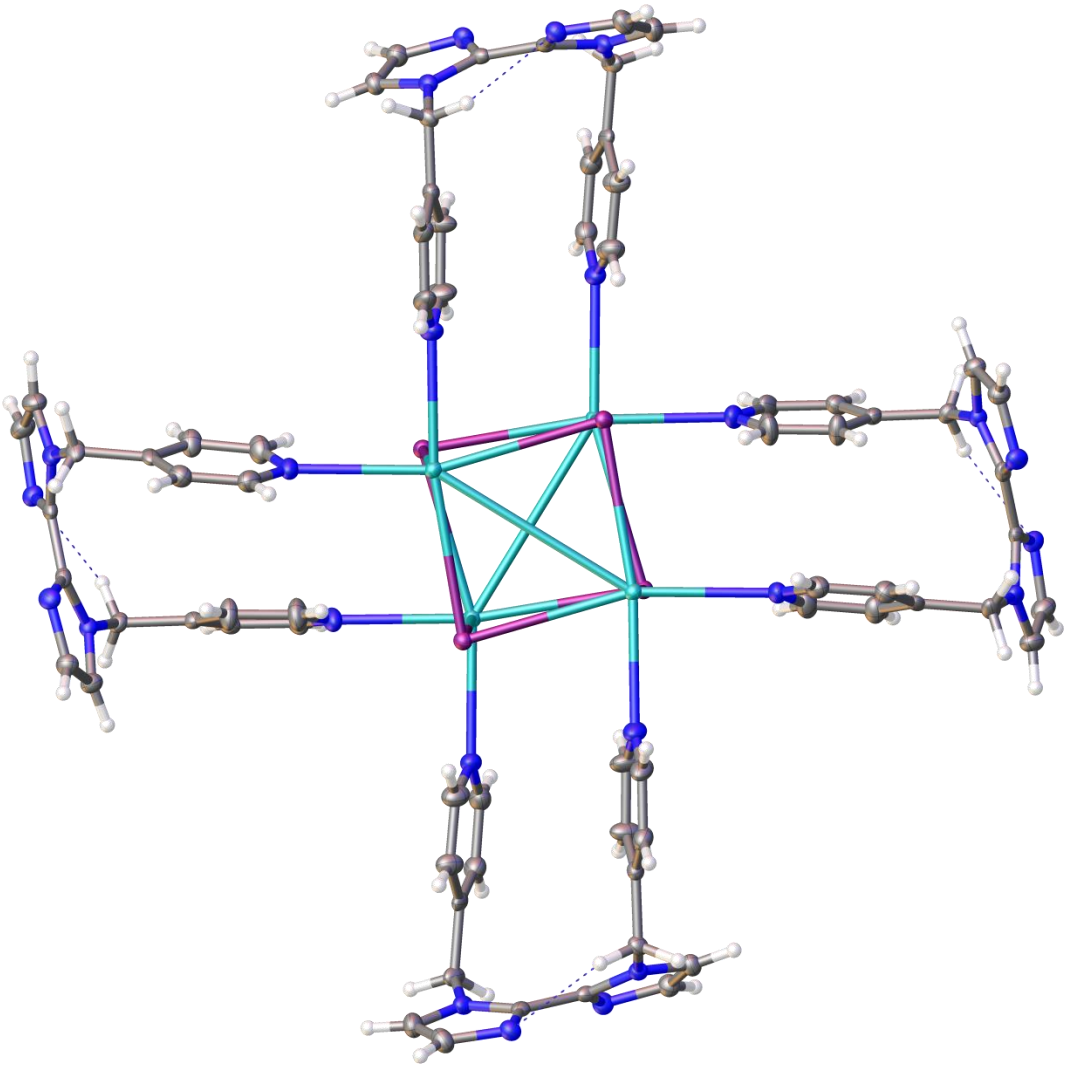

Figure 79. Structure of the complex of KI and L1.

15.CONCLUSIONS

In this thesis, the coordinative properties of biimidazole-derived ligands were studied. To understand the nature of these properties, different types of possible contacts were discussed. The definition, nature, and examples of hydrogen and different types of π-bonding were considered in detail. In order to understand the chemical properties of biimidazole-derived compounds, the chemistry of imidazole itself and that of biimidazole were discussed. The application of biimidazole-derived compounds in medicine, supramolecular chemistry, and coordination chemistry were discussed in order to plan further experiments.

Due to the interest into the coordination and supramolecular chemistry, several biimidazole-based ligands with promising supramolecular properties were synthesized and their ability to bind d-block transition metals such as Fe(II), Zn(II), Ru(II), Ag(I), Re(III), Pt(II), Au(I) were studied. It was shown that a variety of coordinating patterns could be synthesized using biimidazole-based compounds when constructing coordination frameworks. Furthermore, a novel coordination compound was synthesized and investigated.

However, in the future, it would be useful to obtain crystal structures for the synthesized complexes. In addition, further experiments are being planned to investigate the coordination reactions of L1 and salts of the 1st group metals in order to further study this coordination type. In additional research, a modification of L1 is planned to be synthesized and the geometry of binding of a new ligand is planned to be studied. Further research will also look into the synthesis of L3 *in situ* due to the instability of L3 itself.

Furthermore, the interactions between organic molecules, transitional metals, and the surface of oxides for the purpose of obtaining recyclable multifunctional catalysts will be investigated in future research. Therefore, it would be interesting to synthesize polyoxometalate (POM) organic–inorganic hybrid compounds based on discussed ligands and to study the catalytic properties of the obtained compounds.

16.EXPERIMENTAL PROCEDURES

1 Synthesis of ligands

1. Synthesis of 1H,1H'-2,2'-biimidazole (H_2Biim)

To a mixture of ammonium acetate (31.8 g, 0.4 mol) and water (20 ml), 40 % glyoxal (6 ml, 0.04 mol) was added dropwise at 40 ^{o}C over 1 h. After complete addition of glyoxal the reaction mixture was stirred additionally 5 h at r.t., than the 2.4 g of the beige product was filtered and washed with H_2O and acetone, than dried under vacuum.

Yield: 2.4 g (45 %)

2. Synthesis of L1

A mixture of H_2Biim (254.9 mg, 1.9 mmol), 35% w/w NaOH (1.8 ml), and 16 ml of acetonitrile was stirred under argon at r.t. for 3 h in 50 ml round-bottom flask equipped with magnetic stirrer. Than 4-(bromomethyl)pyridine*HBr (1.0117 g, 4 mmol) was added followed by 14 ml of acetonitrile. Resulted mixture was stirred overnight at RT. Resulted solution was purified by column chromatography (Silica gel 60, 90% DCM, 10% MeOH) to give yellowish solid.

Yield: 317.9 mg (52.8 %)

^{1}H NMR (400 MHz; DMSO-*d6*) δ, ppm: 8.43-8.42(m, 4H, H1&H1'), 7.41-7.40 (d, 2H, H2&H2', J = 1Hz), 7.08 (d, 2H, H5&H5', J = 1Hz), 6.94-6.92 (m, 4H, H6&H6'), 5.83 (s, 4H, H4&H4') (Appendix 1).

^{13}C{^{1}H} NMR (101 MHz, DMSO-*d6*) δ, ppm: 149.7 (2C, C7&C7'), 147.1 (4C, C1&C1'), 137.4 (2C, C3&C3'), 128.2 (2C, C6&C6'), 122.9 (4C, C2&C2'), 121.6 (2C, C5&C5'), 49.0 (2C, C4&C4') (Appendix 2).

Elemental analysis ($C_{18}H_{16}N_6$): C, 67.82; H, 5.01; N, 26.15; Calc.: C, 68.34; H, 5.10; N, 26.56.

3. Synthesis of L2

A mixture of H_2Biim (500 mg, 3.9 mmol), 35% w/w NaOH (1.8 ml) and acetonitrile (16 ml) were stirred under nitrogen for 1 h. A mixture of ethylchloroacetate (8 mmol, 0.856 ml) in 1 ml of acetonitrile was added dropwise over 10 min to the reaction mixture, then it was refluxed for 1 d. Reaction was quenched with water, precipitate was filtered.

Filtrate was extracted with DCM. DCM layer was washed with water, dried over $MgSO_4$. Solvent was evaporated to give light-beige residue.

Yield: 823.1 mg (68.9 %)

^{1}H NMR (400 MHz; DMSO-*d6*) δ, ppm: 7.29-7.28 (d, 2H, H5&H5', J = 1Hz), 6.99 (d, 2H, H6&H6', J = 1Hz), 5.37 (s, 4H, H4&H4'), 4.14-4.09 (q, 4H, H2&H2', J = 2Hz), 1.19-1.15 (t, 6H, H1&H1', J = 2Hz) (Appendix 3).

^{13}C NMR (101 MHz, DMSO-*d6*) δ, ppm: 168.9 (2C, C3&C3'), 138.3 (2C, C7&C7'), 128.6-126.7 (d, 2C, C6&C6', J = 190 Hz), 124.9-122.9 (d, 2C, C5&C5', J = 191 Hz), 62.7-59.7 (t, 2C, C2&C2', J = 148 Hz), 50.9-48.1 (t, 2C, C4&C4', J = 143 Hz), 16.4-12.6 (q, 2C, C1&C1', J = 127 Hz) (Appendix 4).

Elemental analysis ($C_{14}H_{18}N_4O_4$): C, 54.53; H, 5.77; N, 17.90; Calc.: C, 54.89; H, 5.92; N, 18.29.

4. Synthesis of L3

A suspension of potassium tert-butoxide (44.9 mg, 0.4 mmol) in 50 ml of dry ether was stirred for 10 min at 0°C, then H_2O (1.8 ml, 0.1 mmol) was added dropwise via syringe and resulted slurry was stirred for 5 min. To this, L2 (15.3 mg, 0.05 mmol) was added and the reaction mixture was then stirred at RT overnight. The reaction mixture was quenched by addition of ice-cold H_2O until two clear layers formed. The aqueous layer was separated and acidified with concentrated HCl, and then it was extracted with ether. Ether fractions were combined and dried under a vacuum to give colorless residue.

Yield: 3.2 mg (26 %)

^{1}H NMR (400 MHz; methanol-d_4) δ, ppm: 7.62 (s, 2H, H3&H3'), 7.47 (s, 2H, H4&H4'), 5.37 (s, 4H, H2&H2') (Appendix 5).

2 Synthesis and structure determination of the transitional metal complexes with L1

1. Synthesis of Fe(II) complex with L1 (MM-COML1Fe)

A mixture of $FeCl_2$*$4H_2O$ (19.8 mg, 0.1 mmol) and 3 ml of ethanol was degassed (N_2, bubbling for 15 min) whine stirring. To the resulted solution was added L1 (31.7 mg, 0.1 mmol) fully dissolved in 2 ml of EtOH and reaction mixture was refluxed overnight.

Then precipitate was filtered, washed with chloroform and dried under a vacuum to give 10.4 mg of the reddish-brown product.

Yield: 10.4 mg

^{1}H NMR (400 MHz; DMSO-*d6*) δ, ppm: 8.66-8.41(br, 4H, H1&H1'), 7.41 (s, 2H, H2&H2'), 7.08 (s, 2H, H5&H5'), 7.07-6.88 (br, 4H, H6&H6'), 5.83 (s, 4H, H4&H4') (Appendix 6)

2. Synthesis of Pt(II) complex with L1 (MM-COML1Pt)

A mixture of K_2PtCl_4 (41.5 mg, 0.1 mmol) and KI (180.9 mg, 1.09 mmol) were dissolved in 10 ml of MeOH while stirring. The resulting dark-yellow solution was stirred at RT for 1 h and L1 (31.7 mg, 0.1 mmol) dissolved in 2 ml of MeOH was added to the reaction mixture and it was stirred over night at reflux temperature. After the reaction precipitate was filtered, washed with chloroform and dried under a vacuum to give 17.94 mg of the yellowish product.

Yield: 17.94 mg

^{1}H NMR (400 MHz; DMSO-*d6*) δ, ppm: 8.80 (m, 2H, H1 or H1'), 8.62-8.54 (m, 2H, H1 or H1'), 7.45 (br s, 2H, H2 or H2'), 7.23-7.01 (m, 4H, H5&H5&H6&H6'), 7.09 (br s, 2H, H2 or H2'), 5.94 (br s, 4H, H4&H4') (Appendix 7)

3. Synthesis of Au(I) complex with L1 (MM-COML1Au)

To a stirred mixture of L1 (31.7 mg, 0.1 mmol) in 3 ml of DCM was added $Au(SMe_2)Cl$ (29.4 mg, 0.1 mmol) in 3 ml of DCM and the mixture was stirred overnight in darkness for 1 d. Then most of solvent was removed by centrifugation and decantation, the least of solvent was removed under a vacuum, and the residue was washed with ether to give a light beige solid 33.6 mg.

Yield: 33.6 mg

^{1}H NMR (400 MHz; DMSO-*d6*) δ, ppm: 8.7(br s, H1 or H1'), 8.5(br s, H1 or H1'), (m, 4H, H1&H1'), 7.42 (br s, H2&H2'), 7.08 (d, 2H, H5&H5', J = 1Hz), 6.94-6.92 (m, 4H, H6&H6'), 5.83 (s, 4H, H4&H4') (Appendix 8).

Elemental analysis ($C_{18}H_{16}Au_2Cl_2N_6$): C, 26.15; H, 2.25; N, 10.41; Calc.: C 27.67; H, 2.06; N, 10.76.

4. Attempt of synthesis of Ru(II) complex with L1 (MM-COML1Ru)

To the dichlorotetrakis(dimethylsulfoxide) ruthenium(II) (41.6 mg, 0.1 mmol) in 3 ml of EtOH was added L1 (31.7 mg, 0.1 mmol). Then 2 ml of THF were added to dissolve the suspension and resulted mixture was stirred at reflux overnight. The solvent was evaporated to give a dark green solid and it was determined to be starting materials.

5. Attempt of synthesis of Re(III) complex with L1 (MM-COML1Re)

To the ReI_3 (56.8 mg, 0.1 mmol) in 3 ml of EtOH was added L1 (31.7 mg, 0.1 mmol). Then resulted mixture was stirred at reflux overnight. The black precipitate was filtered and dry under vacuum; the filtrate fraction was evaporated to give a yellow solid; both solids were determined to be starting materials (ligand and Re salt).

3 Synthesis and structure determination of the transitional metal complexes with L2

1. Synthesis of Fe(II) complex with L2 (MM-COML2Fe)

A mixture of $FeCl_2*4H_2O$ (19.8 mg, 0.1 mmol) and 4 ml of ethanol was degassed (N_2, bubbling for 15 min) while stirring. To the resulted solution was added L2 (30.6 mg, 0.1 mmol) fully dissolved in 4 ml of EtOH and the reaction mixture was refluxed overnight. Then the precipitate was filtered, washed with chloroform, and dried under a vacuum to give 9.2 mg of the dark-orange product.

Yield: 9.2 mg

Due to the poor solubility NMR spectra could not be presented for this compound.

2. Synthesis of Pt(II) complex with L2 (MM-COML2Pt)

A mixture of K_2PtCl_4 (41.5 mg, 0.1 mmol) and KI (180.9 mg, 1.09 mmol) were dissolved in 10 ml of MeOH while stirring. The resulting dark-yellow solution was stirred at RT for 1 h and L2 (30.6 mg, 0.1 mmol) dissolved in 2 ml of MeOH was added to the reaction mixture and it was stirred over night at reflux temperature. After the reaction precipitate was filtered, washed with chloroform and dried under a vacuum to give the light-yellow product.

Yield: 23.8 mg

^{1}H NMR (400 MHz; DMSO-*d6*) is presented in the Appendix 9.

3. Synthesis of Au(I) complex with L2 (MM-COML2Au)

To the stirred for 10 min mixture of L2 (44.3 mg, 0.15 mmol) in 3 ml of DCM was added $Au(SMe_2)Cl$ (47.5 mg, 0.15 mmol) in 3 ml of DCM was added and resulted mixture was stirred 3 d in darkness to give greenish liquid. After that solvent was evaporated, the solid was re-dissolved in chloroform and the precipitate was centrifuged to separate undissolved solid from liquid fraction. The resulted ppt was dried under a vacuum overnight to give 19.5 mg of the product.

Yield: 19.5 mg

^1H NMR spectrum of the compound was found to be the same as for L2.

Elemental analysis ($C_{15}H_{19}Au_2Cl_5N_4O_4$): C, 19.46; H, 2.21; N, 6.55; Calc.: C C, 20.23; H, 2.15; N, 6.29

4. Attempt of synthesis of Ru(II) complex with L2 (MM-COML2Ru)

To the dichlorotetrakis(dimethylsulfoxide) ruthenium(II) (41.6 mg, 0.1 mmol) in 3 ml of acetonitrile was added L2 (30.6 mg, 0.1 mmol). Then the resulted mixture was stirred at reflux 2 d. Solvent was evaporated to give a dark green solid and it was determined to be starting materials.

5. Attempt of synthesis of Re(III) complex with L2 (MM-COML2Re)

To the ReI_3 (56.8 mg, 0.1 mmol) in 3 ml of chloroform was added L2 (30.6 mg, 0.1 mmol). Then the resulted mixture was stirred at reflux 1 d. A black precipitate was filtered and dry under vacuum; the filtrate fraction was evaporated to give yellow solid; both solids were determined to be starting materials (ligand and Re salt).

4 Synthesis and structure determination of KI complex with L1

In a 50 ml round-bottom flask KI (16.6 mg, 0.1 mmol), L1(15.8 mg, 0.05 mmol) and 5 ml of MeOH were added. The mixture was stirred at 40 ^oC overnight, then the solution was slowly evaporated to get light-brown crystals that were further analyzed by single X-ray diffraction analysis (Appendix 11).

REFERENCES

(1) E. Baranoff; B. F. E. Curchod. *FIrpic: archetypal blue phosphorescent emitter for electroluminescence*; The Royal Society of Chemistry, 2015.

(2) A. Dervisi. *Inorg. Chem.* **2012**, *108* (0), 211–219.

(3) X. You; Z. Wei. Two multidentate ligands utilizing triazolyl, pyridinyl and phenolate groups as donors for constructing dinuclear copper(II) and iron(III) complexes: Syntheses, structures, and electrochemistry. *Inorganica Chimica Acta*, 2014, *423, Part* , 332–339.

(4) A. D. McNaught; A. Wilkinson. *IUPAC. Compendium of Chemical Terminology (the "Gold Book")*; Blackwell Scientific Publications: Oxford, 1997.

(5) C. F. Albert; W. Geoffrey. *Advanced inorganic chemistry. A comprehensive text*, 4th ed.; 1980; p 1396.

(6) P. Mercandelli; A. Sironi. *J. Am. Chem. Soc.* **1996**, *118* (46), 11548–11554.

(7) P. A. Gale; J. L. Sessler; J. W. Steed. *Chem. Commun.* **2011**, *47* (21), 5931–5932.

(8) J. W. Steed; J. L. Atwood. *Supramolecular Chemistry*; Wiley, 2009.

(9) http://pandasthumb.org/archives/images/lock%26key.gif (accessed Dec 25, 2014).

(10) http://users-phys.au.dk/kibs/Graphics/Science/Images/DNA.jpg (accessed Dec 27, 2014).

(11) http://semoneapbiofinalexamreview.wikispaces.com/file/view/02_16HydrogenBond-L.jpg/289154631/434x348/02_16HydrogenBond-L.jpg (accessed Jan 15, 2015).

(12) G. A. Jeffrey. *An Introduction to Hydrogen Bonding*; Topics in Physical Chemistry - Oxford University Press; Oxford University Press, 1997.

(13) A. Olbert-Majkut; J. Lundell; M. Wierzejewska. *J. Phys. Chem. A* **2014**, *118* (2), 350–357.

(14) P. G. Sennikov. *J. Phys. Chem.* **1994**, *98* (19), 4973–4981.

(15) P. Kebarle; K. Nishizawa; J. Sunner. *J. Phys. Chem.* **1981**, *85* (1814), 1814–1820.

(16) D. A. Stauffer; D. A. Dougherty. *Tetrahedron Lett.* **1988**, *29* (47), 6039–6042.

(17) T. J. Shepodd; M. A. Petti; D. A. Dougherty. *J. Am. Chem. Soc.* **1986**, *108*, 6085–6087.

(18) S. Yamada; J. S. Fossey. *Org. Biomol. Chem.* **2011**, *9* (21), 7275–7281.

(19) C. A. Ilioudis; D. A. Tocher; J. W. Steed. *J. Am. Chem. Soc.* **2004**, *126* (39), 12395–12402.

(20) Y. S. Rosokha; S. V Lindeman; S. V Rosokha; J. K. Kochi. *Angew. Chemie Int. Ed.* **2004**, *43* (35), 4650–4652.

(21) M. Staffilani; K. S. B. Hancock; J. W. Steed; K. T. Holman; J. L. Atwood; R. K. Juneja; R. S. Burkhalter. *J. Am. Chem. Soc.* **1997**, *119* (27), 6324–6335.

(22) B. L. Schottel; H. T. Chifotides; M. Shatruk; A. Chouai; L. M. Prez; J. Bacsa; K. R. Dunbar; L. M. Pe. *J. AM. CHEM. SOC.* **2006**, *128* (17), 5895–5912.

(23) J. Vrbancich; G. L. D. Ritchie. *J. Chem. Soc. Faraday Trans. 2 Mol. Chem. Phys.* **1980**, *76* (0), 648–659.

(24) C. A. Hunter; K. R. Lawson; J. Perkins; C. J. Urch. *J. Chem. Soc.* **2001**, *2*, 651–669.

(25) C. A. Hunter; J. K. M. Sanders. *J. Am. Chem. Soc.* **1990**, *112* (14), 5525–5534.

(26) C. A. Hunter; M. N. Meah; J. K. M. Sanders. *J. Am. Chem. Soc.* **1990**, *112* (15), 5773–5780.

(27) W. H. Favre, H. A.; Powell. *IUPAC. Nomenclature of Organic Chemistry, Section B, Fundamental Heterocyclic Systems (The "Blue Book")*; Pergamon Press: Oxford, 2013.

(28) K. Ebel; H. Koehler; A. O. Gamer; R. Jäckh. *Ullmann's Encyclopedia of Industrial Chemistry*; Wiley-VCH Verlag GmbH & Co. KGaA, 2000.

(29) Z. Wang. In *Comprehensive Organic Name Reactions and Reagents*; John Wiley & Sons, Inc., 2010.

(30) Bhatnagar A.; Sharma P. K.; K. N. *Int. J. PharmTech Res.* **2011**, *3* (1), 268–282.

(31) W. Beker; P. Szarek; L. Komorowski; J. Lipiński. *J. Phys. Chem. A* **2013**, *117* (7), 1596–1600.

(32) C. Sen; A. Nandi; D. Mallick; S. Mondal; K. K. Sarker; C. Sinha. *Spectrochim. Acta Part A Mol. Biomol. Spectrosc.* **2015**, *137* (0), 935–944.

(33) H. Tang; G. Meng; Z. Chen; Y. Liu; L. Wei; Z. Wang. *J. Mater. Sci. Mater. Electron.* **2015**, 1–6.

(34) http://www.chemspider.com/Chemical-Structure.91683.html (accessed Jan 5, 2015).

(35) B. F. Fieselmann; D. N. Hendrickson; G. D. Stucky. *Inorg. Chem.* **1978**, *17* (8), 2078–2084.

(36) J. R. Cho; S. G. Cho; E. M. Goh; J. K. Kim. Preparation method of 2,2'-bi-1H-imidazole using glyoxal and an ammonium salt, 2004.

(37) Y. Cui; H.-J. Mo; J.-C. Chen; Y.-L. Niu; Y.-R. Zhong; K.-C. Zheng; B.-H. Ye. *Inorg. Chem.* **2007**, *46* (16), 6427–6436.

(38) T. Murata; Y. Yakiyama; K. Nakasuji; Y. Morita. *Cryst. Growth Des.* **2010**, *10* (11), 4898–4905.

(39) A. Pavlopoulou; D. A. Spandidos; I. Michalopoulos. *Oncol. Rep.* **2015**, *33* (1), 3–18.

(40) J. S. Casas; A. Castiñeiras; Y. Parajó; M. L. Pérez-Parallé; A. Sánchez; A. Sánchez-González; J. Sordo. *Polyhedron* **2003**, *22* (8), 1113–1121.

(41) M. J. Bloemink; H. Engelking; S. Karentzopoulos; B. Krebs; J. Reedijk. *Inorg. Chem.* **1996**, *35* (3), 619–627.

(42) Y. Parajó; J. L. Arolas; V. Moreno; Á. Sánchez-González; J. Sordo; R. de Llorens; F. X. Avilés; J. Lorenzo. *Inorganica Chim. Acta* **2009**, *362* (3), 946–952.

(43) P. A. Boo; J. S. Casas; M. D. Couce; E. Freijanes; A. Furlani; V. Scarcia; J. Sordo; U. Russo; M. Varela. *Appl. Organomet. Chem.* **1997**, *11* (12), 963–968.

(44) C. Tan; S. Hu; J. Liu; L. Ji. *Eur. J. Med. Chem.* **2011**, *46* (5), 1555–1563.

(45) Y. Li; Y. Wu; J. Zhao; P. Yang. *J. Inorg. Biochem.* **2007**, *101* (2), 283–290.

(46) J. L. Ferguson; C. M. Fitchett. *Cryst. Growth Des.* **2015**, *15* (3), 1280–1288.

(47) C.-Y. Yang; L.-C. Zhang; Z.-J. Wang; L. Wang; X.-H. Li; Z.-M. Zhu. *J. Solid State Chem.* **2012**, *194* (0), 270–276.

(48) M. C. Llinàs; J. Farran; M. V Capparelli; G. Anguera; D. Sánchez-García; J. Teixidó; S. Borrós. *Tetrahedron Lett.* **2014**, *55* (33), 4667–4670.

(49) S. Fortin; A. L. Beauchamp. *Inorg. Chem.* **2001**, *40* (1), 105–112.

(50) H.-J. Zhang; R.-Q. Fan; X.-M. Wang; P. Wang; Y.-L. Wang; Y.-L. Yang. *Dalt. Trans.* **2015**, *44* (6), 2871–2879.

(51) T. K. W. Christer B. Aakeröy John Desper. *J. Mol. Struct.* **2014**, *1072*, 20–27.

(52) Y.-H. Xu; Y.-Q. Lan; S.-X. Wu; K.-Z. Shao; Z.-M. Su; Y. Liao. *CrystEngComm* **2009**, *11* (8), 1711–1715.

APPENDICES

^{1}H NMR spectrum of 1,1'-bis(pyridin-4-ylmethyl)-1H,1'H-2,2'-biimidazole (L1) in DMSO-*d6* at 30 °C at 400 MHz

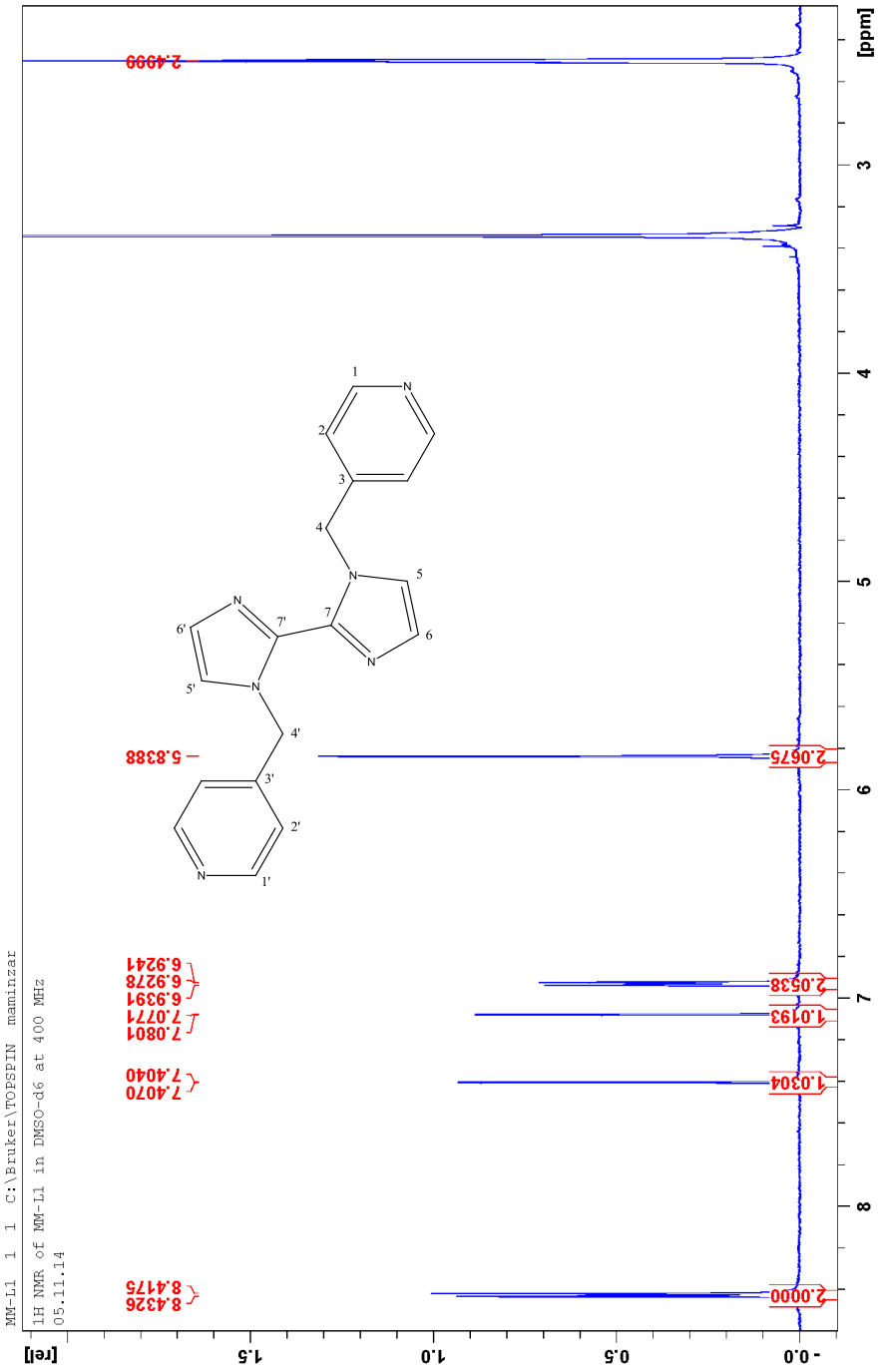

$^{13}C\{^{1}H\}$ NMR spectrum of 1,1'-bis(pyridin-4-ylmethyl)-1H,1'H-2,2'-biimidazole (L1) in DMSO-*d6* at 30 °C at 101 MHz

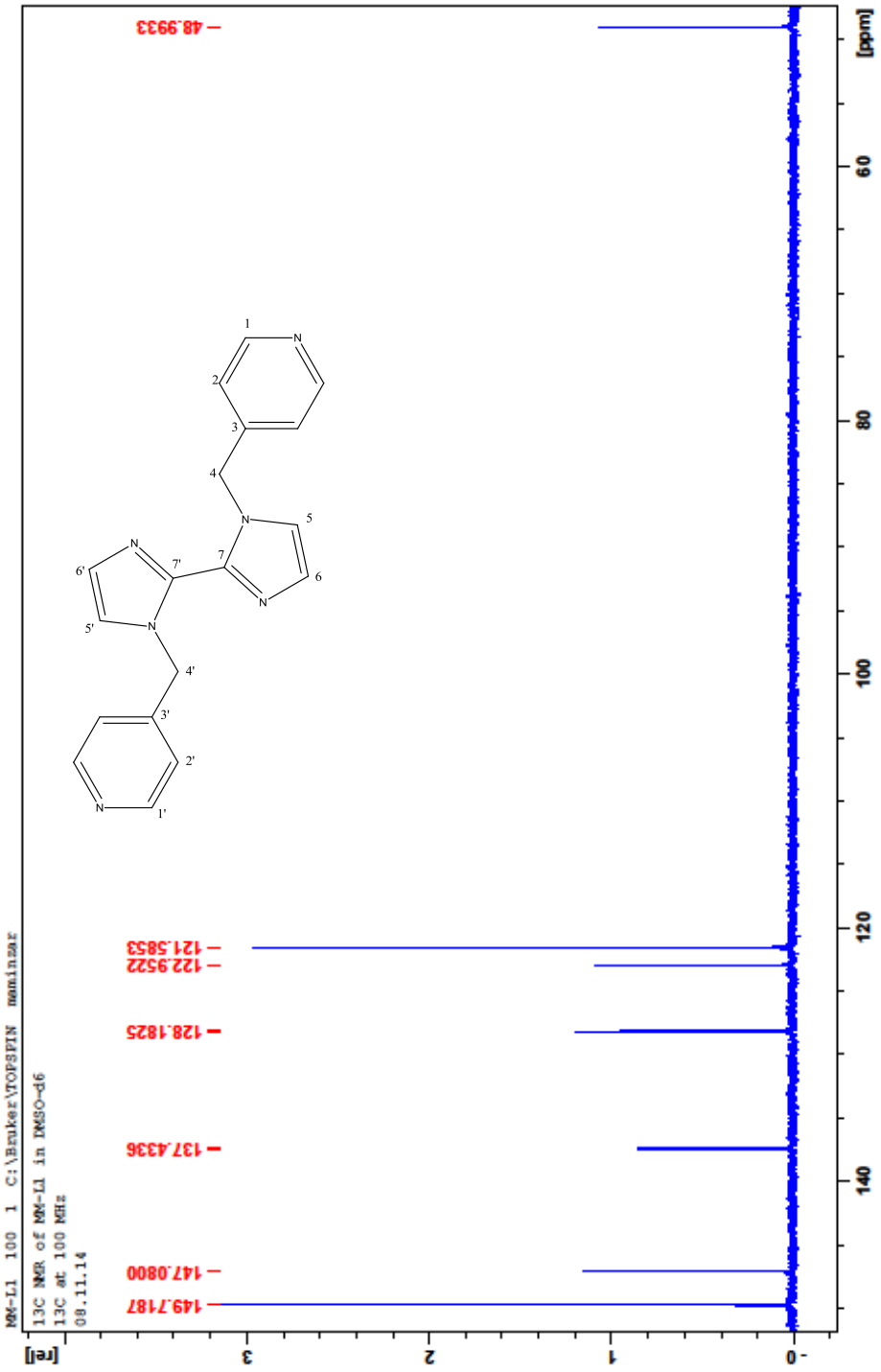

^{1}H NMR spectrum of diethyl 2,2'-(1H,1'H-[2,2'-biimidazole]-1,1'-diyl)diacetate (L2) in DMSO-*d6* at 30 °C at 400 MHz

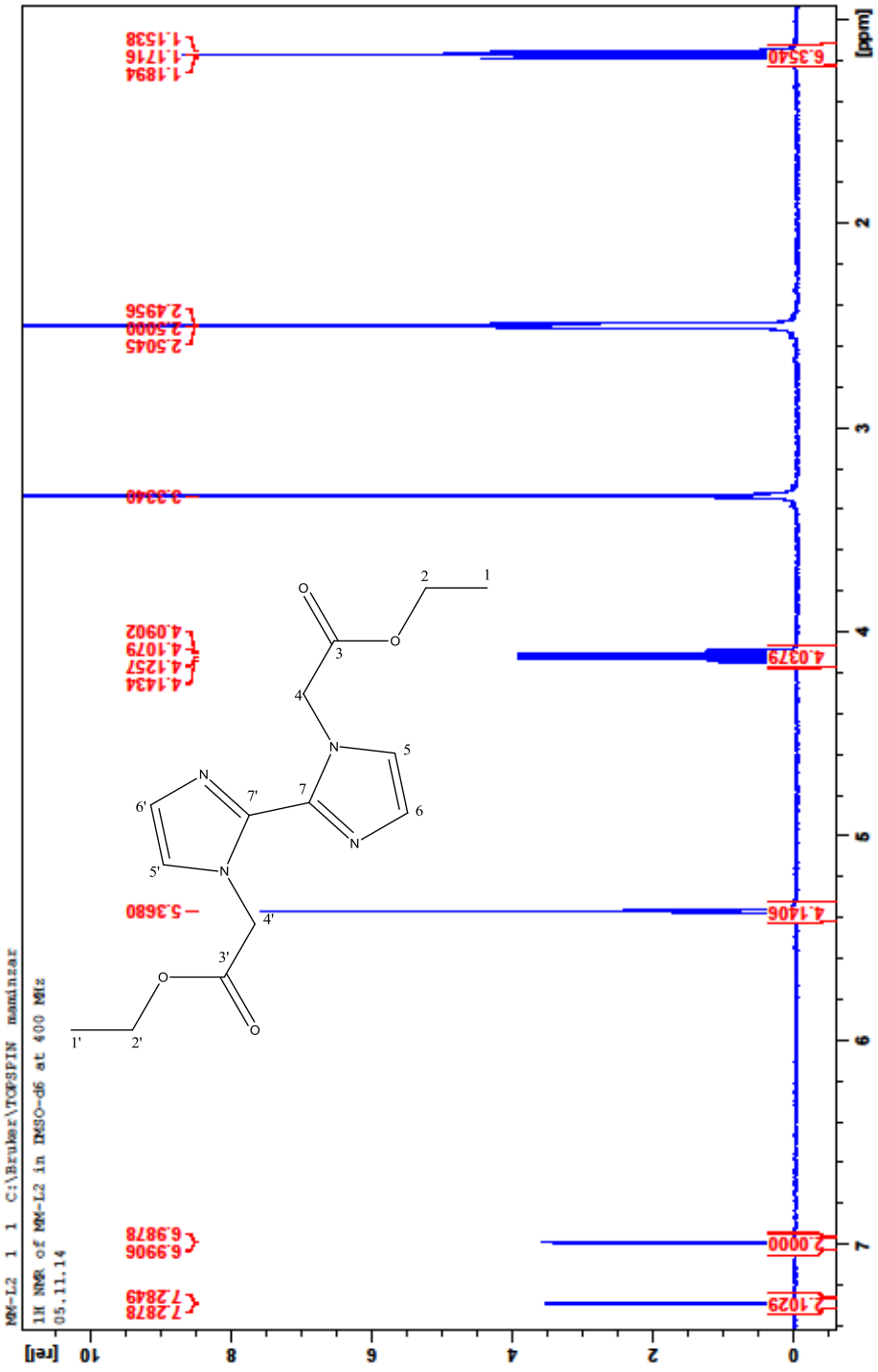

^{13}C NMR spectrum of diethyl 2,2'-(1H,1'H-[2,2'-biimidazole]-1,1'-diyl)diacetate (L2) in DMSO-*d6* at 30 °C at 400 MHz

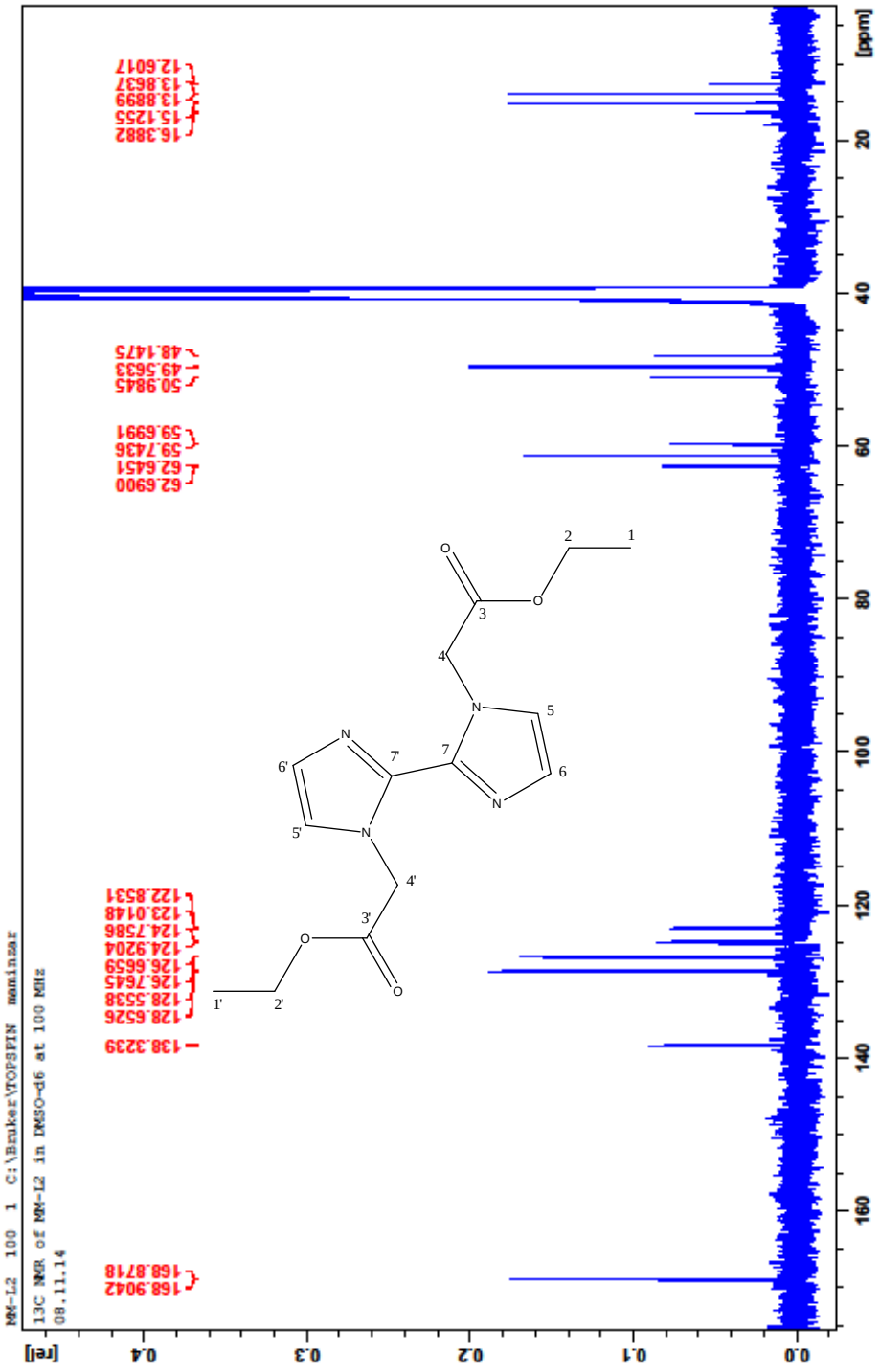

^{1}H NMR spectrum of diethyl 2,2'-(1H,1'H-[2,2'-biimidazole]-1,1'-diyl)diacetic acid (L3) in MeOD at 30 °C at 400 MHz

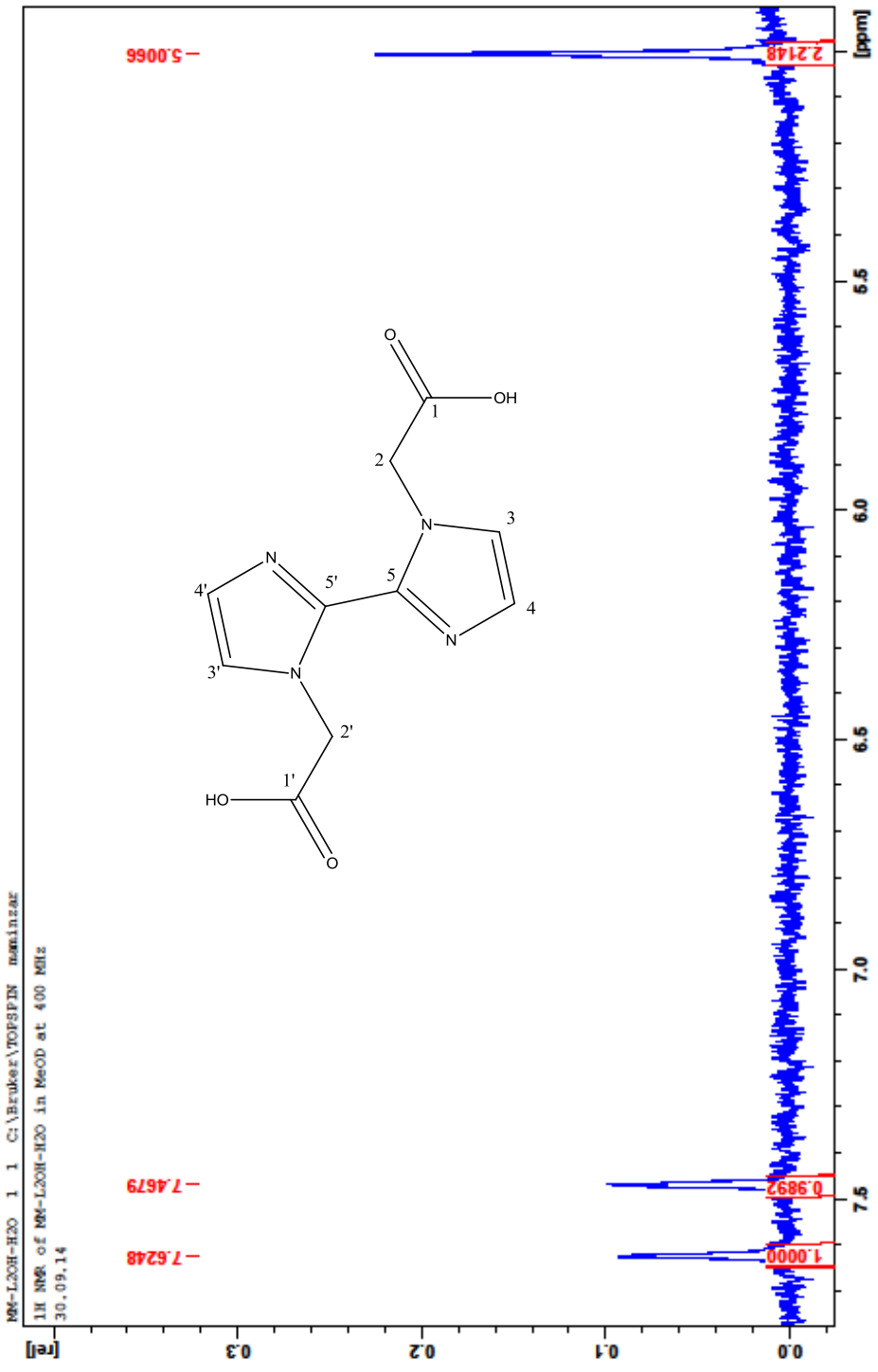

^{1}H NMR spectrum of Fe(II) complex with L1 in DMSO-*d6* at 30 °C at 400 MHz

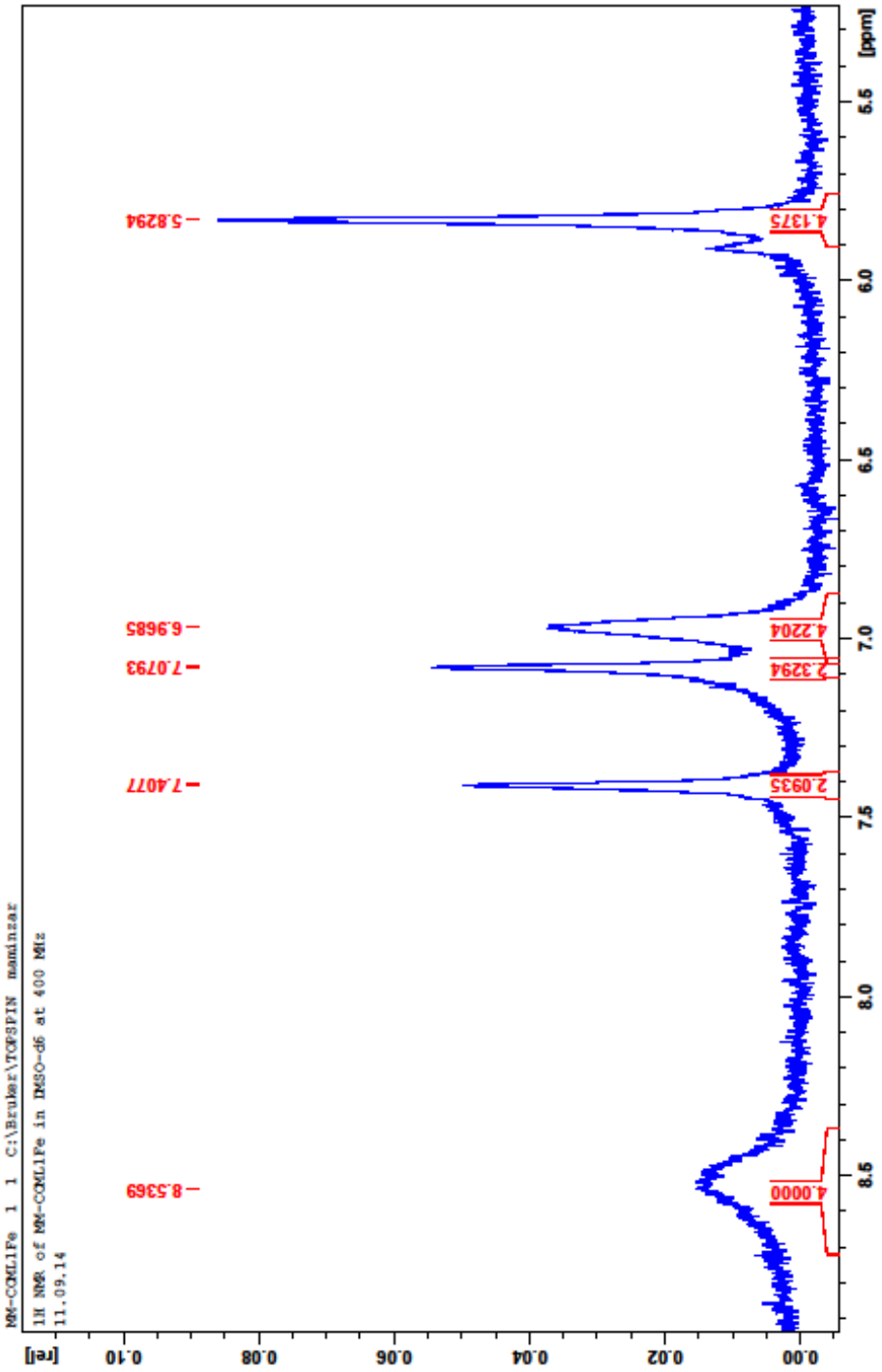

^{1}H NMR spectrum of Pt(II) complex with L1 in DMSO-*d6* at 30 °C at 400 MHz

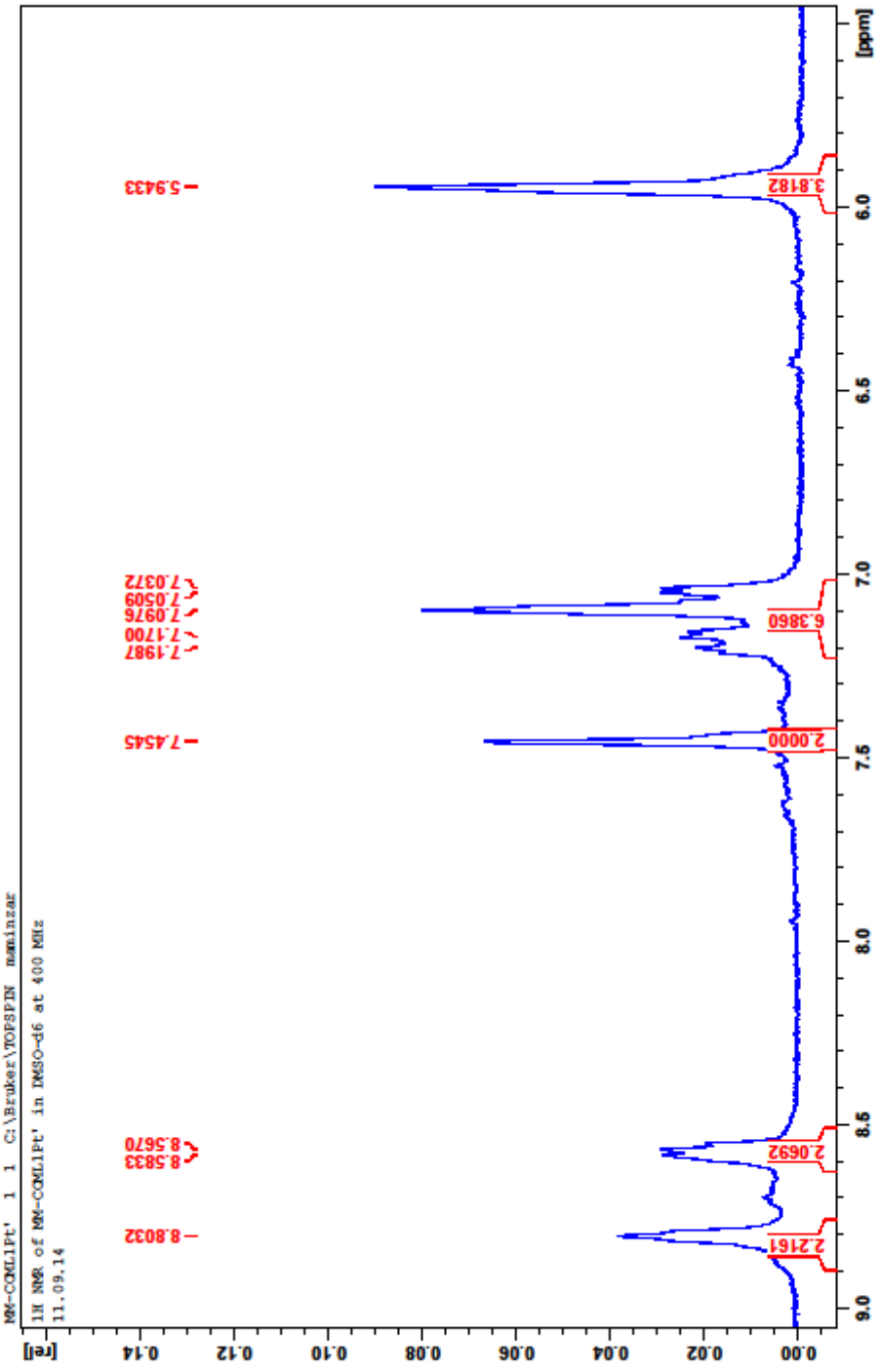

^{1}H NMR spectrum of Au(I) complex with L1 in DMSO-*d6* at 30 °C at 400 MHz

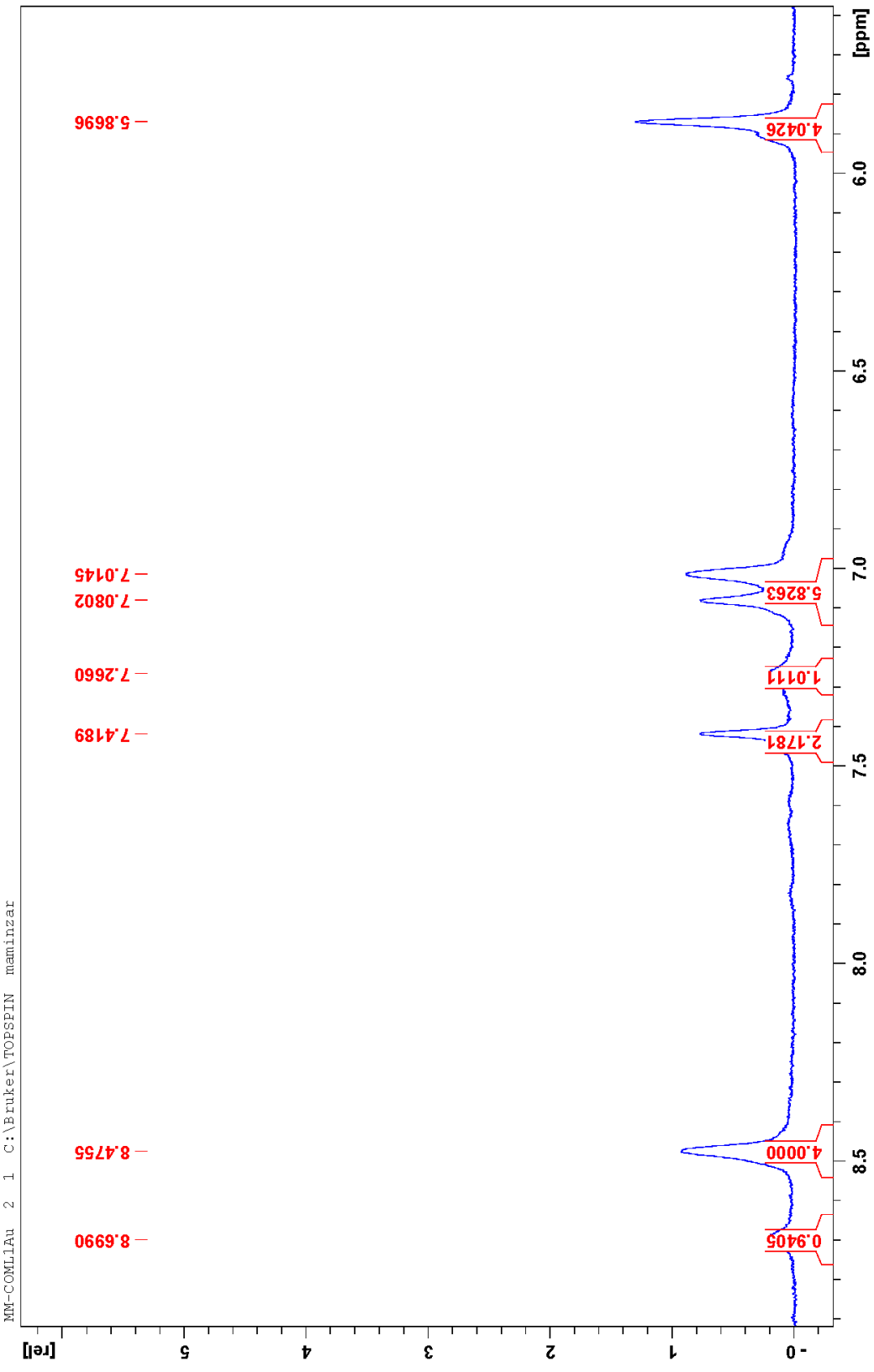

^{1}H NMR spectrum of Pt(II) complex with L2 in DMSO-*d6* at 30 °C at 400 MHz

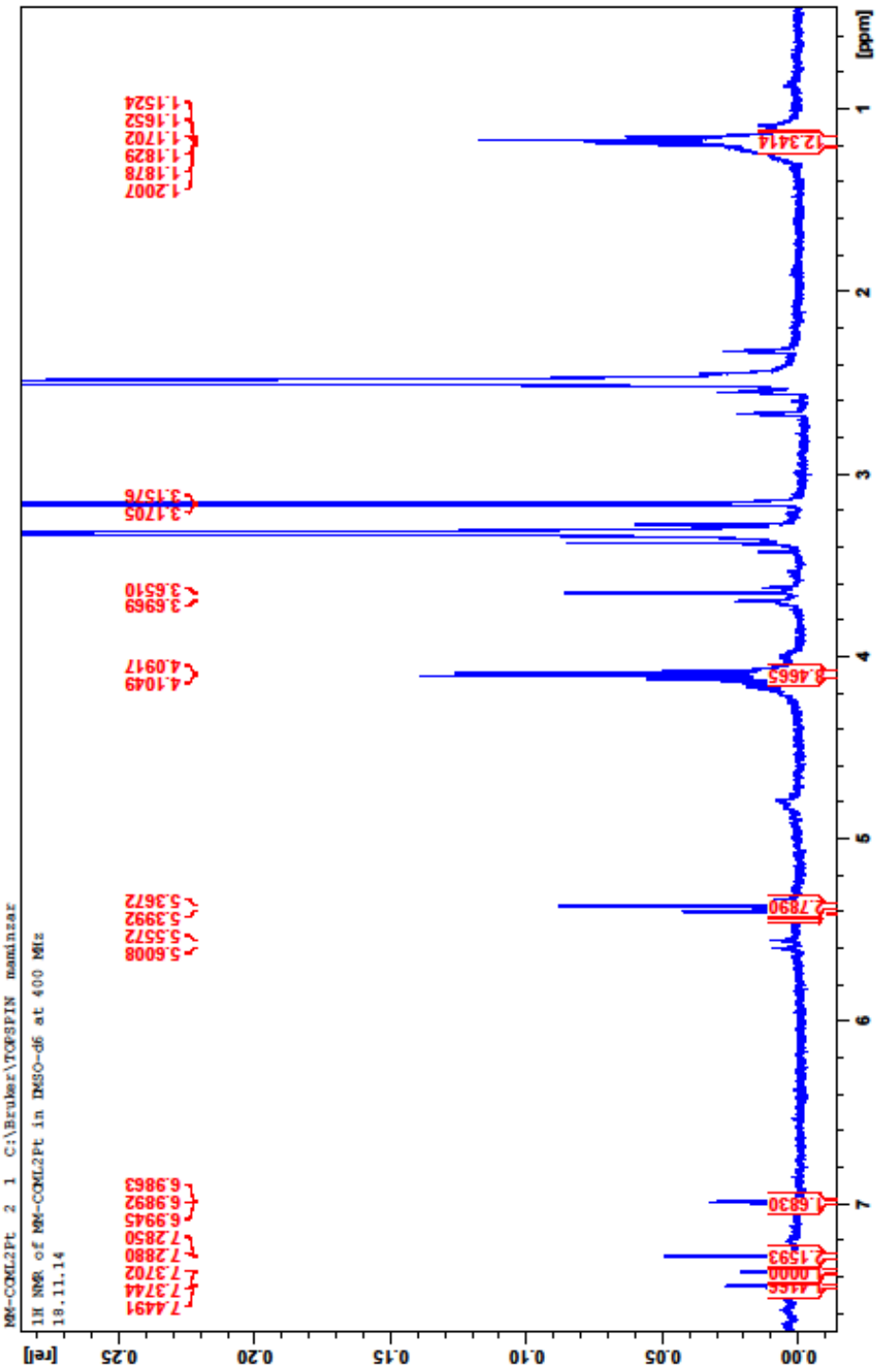

Single crystal X-ray diffraction parameters for L1

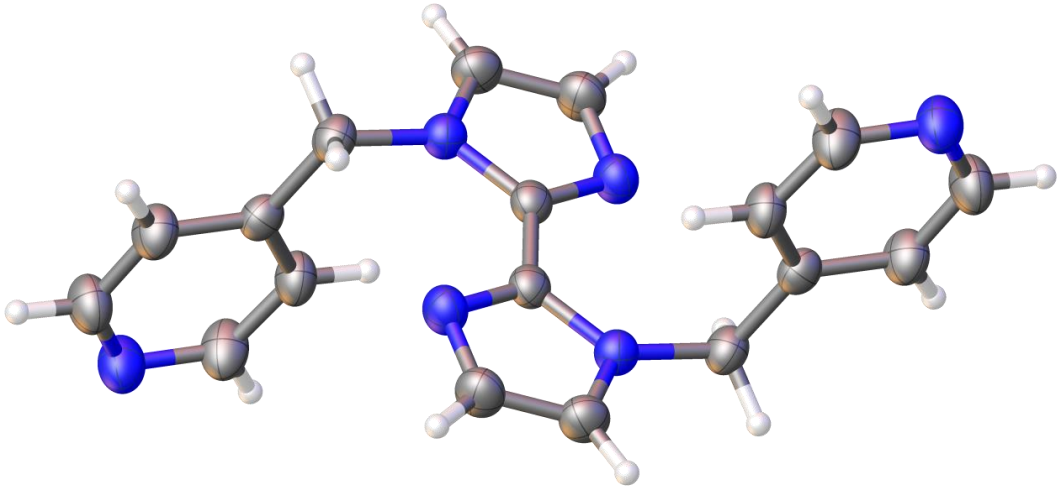

Compound		L1
Formula		$C_{18}H_{16}N_6$
Space group		P 2_1/c
Cell lenghts, Å	a	5.18061(12)
	b	16.7663(5)
	c	9.1665(2)
Cell angles,°	α	90.00
	β	98.062(3)
	γ	90.00
Cell volume, $Å^3$		788.33

Single crystal X-ray diffraction parameters for L2

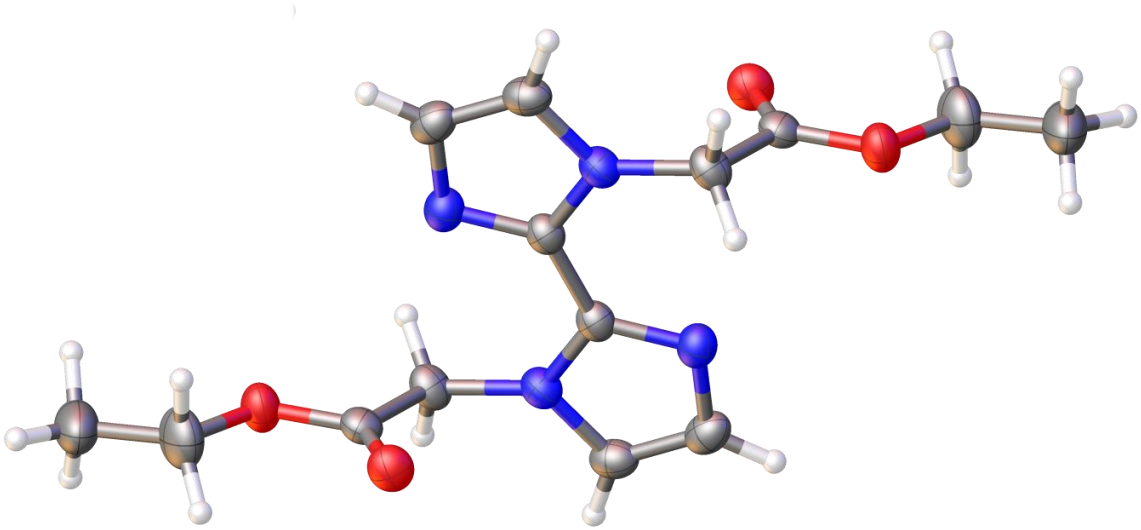

Compound		L2
Formula		$2(C_7H_9N_2O_2)$
Space group		P 2_1/n
Cell lenghts, Å	a	14.4601(4)
	b	4.97906(10)
	c	21.9013(5)
Cell angles,°	α	90.00
	β	107.531(3)
	γ	90.00
Cell volume, $Å^3$		1503.61

Single crystal X-ray diffraction parameters for KIL1 complex

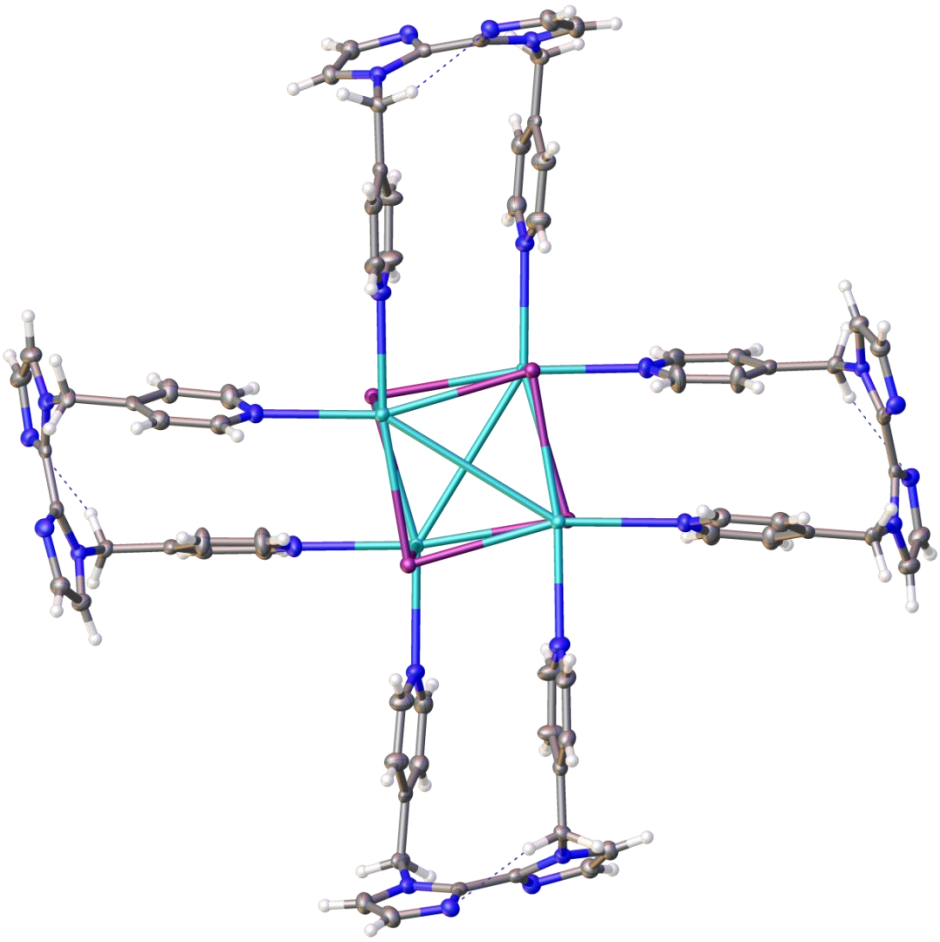

Compound		KIL1 complex
Formula		$C_{18}H_{16}IKN_6$
Space group		P 4_2/n
Cell lenghts, Å	a	23.56060(19)
	b	23.56060(19)
	c	6.92267(8)
Cell angles,°	α	90.00
	β	90.00
	γ	90.00
Cell volume, $Å^3$		3842.79

Single crystal X-ray diffraction parameters for ZnL1complex

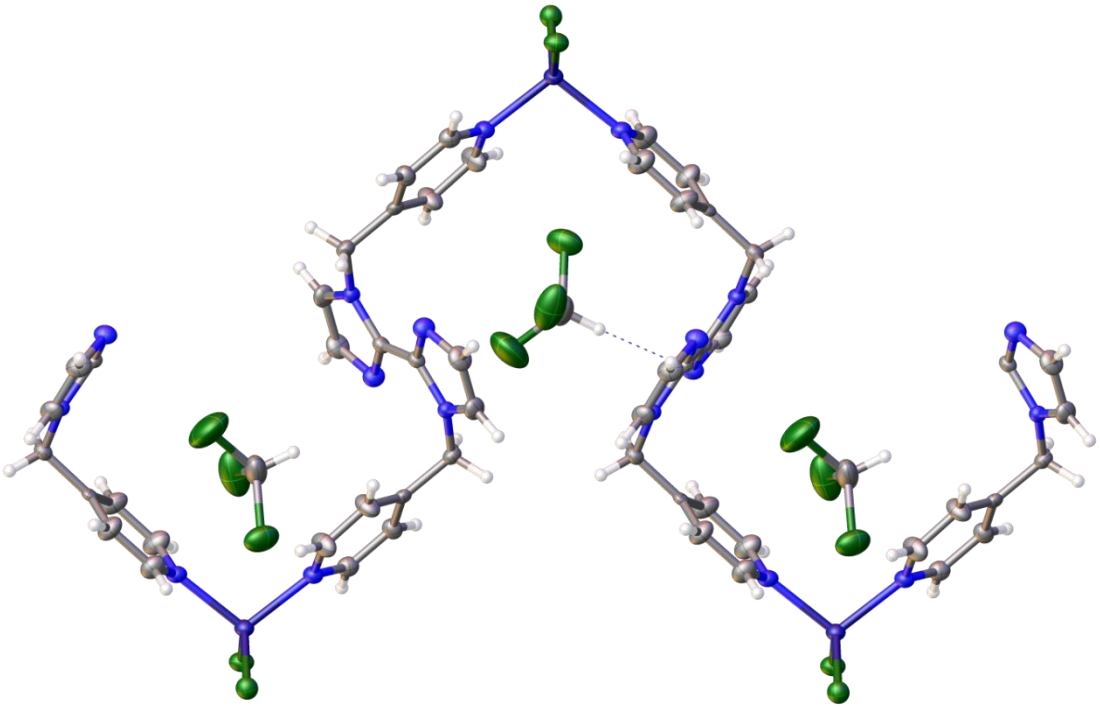

Compound		ZnL1 complex
Formula		$C_{18}H_{16}Cl_2N_6Zn,C\ HCl_3$
Space group		P $2_1/c$
Cell lenghts, Å	a	12.2909(3)
	b	13.9051(3)
	c	14.8081(4)
Cell angles,°	α	90
	β	110.538(3)
	γ	90
Cell volume, $Å^3$		2369.94

Single crystal X-ray diffraction parameters for AgL1complex

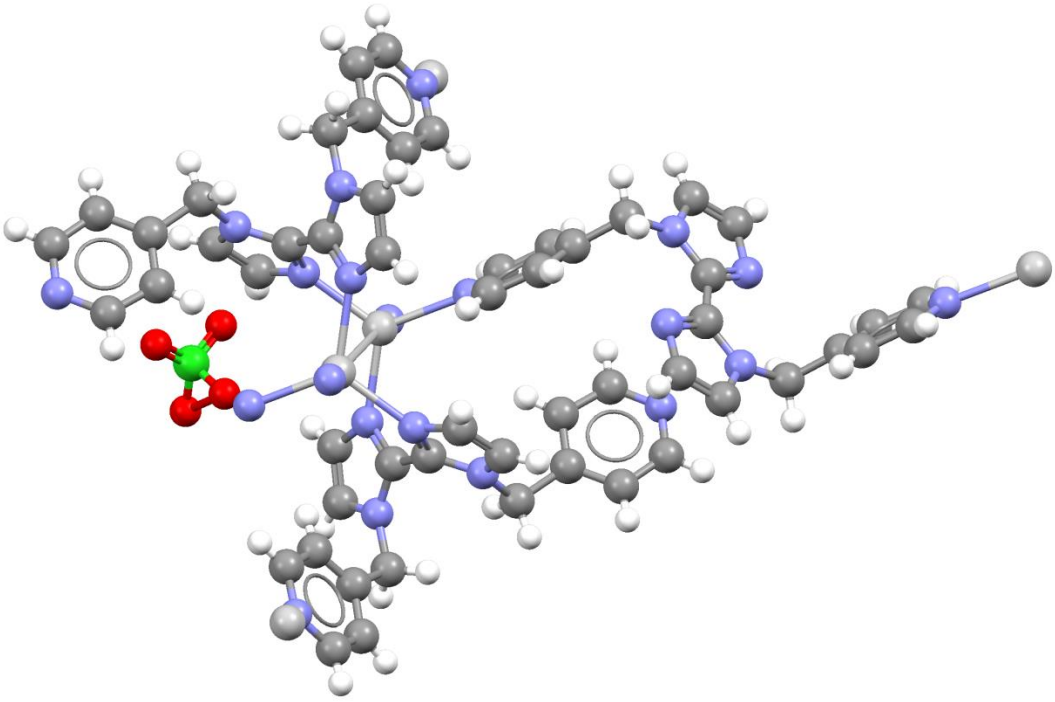

Compound		AgL1 complex
Space group		P -1
Cell lenghts, Å	a	9.6948(9)
	b	10.8492(17)
	c	16.1159(18)
Cell angles,°	α	72.746(12)
	β	76.739(8)
	γ	76.259(10)
Cell volume, $Å^3$		1549.22

Single crystal X-ray diffraction parameters for AgL1complex

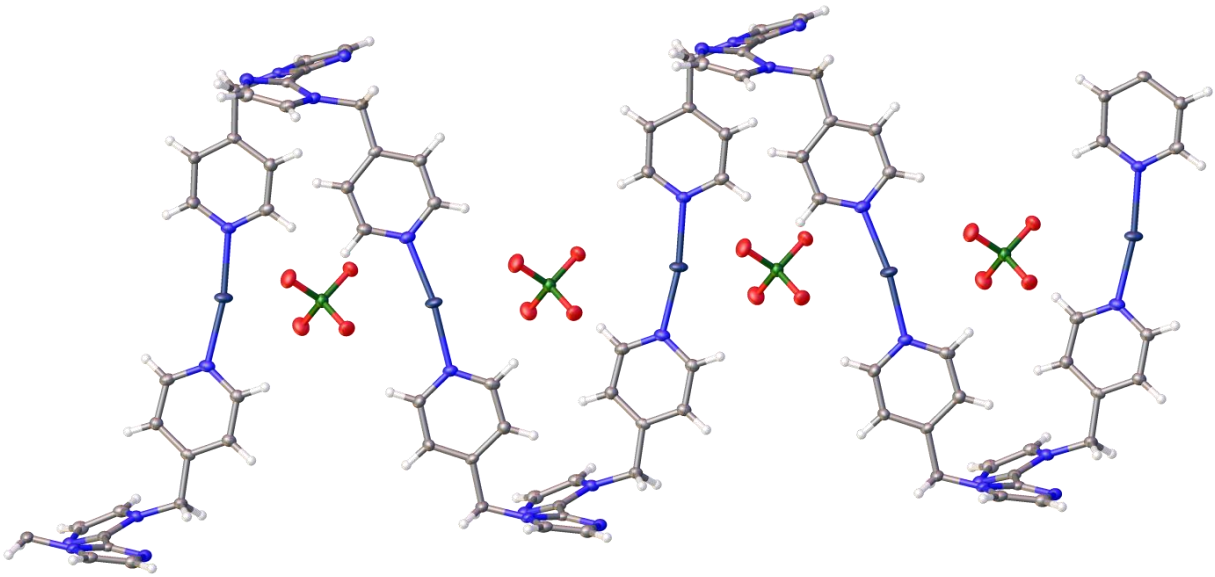

Compound		AgL1 complex
Formula		$2(C_{18}H_{16}AgN_6),4(Cl_{0.5}\ O_2)$
Space group		P 2_1 2_1 2
Cell lenghts, Å	a	23.02023(17)
	b	22.77892(17)
	c	7.07377(6)
Cell angles,°	α	90.00
	β	90.00
	γ	90.00
Cell volume, $Å^3$		3709.32